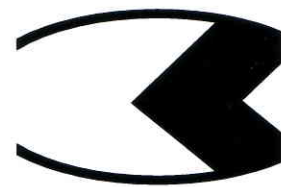


VLAKNA TEXTIL



Ročník 21.
September
2014

ISSN1335-0617

Indexed in:

Chemical
Abstracts,

World Textile
Abstracts

EMDASE

Elsevier
Biobase

Elsevier
GeoAbstracts



FIBRES AND TEXTILES VLÁKNA A TEXTIL

Vydáva

- Slovenská technická univerzita v Bratislave, Fakulta chemickej a potravinárskej technológie
- Technická univerzita v Liberci, Fakulta textilní
- Trenčianska univerzita A. Dubčeka v Trenčíne, Fakulta priemyselných technológií
- Výskumný ústav chemických vlákien, a.s. Svit
- Slovenská spoločnosť priemyselnej chémie, Bratislava
- VÚTCH – CHEMITEX, spol. s r.o., Žilina

Published by

- Slovak University of Technology in Bratislava, Faculty of Chemical and Food Technology
- Technical University of Liberec, Faculty of Textile Engineering
- A. Dubček University in Trenčín, Faculty of Industrial Technologies
- Research Institute of Man-Made Fibres, j.s.c., Svit
- Slovak Society of Industrial Chemistry, j.s.c., Bratislava
- VÚTCH – CHEMITEX, Ltd., Žilina

Šéfredaktor (Editor in Chief): A. Ujhelyiová

Redakčná rada

M. Hricová, M. Jambrich, J. Kochan, P. Lizák, P. Michlík, M. Pajtášová, M. Prášil, M. Révus, I. Sroková, V. Váry

Editorial Board

Čestní členovia redakčnej rady

R.U. Bauer (DE), D. Ciechanska (PL), T. Czigani (HU), J. Drašarová (CZ), A.M. Grancarić (HR), M. Krištofič (SK), I. Krucinska (PL), A. Marcinčin (SK), A.M. Marechal (SL), J. Militký (CZ), R. Redhammer (SK), J. Šajbidor (SK), J. Šesták (SK), M. Budzák (SK), J. Vavro (SK), V. Vlasenko (UA)

Honourable Editorial Board

Výkonný redaktor (Executive Editor): M. Hricová

Redakcia a distribúcia časopisu:
(Editorial Office and distribution of the journal)

STU in Bratislava, FCHPT, Oddelenie vlákien a textilu,
Radlinského 9, 812 37 Bratislava, SK
IČO 00 397 687
Tel: 00 421 2 59 325 575
Fax: 00421 2 524 931 98
e-mail: marcela.hricova@stuba.sk

Objednávka a inzercia časopisu:
(Order and advertisement of the journal)

Slovenská spoločnosť priemyselnej chémie,
člen Zväzu vedecko-technických spoločností
Radlinského 9, 812 37 Bratislava, SK
Tel: 00 421 2 59 325 575, Fax: 00421 2 524 931 98
e-mail: marcela.hricova@stuba.sk

Objednávka časopisu zo zahraničia – okrem Českej Republiky

Order of the journal from abroad – excepting Czech Republic

SLOVART G.T.G, s.r.o. EXPORT-IMPORT
Krupinská 4, P.O.Box 152, 852 99 Bratislava, SK
Tel: 00421 2 839 471-3, Fax: 00421 2 839 485
e-mail: info@slovart-gtg.sk

Sadzba a tlač

FOART, s.r.o., Bratislava

Typeset and printing at

Časopis vychádza 4x ročne
Ročné predplatné 60 EUR

Journal is published 4x per year
Subscription 60 EUR

Contributions are issued without any proof-readings

ISSN 1335-0617

Evidenčné číslo MKCR SR Bratislava EV 4006/10

Fibres and Textiles (3) 2014

Vlákna a textil (3) 2014

September 2014

Special issue venue 4th International Conference TEXCO'14 held on August 27.-28.2014 in Ružomberok, Slovakia

CONTENT	OBSAH
3 <i>P. Lizák</i> Information about 4 th International Conference TEXCO'14	3 <i>P. Lizák</i> Informácie o 4-tej medzinárodnej konferencii TEXCO'14
4 <i>V. Bajzik, Z. Bečicová and A. Havelka</i> The influence of time of work on the wear of needle surface	4 <i>V. Bajzik, Z. Bečicová a A. Havelka</i> Vliv délky pracovního zatížení na poškození povrchu šicí jehly
8 <i>L. Balogová, B. Babušiak and M. Gála</i> Biopotential sensing with electroconductive fabrics	8 <i>L. Balogová, B. Babušiak a M. Gála</i> Snímanie biopotenciálov pomocou elektricky vodivých textílií
11 <i>P. Benesovsky and H. Polaskova</i> Classification of thermoregulatory properties of outdoor clothing in standards and technical reports	11 <i>P. Benesovsky a H. Polaskova</i> Klasifikace termoregulačních vlastností textilu pro outdoorové oděvy v normách a technických zprávách
14 <i>J. Bezečný, R. Vavřík and A. Dubec</i> The influence of the selected parameters on the initiation of hydrogen embrittlement	14 <i>J. Bezečný, R. Vavřík a A. Dubec</i> Vplyv vybraných parametrov morenia na vznik vodíkovej krehkosti
18 <i>P. Gilewicz, J. Rutowicz, I. Frydrych and A. Cichocka</i> Color change measurement on DigiEye	18 <i>P. Gilewicz, J. Rutowicz, I. Frydrych a A. Cichocka</i> Meranie farebnej zmeny na prístroji DigiEye
22 <i>I. Kopal</i> Design of DMA experiments for polymers	22 <i>I. Kopal</i> Experimentálny dizajn DMA polymérov
25 <i>I. Kopal and K. Kováč</i> Temperature dependency of DC electrical conductivity of hardened polyurethane based carbon nanocomposites	25 <i>I. Kopal a K. Kováč</i> Teplotná závislosť jednosmernej elektrickej vodivosti uhlíkových nanokompozitov na báze matrice z tvrdého polyuretánu
28 <i>I. Kopal and L. Polka</i> FTIR spectroscopy measurements of oriented polypropylene films	28 <i>I. Kopal a L. Polka</i> FTIR spektroskopia orientovaných polypropylénových filmov
31 <i>J. Krmela and M. Vančo</i> Bike tire with textile reinforcement – experiment and computational modelling	31 <i>J. Krmela a M. Vančo</i> Bicyklová pneumatika s textilní výztuží – experiment a výpočtové modelování
35 <i>V. Krmelová, M. Halaj, J. Pleváková, I. Sroková and V. Sasinková</i> Cationic esters of hydroxyethylcellulose: synthesis, characterization and properties	35 <i>V. Krmelová, M. Halaj, J. Pleváková, I. Sroková a V. Sasinková</i> Kationové estery hydroxyetylcelulózy: príprava, charakterizácia a vlastnosti
39 <i>J. Legerská</i> Model calculation of the thermal conductivity and thermal resistance for the layered laminated textile fabrics	39 <i>J. Legerská</i> Modelový výpočet tepelnej vodivosti a tepelného odporu poťahu automobilového sedadla

44	<i>J. Ligas and K. Huljaková</i> Preparation of blended yarns with multifunctional properties	44	<i>J. Ligas a K. Huljaková</i> Príprava zmesných priadzí s multifunkčnými vlastnosťami
47	<i>P. Lizák</i> Textile design as symbiosis of technical and artistic aspect	47	<i>P. Lizák</i> Textilný dizajn ako symbióza technického a umeleckého hľadiska
51	<i>P. Lizák, S. Ibrahim and A. Schlosser</i> Impact of fiber macrostructure on transport properties of textile fabrics	51	<i>P. Lizák, S. Ibrahim a A. Schlosser</i> Vplyv makroštruktúry vlákien na transportné vlastnosti textilných vláknových útvarov
55	<i>A. Mazari, A. Havelka and F. Buyuk Mazari</i> Effect of DLC-coated needle on sewing performance	55	<i>A. Mazari, A. Havelka a F. Buyuk Mazari</i> Vplyv DLC náterov ihly na šijací výkon
59	<i>R. Mishra, V. Baheti, J. Militky, D. Kremenakova, B.K. Behera, M. Venkataraman and V. Arumugam</i> Functional advantages of 3D woven glass nanocomposites	59	<i>R. Mishra, V. Baheti, J. Militky, D. Kremenakova, B.K. Behera, M. Venkataraman a V. Arumugam</i> Výhody 3D tkaných sklenených nanokompozitů s ohledem na jejich funkční vlastnosti
62	<i>F. Pešlová, P. Lizák, M. Ďurovcová, M. Janeková, A. Pavůčková and D. Košťáliková</i> PVD method used for deposition of silver and tungsten layer on the cotton woven fabric	62	<i>F. Pešlová, P. Lizák, M. Ďurovcová, M. Janeková, A. Pavůčková a D. Košťáliková</i> PVD povlakovaná bavlna striebrom a volfrámom
67	<i>P. Rusko</i> Computer graphics in textile design	67	<i>P. Rusko</i> Počítačová grafika v textilnom dizajne
70	<i>V. Šafářová and J. Militký</i> Analysis of the electrical and mechanical properties of hybrid yarns designated for protection against electromagnetic field	70	<i>V. Šafářová a J. Militký</i> Analýza elektrických a mechanických vlastností hybridních přízí určených pro ochranu proti elektromagnetickému poli
74	<i>A. Schlosser, P. Lizák and L. Žila</i> Effect of consumer wear and tear on transport properties of knitted fabrics	74	<i>A. Schlosser, P. Lizák a L. Žila</i> Vplyv zmeny parametrov spotrebiteľských vlastností na transportné vlastnosti pletenín
78	<i>L. Techniková, M. Tunák and J. Janáček</i> A procedure of 3D surface reconstruction of unicolor and patterned fabrics and pills detection	78	<i>L. Techniková, M. Tunák a J. Janáček</i> Postup 3D rekonstrukce povrchu jednobarevných a vzorovaných textilií a detekce žmolků
81	<i>M. Tunák and M. Řiřicová</i> Monitoring of nanofiber layer structure with the aid of image analysis	81	<i>M. Tunák a M. Řiřicová</i> Monitorování struktury nanovláknenných vrstev pomocí obrazové analýzy
85	<i>M. Venkataraman, R. Mishra, J. Militky, D. Kremenakova, A. Veerakumar and S. Misra</i> Thermal properties of high performance nonwoven padding fabrics at sub zero temperatures	85	<i>M. Venkataraman, R. Mishra, J. Militky, D. Kremenakova, A. Veerakumar a S. Misra</i> Tepelné vlastnosti vysocefunkčních netkaných výplňkových textilií za nízkých teplot
88	<i>M. Vik, M. Viková and M. Kašparová</i> Color difference evaluation at high chromatic colors	88	<i>M. Vik, M. Viková a M. Kašparová</i> Hodnocení barevných rozdílů u materiálů s vysokou čistotou odstínu

Information about 4th INTERNATIONAL CONFERENCE on Textile and Material Science TEXCO'14



On 27 - 28.08.2014 the fourth international conference on textile materials was held in Slovakia, Ružomberok. The conference brought together experts not only from Slovak Republic, but also experts from the Czech Republic and Poland. This conference offered 29 lectures. Within the conference

fashion trends in textile design were presented via fashion show realized by the students of the School of Applied Arts. These were completed by special lectures. The main conference topics were focused on: Clothing and Comfort; Technical Textiles; Design Engineering; Textile Chemical Technologies

In the first of plenary lectures not only current situation in the textile and clothing industry was evaluated but also new view on textile design trends. It was emphasized that the current designer is not only the creator of innovation in relation to seasonal fashion offer, but often also gives suggestions to new technical and technological solutions, or is involved in their selection and implementation into production practice. Fabric design is the overall appearance including the structure of the fabric and the design is just drawing on the fabric surface.

Textile design is a complex field of practice which operates in a competitive, global industry. Textile designers are often unacknowledged in the process of design, obscured by the names of companies, brands and fashion designers. This lecture attempts to bring clarity to the subject by revealing some of its hidden structures and interrelationships. It also seeks to capture the diversity of textile design through documenting technical and aesthetic considerations together with some of the traditional craft and advanced digital approaches currently applied by different sectors of the industry. There were defined three areas of textile design:

1. *Fabric construction approaches to textile design*
 - Fibers, yarns and fabrics – fundamental principles for the textile designers
 - Textile pattern of fabrics and knits
2. *Surface approaches to textile design*
 - Printed textile design
 - Embroidered textile design
 - The use of color in textile design
3. *Applications and advances*
 - Fashion design – the dynamics of textiles in advancing cultural memes
 - Interior textile design
 - The design of technical textiles (textile architecture, vehicles, etc.).

Nowadays the extraordinary task of designers and manufacturers cooperation is emphasized especially in the area of innovation, quality, technical possibilities and also cooperation in the European economic area in clothing and home textiles is considered to be very important. In the second Invitive lecture "*Prediction of Side Emitting Optical Fibers Illumination Length*" is evaluation of SEPOF loss of illumination intensity in dependence on the distance from light source and prediction of real illumination length. The four blocks of lectures were focused mainly on textile material. It was informed about the optical fibers and the impact of working load on surface damage of sewing needles (The influence of work time on needle surface). There were also presented innovations in the field of multifunctional textiles for the military sector and also car industry.

As usual the conference in Ružomberok paid a considerable attention to sportswear. The lectures showed that about 60% of the total energy consumes human organism for its conditioning. In sportswear prevails the trend to construct „mixed“ material for each part of the body to maintain thermal balance. Producers prefer mainly POP fibers and their usage for thermal underwear. POP fiber with its excellent transport properties had the special position. Our designers presented new clothes using recycled fabrics, which on one side allow to increase the wearing comfort, but on the other hand the price of clothing corresponds to the current state of the Slovak economy. Special attention was paid to fibers with anti-allergic finishing for consumers who have sensitive skin in contact with other fabrics.

New clothes tested for wearing comfort are marked as "wearing comfort", which gives consumers confidence in the decision when purchasing it. Comfort is a complex function, involving many properties of the fabric. Comfort is measurable based on modern test procedures which represent the benefit of science in recent years.

In the field of work clothing materials are used new fabrics with special features and new textile structures are formed that provide protection in harsh and extreme working conditions. Work-wear requires high thermo-physiological comfort. Special textile materials are produced through nanotechnology to make the surface of fibers and textiles functional. The new procedures as plasma surface treatment and other nanotechnology procedures or its combinations are used.

doc. Ing. Pavol LIZÁK, PhD.
Chair of Scientific Committee

THE INFLUENCE OF TIME OF WORK ON THE WEAR OF NEEDLE SURFACE

Vladimir Bajzik¹, Zuzana Bečicová¹ and Antonín Havelka²

Technical University of Liberec, Faculty of Textile Engineering

¹*Department of Textile Evaluation*

²*Department of Clothing*

Studentská 2, 461 17, Liberec, Czech Republic

vladimir.bajzik@tul.cz

Abstract: *In the paper the influence of surface finish of needles (titanium nitride finish and chrome finish), air cooling and the placement of needles in the needle bar during 24 hour period of sewing of seat covers for car seats made of leather is presented. Damaged sewing thread reduces high quality appearance of the seat cover at the site of sewing and also the durability of the joint. Simultaneously, the sewing needles must be replaced more frequently which leads to an increase in costs and loss of productivity. The test was carried out on two-needles sewing machine using the lockstitch. The degree of the wear of needle surface was measured after 8, 16 and 24 hours of work. The one was determined subjectively by analyzing images from a scanning electron microscope. To analyze the extent of surface wear the grid was used. The results show that the damage surface of the left needle is considerably larger than at the right, which may be caused by the different direction of rotation of the loopers. Neither the cooling effect nor the influence of surface finish has the influence on the changes of size of surface wear.*

Keywords: *Car seat, cooling, lockstitch, sewing needle, surface finish*

1 INTRODUCTION

Sewing process is basic operation which can be met when the clothing is produced under home conditions. Also this one is common operation for industrial production and can be found in very wide spectrum of products not only in the clothing industry but also in technical textiles, eg. in automotive. Generally, it is valid for industrial production that the emphasis is put on productivity and quality. Therefore, even a small improvement may play significant role in firm benefits especially it is valid for heavy industry sewing, such as sewing of seat cushions, backs and airbags in automotive, where lifetime of needles is standardly lower than at apparel industry. The high quality of product is connected also with quality of sewing, where appearance and long-lasting stitches at seat cushions can be affected by sewing quality.

1.1 The stress of machine sewing needles

Machine sewing needles in the sewing process are stressed mechanically and thermally. Their main role is to penetrate the sewing material without damage of sewn or sewing material and without their wear. The cause of the mechanical and subsequent thermal stress and wear of the

needle is work that is held by needle at high speeds despite the resistance of the material. The resistance of the material to penetration by the needle and subsequent wear of the needle is greater, the harder material is. Method of sewing machine needles stress has a direct impact on the life of sewing needles. Their life are stirred in part design and surface finish of the needles themselves, adjusting of the sewing machine, sewn and sewing material, number of layers of material and, last but not least, how the machine is operated by an operator.

In industrial production, especially technical textiles, arose due to the high-speed sewing problem with overheating needles, which limits the possible further acceleration of the sewing process and affects productivity. At seat cushions, typically, the material being sewn includes single and multiple plies of synthetic fabric or leather, and sometimes backed with plastics. These materials are much more difficult to sew compared to ordinary sewing applications. The high temperature of sewing needles may negatively affect the strength of sewing thread and to melt sewn material at the point of a penetration of the needle. Standard sewing speeds range from 1000 to 3000 rpm in heavy industrial sewing but sewing speeds in the range

from 2000 to 6000 rpm are used in present time. The high sewing speed leads to needle heating which can reach up to 300°C [1]. At the work [2] is presented that thread tensile strength is negatively affected by needle heating and high temperature leads to weakening of thread.

Needle heating arose due to the friction between the needle and the fabric and between thread and needle eye. The heat is partially absorbed by the fabric and partially by the needle. The heat absorbed by the fabric is spread out along the seam, but the heat absorbed by the needle accumulates and the high temperature of needle can lead to wear of thread. The resistance to needle wear can be improved by the hardness of the needle surface. It should be as great as possible when the technical textiles are sewn. The high hardness leads to high life-time of sewing needles. This one is ensured by means of surface treatment of sewing needles. The surface treatment leads to improve the mechanical and thermal properties of the needle during sewing.

Also set up and maintenance of the machine has the big influence on the mechanical wear of the needle. In the case that the sewing machine is not tuned well the friction may arise between the needle and the other parts of device where stitch is created and this leads to abrasion of the needle. On the needle surface sharp edges and rough places can occur, which may cause increased heating and subsequently reducing of quality of stitching. The right choice of parameters of needles helps to eliminate defects during the sewing process [3], too. Generally, the temperature of the needle can be cut down, eg, by installing a cooling or lubrication of sewing thread by silicone oil or using less common way by dampen of the sewing thread. But cooling must not lead to effective reduction of heating when heavy materials are sewn [2].

As an important problem connected with damage of sewing thread the wear of needle surface is as the aim of this work the comparison of the course of wear of needle surface during 24 were chosen. The wear during time for two types of surface finish – chrome finish and coating by titanium nitride was investigated.

2 EQUIPMENT AND THE COURSE OF EXPERIMENT

Except the investigation of wear of needle the influence of cooling was observed. The arranging of experiment is presented in the Table 1.

Table 1 Design of experiments

surface finish (marking)	cooling	L/R
Chrome (Cr)	C	L
	C	R
Chrome (Cr)	noC	L
	noC	R
titanium nitride (Ti)	C	L
	C	R
titanium nitride (Ti)	noC	L
	noC	R

Notice: C – with cooling, noC – without cooling, L – needle on left side, R - needle on right side

At each combination three needles were measured, together 24 needles was evaluated. The sewn length was always 74 cm, then the bonded material was exchanged and new layers were connected. The wear of surface was evaluated after 8, 16 and 24 hours of operations.

Following equipments for experiments were used:

- 1) needles
 - needle with chrome surface finish, with fineness, needle tip type R (Figure 1),
 - needle with titanium nitride surface finish, with the same other parameters (Figure 1),
- 2) lockstitch flat bed sewing machine with installed cooling equipment for cooling of needle. Cooling is realized by means of airflow.
- 3) stitch – double lock stitch,
- 4) threads – polyester sewing threads (100 % PET, 148 tex),
- 5) material – fur and foam (thickness of foam 6 mm).

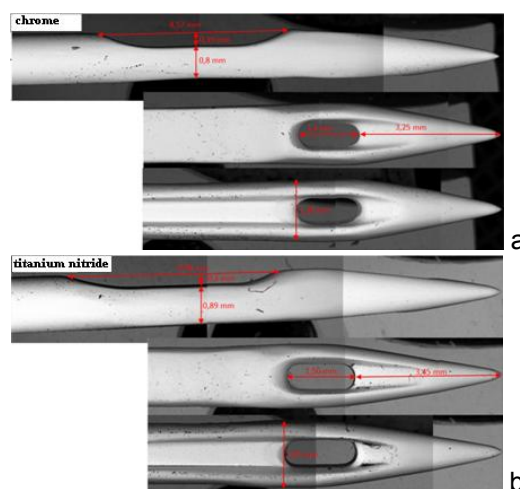


Figure 1 Dimensions of the needle with chrome finish (a) and titanium nitride finish (b)

Cooling of the needle's eye (Figure 2) was installed on the machine and it was realized by a stream of air guided from the compressor tube which at the needle eye results in a shaped tube, towards the needles eye.

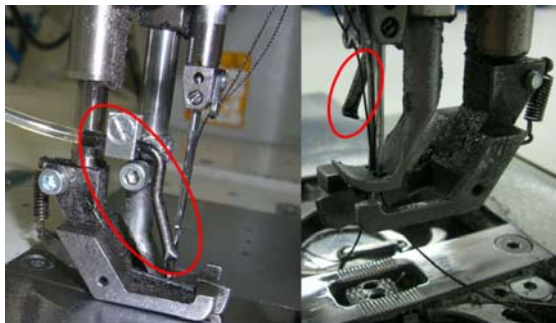


Figure 2 Cooling of needle

2.1 Needle Surface Wear Evaluation

At the same combinations three replications were realized for all time period. The degree of surface wear was determined subjectively by analyzing images from a scanning electron microscope. To analyze the extent of mechanical wear the grid was used. The grid was always placed in a central point, which was defined as the center of the eye of a needle (Figure 3). Placing a grid to a central point leads to prevention of its accidentally laying on the photo, and thus distortion in the subsequent analysis. The degree of wear was determined by number of squares in which the wear was observed.

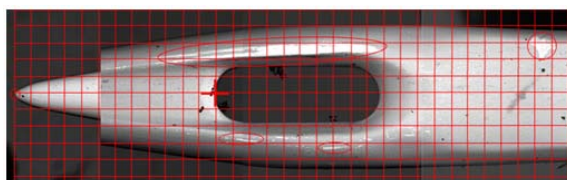


Figure 3 The grid placing and subjective evaluation of damage

To determine the repeatability and reproducibility measurement system analysis was used. This method can apply not only for evaluation of the repeatability and reproducibility but as well as for evaluation of the influence of the operators. Verification was realized by means of 2 evaluators who evaluated 10 needles two times. The low variation of measurements on the single needles realized by the single operators exists what indicates good repeatability. Also low variability between operators exists what indicates good reproducibility. The greatest

variability is represented by the values measured among samples. It shows different level of the wear of the single needles but it has no meaning for evaluation of the repeatability and reproducibility in this case. The analysis showed that subjective determination of the wear of the needle using a grid is repeatable and reproducible.

2.2 Analysis of the needle wear

The size of the wear of needle surface was measured after 8, 16 and 24 hours of work. The analysis of variance (ANOVA) and software MINITAB 16 were used for analysis. The level of the significance α is 0.05. The influence of side of placement of needles in the needle bar (side – L: left side, R: right side), surface finish (surface finish – Cr: Chrome finish, Ti: Titanium Nitride) and cooling (C: with cooling. noC: without cooling) was investigated during time period 24 hours.

Results are shown on Figure 4. Results on Figure show the course of needle wear after 8, 16 and 24 hours of the work. It is worth noting in particular the difference in the wear of needles placed on right (R) and left sides (L) where the wear of needles placed on right increased slowly in comparison with needles placed on the left sides where the wear increased mostly sharply.

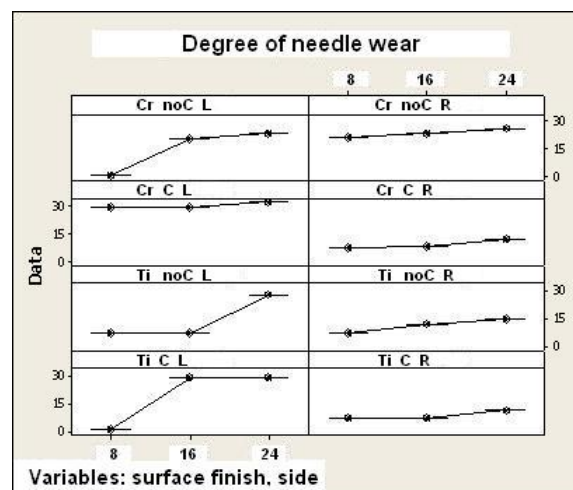


Figure 4 The degree of the wear of needles after 8, 16 and 24 hours (axis y – number of squares with visible surface wear)

Results flowing from ANOVA show that neither factor surface finish nor side of placement of needles have the statistically significant influence on the wear of needles after 8 hours of operations. Although results indicate that needles coated by titanium nitride have rather lower degree of surface wear that needles with chrome

finish the difference is not significant. Also the influence of cooling was not generally confirmed. The same conclusion is valid for surface wear of needles after 16 hours of work. Here also results show that neither factor surface finish nor side of placement of needles in the needle bar has the statistically significant influence on the wear. On Figure 4 is shown noticeable increase in the wear of the needle placed on the left side and the lower degree of wear of needles without cooling compared with cooling. But results are not statistically significant.

Results of experiment after 24 hours of operations show that as side of store as surface finish has minimal influence on difference in surface wear of needles after 24 hours of operations. Although areas of surface wear at the most left needles are more than one half greater than the right needles it is not valid generally. It is possible to see at the factor Surface finish the similar size of damage at all type of experiments except the needle with chrome surface finish without cooling where it is much less. At factor Side it is evident that degree of the wear at needles placed on the left side is higher than at needles placed on the right side except the needle with chrome surface finish without cooling.

3 CONCLUSION

The influence of the surface finish using chrome and titanium nitride, placement of needles in the needle bar and cooling on the wear of sewing needle surface was investigated during time period 24 hours of work. The analysis of results after 8 hours of work indicated less wear of needle coated by titanium nitride but the result are not statistically significant at level of

significance $\alpha=0.05$. No influence of cooling or the placement of needles in needle bar was detected. The wear of needles after 16 hours leads to the very similar conclusion. The difference in wear in the placement of needles in needle bar increases but again the result is not statistically significant. The higher degree of wear has the needles placed on the left side.

The analysis of surface damages of sewing needles after 24 hours of work leads to conclusion that the side of placement of needles (left or right) is the biggest problem on double lockstitch sewing machines, more than surface finish of needles. The results show that the damage surface of the left needle is considerably larger than at the right, which may be caused by the different direction of rotation of the loopers. Neither the cooling effect nor the influence of surface finish has the influence on the changes of size of surface wear.

4 REFERENCES

1. Li Q., Liasi E., Zuo H., Du R.: A study on the needle heating in heavy industrial sewing: Part 2: analytical models, *International Journal of Clothing Science and Technology* Vol. 13 (2), 2001, pp 87-105
2. Liasi L., Du R., Simon D.: An experimental study of needle heating in sewing heavy materials using infrared radiometry, *International Journal of Clothing Science and Technology* Vol. 11 (5), 1999, pp 300-314
3. First Rogale S., Bobovcan-Marcelic M., Rogale D., Dragcevic Z., Nikolic G.: Garment seam strength depending on needle size and stitch length. *Annals & Proceedings of DAAAM International 2012*, Vol. 23 (1), 2012, pp 875-878

VLIV DÉLKY PRACOVNÍHO ZATÍŽENÍ NA POŠKOZENÍ POVRCHU ŠICÍ JEHLY

Předložený příspěvek se zabývá opotřebením šicích jehel při šití automobilových sedaček. Způsob seřízení šicího stroje výrazně ovlivňuje opotřebení šicí jehly, které se následně projevuje na poškození šicí nitě. Poškozená šicí nit' snižuje jednak kvalitu vzhledu v místě šití, jednak trvanlivost spoje. Předmětem zkoumání bylo sledování vlivu povrchové úpravy jehel (úpravy nitridu titanu a chromová úprava) a chlazení na životnost šicích jehel. Test byl uskutečněn na dvojehlovém stroji šijícím vázaným stehem.

Po 8, 16 a 24 hodinách provozu bylo zjišťováno, zda došlo k mechanickému poškození jehly a jak veliké bylo. Míra poškození byla určována subjektivně analýzou fotografie z rastrovacího elektronového mikroskopu. Pro analýzu míry mechanického poškození byla použita mřížka. Výsledky ukázaly, že ani chlazení ani typ úpravy z dlouhodobého hlediska (po 24 hodinách) nemají vliv na snížení opotřebení jehel.

BIOPOTENTIAL SENSING WITH ELECTROCONDUCTIVE FABRICS

Ludmila Balogová¹, Branko Babušiak² and Michal Gála²

¹VÚTCH-CHEMITEX, spol. s r.o., Rybníky 954, 011 68 Žilina, Slovak Republic

² Department of Theoretical Electrical Engineering and Biomedical Engineering,
Faculty of Electrical Engineering, University of Žilina, Slovak Republic
balogova@vutch.sk, branko.babusiak@fel.uniza.sk, michal.gala@fel.uniza.sk

Abstract: On-going and continuously progressing multidisciplinary research in the field of textile fibres, special yarns, biomedical textile sensors, wireless and mobile communication, relating to telemedicine, is directed mainly to development of progressive smart biomedical clothing today. Mobile monitoring of human physiological functions using smart clothing enables to sense, record, process and transmit the measured biological signals such as muscle activity (breathing), heart activity (ECG), activity of neural system (EEG), body temperature and other impulses.

The paper focuses on application of special electroconductive textiles - knitted fabrics, from which textile sensors and active capacitive electrodes designed for monitoring and sensing of human physiological signals (ECG) were prepared. Results of measurement of human electrocardiosignal using active capacitive electrodes without direct contact with human skin will be presented as well.

Keywords: electroconductive fibres, electroconductive blended yarns, textile sensors, biopotentials, electrocardiosignal

1 INTRODUCTION

This contribution focuses on evaluation of performance of the electroconductive textiles incorporated into construction of active capacitive ECG electrodes used to sense human ECG biopotential in real time. A goal of the contribution is to present results of research focused on possibilities of heart frequency (ECG) monitoring based on application of active capacitive electrode, sensing part of which is an electroconductive fabric. Performance of model samples of the developed active capacitive electrodes has been evaluated by control measurement on a real subject. This is an efficient and modern solution for smart clothing in a form of textile interface allowing integration of the sensors, power and communication components as well as collecting data units to create a comprehensive system for monitoring of human physiological functions.

2 EXPERIMENTAL

2.1 Materials

Electroconductive fabrics

Functional component of the electro-conductive fabrics are electroconductive fibres, electrical conductivity of which differs in dependence on their material composition. High-quality silver-coated multifilament electroconductive polyamide textile filament was used for preparation of the electroconductive blended yarns.

Electroconductive yarns based on a blend of electroconductive fibre and standard non-conductive fibres were prepared on DirecTwist 2B multifunctional twisting device using twisting technology. Bi-component electroconductive blended yarns have been prepared in the frame of our experimental works using method of simple twisting as well as „Cabling“ and „Diamant“ double twisting with different number of conductive fibres in their construction. The best electroconductive properties of the tested yarns showed Diamant type yarn, incorporating 10 conductive fibres in the construction, whose electrical resistance was on a level of 129 Ω /m of the yarn [6]. This yarn was selected for further experimental works on the base of the achieved electrical resistance. The electroconductive yarn was successfully incorporated into construction of a plain tubular jersey fabric prepared on circular knitting machine. The final knitted electroconductive fabric showed homogeneous properties, it was without any non-uniform places or parts.

Electroconductive textile sensors

Squares with dimensions of 5 x 5 cm were cut from the prepared knitted fabric for the purpose of preparation of textile sensors in the frame of the experimental works. They were overedged with a conductive sewing thread. Performance of the developed sensors was evaluated by measurement of electric resistance in quiescent condition. Basic criterium was achievement of as low length electric resistance as possible (<1 Ω)

in each direction on an area of 3x3 cm. Electrical resistance of the prepared textile sensors was achieved on a level of about 0.57 Ω in each direction of the area of 3 x 3 cm. Textile sensor prepared this way was used in the construction of active capacitive textile electrodes.

2.2 Preparation of active capacitive electrode and its application in the clothing

Textile electrodes designed for monitoring of health state were designed so that they were as small as possible and minimally influenced by disturbing impacts caused e.g. by movement. Design of the active capacitive electrode was proposed and inspired. It consists of four layers. The first layer is conductive textile sensor which is a sensitive part of the electrode and ensures sensing and transfer of the signal to collecting unit. The second layer is non-conductive fabric performing as insulation. Microelectronics creating the third layer of the electrode is placed in the middle of the layered structure. All electronic components are placed on a flexible board enabling simple incorporation of microelectronics into the active electrode. The active electrode includes low-noise operational amplifier in connection of a voltage tracker. Function of such a connection is to transform high input impedance between electrode surface and skin to low output impedance. The active electrode consists of printed circuit board (PCB) with operational amplifier and textile layer. Connection of the active sensing face to the amplifier input is realized by an electroconductive yarn. The fourth layer is again non-conductive one operating as an insulation protecting the electrode against disturbing impacts.



Figure 1 Position of the active textile electrodes on the first prototype of smart T-shirt

Two active capacitive ECG electrodes were used to prepare the first prototype of so-called „smart clothing“. The electrodes were sewn on back side of back part of a cotton T-shirt, encircling chest of

a monitored person. Therefore the electrodes are in direct contact with human skin without impairing wearing comfort of the clothing. The electrodes were placed about 7 cm under shoulder-bone of the monitored person in distance of about 7 cm from each other (Figure 1). The capacitive electrode was connected to the data collection unit by means of copper wires. Communication between the monitored person and monitoring station ensures USB interface transmitting the sensed data in real time to a computer.

2.3 Methodology

Electrical manifestations in organism are based on electrical properties of muscular and neural tissue. Principle of electrocardiography (ECG) is sensing electrical activity of the heart in electrocardiogram pattern (record of time change of electrical potential, caused by heart activity, in a form of ECG curves). The active electrodes act as sensors, detecting electric signals generated by heart tissue [2]. The electrocardiogram was taken using conductive textile electrodes. The measured data were transferred in real time to the central unit where their analysis was performed.

3 RESULTS AND DISCUSSION

Performance of the active capacitive electrodes was evaluated by several check measurements using patient simulator as well as by ECG measurement of a real person. The measurements were carried out in sitting position of the monitored person (Figures 4 and 5).

ECG signal of the real person was considerably impaired by network noise as it can be seen in Figure 5.

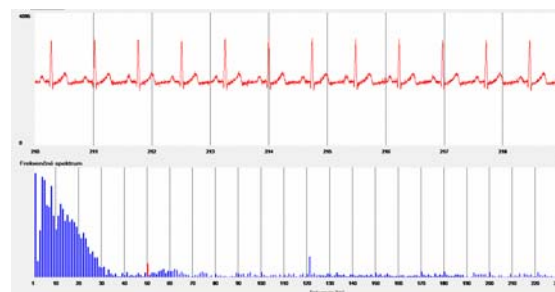


Figure 4 Signal (upper graph, x-axis - time in seconds, y-axis - amplitude in quantization levels) measured by connecting patient simulator to the active textile electrodes including frequency spectrum (bottom graph, x-axis - frequency in Hertz, y-axis - amplitude without dimension)

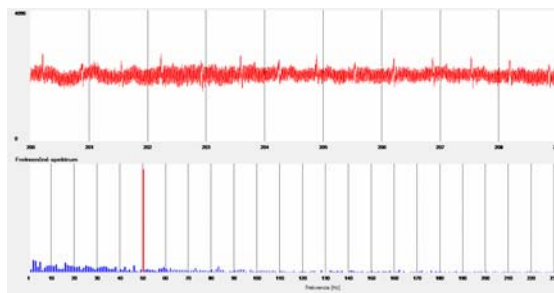


Figure 5 Signal (upper graph, x-axis - time in seconds, y-axis - amplitude in quantization levels) of a real person measured using the active textile electrodes including frequency spectrum (bottom graph, x-axis - frequency in Hertz, y-axis - amplitude without dimension) where considerable network noise (red spectral line) can be seen

Software filter, i.e. band-elimination filter for 50 Hz frequency, will have to be used to eliminate this unacceptable artefact in the future. It is possible to state on the base of the above-mentioned results that the developed textile sensor and active capacitive electrode are able to detect ECG signal and the proposed clothing system creates this way a functional gel-free system for measurement of human ECG signal on dry interface.

4 CONCLUSION

Biopotential sensing with active capacitive electrodes prepared from electroconductive fabrics is a progressive solution of ECG measurement without direct contact with the human skin. Method of contact-free measurement of human ECG signal is an alternative to common methods with Ag/AgCl electrodes, fastened to the body in wet state using gel.

An argument for the claim are results given in this contribution showing that the developed active

capacitive electrodes prepared from electroconductive fabrics are fully functional and sufficiently sensitive to sense human ECG signal. As the sensed signals are impaired by network noise, it will be necessary to eliminate this noise using software filter on signal processing in the next step. Therefore, elimination of the network noise is a task which will be solved in the future so that the imaging software could be used online. Results of the measurement are very encouraging and they became a starting point for further research and experimental works. Our further works will focus on improvement of construction and parameters of the active electrodes as well as optimization of signal transfer. It will be possible to use the developed textile electrodes in smart clothing designed for short-term as well as long-term monitoring of human ECG signal as soon as the problems and noises arising mainly due to movement will be resolved.

5 REFERENCES

1. Yong Gyu Lim; Gih Sung Chung; Kwang-Suk Park: Capacitive driven-right-leg grounding in Indirect-contact ECG measurement, Engineering in Medicine and Biology Society (EMBC), 2010 Annual International Conference of the IEEE, Aug. 31 - Sept. 4, 2010, pp. 1250-1253
2. Baum, O. V.; Voloshin V. I.; Popov, L. A.: Biophysical models of the heart electrical activity, Biofizika 51(6), pp. 1069-1086

Acknowledgement: This contribution was worked out in the frame of solution of the project „Research of technologies and products for smart and technical textiles (VY-INTECH-TEX)“, ITMS code: 26220220134, with financial support of the European Regional Development Fund (ERDF) and Ministry of Education, Science, Research and Sport of the Slovak Republic on the base of contract No. 137/2010/2.2/OPVaV.

SNÍMANIE BIOPOTENCIÁLOV POMOCOU ELEKTRICKY VODIVÝCH TEXTÍLIÍ

Pokračujúci a neustále napredujúci multidisciplinárny výskum v oblasti textilných vlákien, špeciálnych priadzi, elektricky vodivých textílií, biomedicínskych textilných senzorov, bezdrôtovej a mobilnej komunikácie, spojenej s telemedicínou, dnes smeruje najmä k vývoju progresívnych inteligentných biomedicínskych odevov. Mobilné monitorovanie fyziologických funkcií človeka pomocou inteligentných odevov umožňuje snímať, zaznamenávať, spracovávať a prenášať namerané biologické signály, ako sú napr. aktivita svalstva (dýchanie), aktivita srdca (EKG), aktivita nervového systému (EEG), telesná teplota a ďalšie impulzy.

Príspevok je zameraný na využitie elektricky vodivých textílií - pletenín, z ktorých boli pripravené textilné senzory a aktívne, kapacitne viazané elektródy určené na monitorovanie a snímanie fyziologických signálov človeka (EKG). Prezentované budú aj výsledky merania elektrokardiografického signálu človeka pomocou aktívnych, kapacitne viazaných elektród bez priameho kontaktu s pokožkou človeka.

CLASSIFICATION OF THERMOREGULATORY PROPERTIES OF OUTDOOR CLOTHING IN STANDARDS AND TECHNICAL REPORTS

Petr Benesovsky and Hana Polaskova

*Textile Testing Institute, Vaclavska 6, 658 41 Brno, Czech Republic
benesovsky@tzu.cz*

Abstract: *Thermoregulatory properties of textile materials for outdoor clothing strongly affect comfort of the user. Different atmospheric conditions and different physical load during different activities require different combination of levels of thermal insulation, water vapor transmission, water penetration, resistance and repellence or liquid sweat management for every layer of clothing.*

This article reviews international standards and technical reports, containing requirements for and classification of thermoregulatory properties of textile materials for outdoor clothing. The most important of those documents is Technical Report CEN/TR 16422. It tends to become one of the main guides for simple classification of properties of different layers of outdoor clothing in different outer conditions, based on results of tests, carried on according to the methods, described in other referenced international standards.

Keywords: *textile, thermoregulatory properties, outdoor, standardization.*

1 INTRODUCTION

Recently, many new materials and textile structures were developed for use in garments for different outdoor activities. In order to evaluate their "comfort" properties, many technical standards were worked out. Paper summarizes most important standards for evaluation and testing of thermoregulatory properties of outdoor textiles.

1.1 CEN/TR 16 422 [1] Classification of thermoregulatory properties

CEN/TR 16 422 [1] is the first attempt to categorize thermoregulatory properties of textiles, used for manufacturing outdoor garments, according to their intended use (ambient temperature, positioning of textile in contact with skin/in intermediate layer, in upper layer etc.).

It offers system of three performance levels, based on results of tests, carried on according to several well established standards (Table 1). It also contains annexes A and B with another test method, utilizing Skin Model plate, described in EN 31092.

TR then specifies three performance classes A-C (A means very good, C is acceptable) and in seven tables assigns those classes to specific performance levels. Six tables represent values for combination of clothing layer (skin contact, intermediate layer, outer layer) and ambient climate (cold, warm), whereas seventh one

includes classification of outer multilayer material for very cold conditions. For example see Table 2. Report recommends labeling or marking the product by abovementioned classification using simple tables, containing parameter and it's class. From the point of view of accredited textile laboratory it can be stated, that standards listed in Table 1 are "alive" and manufacturers and dealers of flat textiles and garments use them for proving quality of their products (for example within the framework of tenders). As for the classes, unfortunately there is no practical use seen on the market.

2 TESTS INVOLVING MANIKINS

Most standardized testing methods are used for assessment of single or multilayer material itself. However, thermoregulatory properties depend also on design and fit of garments. Different intensity of contact with skin can strongly affect heat or moisture transport. For assessment of real performance of product, tests involving manikins should be used. Among others, this type of tests are described in EN 13 537 *Requirements for sleeping bags* [2], EN ISO 15 831 *Clothing - Physiological effects - Measurement of thermal insulation by means of a thermal manikin* [3], ASTM F1291-10 *Standard Test Method for Measuring the Thermal Insulation of Clothing Using a Heated Manikin* [4] or ASTM F2380-10 *Standard Test Method for Measuring the*

Evaporative Resistance of Clothing Using a Sweating Manikin [5].

All those standards specify human body manikins of different height (adult, child) divided into several zones with independent heating and sensors. Some methods request lying manikin (in sleeping bag), some want them standing still or even “walking” – see Figure 1. Development of manikin able to fulfill the requirements of standards isn't easy, but used physical models simulate real use of outdoor garments more precisely than tests listed in Table 2.



Figure 1 Manikin according to EN ISO 15 831 [3] (left), manikin according to EN 13 537 [2]

Table 1 List of testing standards, named in TR 16422 [1] as methods for testing

Area of testing	Name of the standard	Quantity, unit
Thermal insulation	ISO 5085-1 Textiles – Determination of thermal resistance – Part 1: Low thermal resistance	Thermal resistance [$m^2.K/W$]
	EN 31 092 Textiles – Determination of physiological effects – Measurement of thermal and water-vapour resistance under steady-state conditions (sweating guarded-hotplate test)	Thermal resistance [$m^2.K/W$]
Water vapour transmission	EN 31 092 Textiles – Determination of physiological effects – Measurement of thermal and water-vapour resistance under steady-state conditions (sweating guarded-hotplate test)	Water vapour permeability index [-] Water vapour resistance [$m^2.Pa/W$]
	EN ISO 9237 Textiles – Determination of permeability of fabrics to air	Air permeability [mm/s]
Water penetration resistance and repellence	EN 20 811 Textiles – Determination of resistance to water penetration – hydrostatic pressure test	Water column [cm of H_2O or Pa]
	EN 29 865 Textiles – Determination of water repellency of fabrics by the Bundesmann rain-shower test	Water repellence [grade]
	EN 24 920* Textiles – Determination of resistance to surface wetting (spray test) on fabric	Spray rating [-]
Liquid sweat management	AATCC TM 195 Liquid moisture management properties of textile fabrics	Index OMMC [-]
	Annex A and B of CEN/TR 16 422 (BPI 1.2.1. Hohenstein method)	Liquid sweat transport $g/m^2.h$ Liquid sweat buffering index [-]

* - no longer valid, replaced by EN ISO 4920

Table 2 Classification of performance for intermediate layer materials for cold climate

Property	Unit	A	B	C
Thermal insulation	$m^2.K/W$	≥ 0.09	0.06-0.09	0.04-0.06
Water vapour permeability index	Index 0-1	≥ 0.55	0.45-0.55	0.35-0.45
Water vapour resist.	$m^2.Pa/W$	≤ 5	5-6	6-7
Air permeability	mm/s	> 100	5-100	≤ 5
Liquid moisture management	Index OMMC	≥ 3	2-3	≤ 2

Table 3 Summary of requirements for thermoregulatory properties of protective clothing according to EN 14058 [8]

parameter	Class 1	Class 2	Class 3
Thermal insulation R_{ct} [$m^2.K/W$] EN 31092 or ISO 5085-1	0.06 - 0.12	0.12 - 0.18	0.1 - 0.25
Air permeability AP [mm/s] EN ISO 9237	< 100	5 - 100	≤ 5
Water column W_p [Pa] EN 20811 (optional)	8000 - 13000	> 13000	Not defined
Water vapour resistance R_{ef} [$m^2.Pa/W$] EN 31092	< 55 (for complete set of clothing)		
Resultant effective thermal insulation I_{cler} [$m^2.K/W$] EN ISO 15 831 [3] (optional)	> 0.170		

3 THERMOREGULATORY PROPERTIES FOR PROTECTIVE CLOTHING

Another group of standards containing requirements for thermoregulatory properties are standards dealing with protective clothing (personal protective equipment). The most important of them are EN 342 *Protective clothing - Ensembles and garments for protection against cold* [6], EN 343 *Protective clothing - Protection against rain* [7] and EN 14058 *Protective clothing - Garments for protection against cool environments* [8]. As seen in Table 3 (EN 342 and EN 343 contain requirements for the same properties), they utilize the same testing standards and parameters as CEN/TR 16422 [1] and they divide protective clothing into three categories, too. Moreover, they include parameters measured by means of tests on mannequins. All three standards are harmonized, so they are mandatory for protective garments producers.

4 CONCLUSION

Standards for testing and classification of thermoregulatory properties of outdoor garment textiles represent live praxis used by producers

and salesman and are subject to further development and changes. R&D staff should have good awareness of those standards in order to be able of effective communication with future producers, marketers and end users.

5 REFERENCES

1. CEN/TR 16 422. Classification of thermoregulatory properties, Brussels: CEN, 2012
2. EN 13 537 Requirements for sleeping bags, Brussels: CEN, 2012
3. EN ISO 15 831 Clothing - Physiological effects - Measurement of thermal insulation by means of a thermal manikin, Brussels: CEN, 2012
4. ASTM F1291-10. Standard Test Method for Measuring the Thermal Insulation of Clothing Using a Heated Manikin, Philadelphia: ASTM, 2010
5. ASTM F2380-10. Standard Test Method for Measuring the Evaporative Resistance of Clothing Using a Sweating Manikin, Philadelphia: ASTM, 2010
6. EN 342 Protective clothing - Ensembles and garments for protection against cold, Brussels: CEN, 2004
7. EN 343 Protective clothing - Protection against rain, Brussels: CEN, 2007
8. EN 14058 Protective clothing - Garments for protection against cool environments, Brussels: CEN, 2004

KLASIFIKACE TERMOREGULAČNÍCH VLASTNOSTÍ TEXTILU PRO OUTDOOROVÉ ODĚVY V NORMÁCH A TECHNICKÝCH ZPRÁVÁCH

Termoregulační vlastnosti textilií pro outdoorové oděvy mají zásadní vliv na pohodlí uživatele. Rozdílné okolní podmínky a fyzická zátěž při různých aktivitách vyžadují rozdílné kombinace tepelné izolace, prostupnosti vodních par a vody, nepromokavosti aj u každé vrstvy oblečení.

Článek je přehledem měřicích a požadavkových mezinárodních technických norem a technických zpráv v oblasti termoregulačních vlastností textilií pro outdoorové oděvy. Nejzásadnějším z diskutovaných dokumentů je CEN/TR 16422, technická zpráva, která je návodem pro jednoduchou klasifikaci termoregulačních parametrů různých vrstev outdoorového oblečení v různých klimatických podmínkách. Tato klasifikace je založena na hodnotách parametrů, získaných zkouškami dle dalších zavedených technických norem.

THE INFLUENCE OF THE SELECTED PARAMETRES ON THE INITIATION OF HYDROGEN EMBRITTLEMENT

J. Bezecný, R. Vavřík and A. Dubec

Alexander Dubcek University of Trencin, Faculty of Industrial Technologies, Department of Materials Engineering, I. Krasku 491/30, 020 01 Púchov, SK
jan.bezecny@fpt.tnuni.sk

Abstract: The paper deals with the influence of selected parameters of pickling on the hydrogen embrittlement formation in relation to the high strength steels. In this work, effects of two different acids, different temperatures and different time intervals of pickling were observed in relation to formation of hydrogen embrittlement for the high strength steels. Samples were evaluated by using a wedge test after the application of the mentioned parameters in order to prove the formation of hydrogen embrittlement. Then, some of the selected samples were subjected to pickling process and some of the selected samples were not affected by pickling process in order to make desired mutual comparison and subsequently all of the samples (with and without pickling process) were subjected to tensile tests. After the given tensile tests, the samples were evaluated with help of the fractographic and metallographic method.

Keywords: screws, high strength steel, pickling, acid, hydrogen embrittlement.

1 INTRODUCTION

Hydrogen embrittlement is a phenomenon which occurs in metals due to the action of hydrogen. This phenomenon is most frequently observed in materials having tensile strength higher than 1200 MPa, as well as in materials with a much lower yield strength (550 MPa) [1]. Hydrogen is formed during the surface treatments such as pickling and electroplating. It is important to know which one has a decisive influence for formation of hydrogen embrittlement, because these two operations usually follow each other. Atomic hydrogen generated during these surface treatments subsequently diffuses into the material and it is able to recombine to his molecular form with formation of high internal stresses. The greatest danger of hydrogen embrittlement consists in the fact that it cannot be identified by conventional tests before the introduction of components into practice. Destruction only a small hydrogen charging part can lead to an accident of the whole device including great damages and threat to life. Formation of hydrogen embrittlement is significantly influenced

by the amount of hydrogen diffused into the metal, material strength, the presence of technological notches and size of the external load. A typical manifestation of hydrogen embrittlement is the formation of delayed fracture, which often occurs at low load, often under the value of yield strength of the material. The resulting fracture surface is usually intergranular, with signs of hydrogen interaction. These signs are the hairlines (called "crow legs") and voids in the form of "tunnels" caused by the high pressures effects of hydrogen molecular recombination [2].

2 EXPERIMENTAL MATERIAL

The material used in the experimental part are normally produced screws M16x60 with strength class 12.9 and 10.9 and screws M10x85 with strength class F 130 V. M16x60 screws are made of steel 1.7225 - 42CrMo4. It is a low alloyed stainless chromium - molybdenum steel. M10x85 screws are made of steel 14 140 (equivalent steels are 37Cr4 DIN, ISO 37Cr4).

Table 1 Chemical composition of steel 42CrMo4 and 37Cr4 [3, 4]

	C	Si max.	Mn	P max.	S max.	Cr	Mo
42CrMo4	0.38-0.45	0.40	0.60-0.90	0.025	0.035	0.90-1.20	0.15-0.30
37Cr4	0.37	0.25	0.70	-	0.035	1.05	-

2.1 Hydrogen charging of samples

Hydrogen charging of the samples was carried out by acid pickling. Acids 10% H₂SO₄ and 15% HCl were chosen as pickling baths with respect to the literature data and practical experience. Acid pickling was carried out at room temperature of 20°C and at an elevated temperature of 60°C. For the acids were made weight loss measurements of screws in relation to pickling time in order to determine how the acids react with the surface of the screws at room temperature of 20°C and at an elevated temperature of 60°C. Graph for screws M16x60 10.9 is presented for illustration.

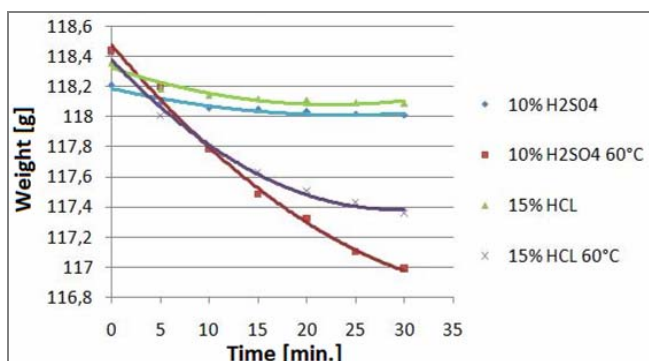


Figure 1 Weight loss in relation to time for M16x60 10.9

Weight loss in relation to time was minimal for both acids and for all types of screws at room temperature. Mentioned weight loss significantly increased by using of elevated temperature. Amount of hydrogen generated on the surface of the screws were inspected visually. Significant increase was observed at temperature of 60°C but at room temperature was comparable for both acids.

2.2 The procedure for the evaluation of hydrogen embrittlement

Screws were evaluated after pickling using international standard wedge test ISO / DIS 10587 [5]. This test is used for the evaluation of embrittlement and degradation of joining components from steel with a tensile strength greater than 1000 MPa. The test apparatus consists of two steel plates but one plate is chamfered at an angle of 6°. Test procedure involves the insertion of investigational screws into the test apparatus in abutting position of bolt heads on the chamfered surface of the plate. The screws are subsequently tightened at 75% of the tensile strength. The duration of the test is at least 48 hours. The screws are visually inspected during this time period at the same time intervals

due to formation of cracks. The maximum length of the test is 200 hours [4]. The evaluation was carried out always at 5 pickled screws (for each tightening torque). Tightening torques were chosen:

- 75% of the maximum tensile strength according to ISO / DIS 10587,
- 100% of the maximum tensile strength,
- according to DIN 898/1 (tightening torque for each steel grade).

Loaded screws were pickled in 10% H₂SO₄ at elevated temperatures of 60°C for 30 minutes after the calculation of required torques for individual types of screws. Used torques represented a force corresponding to 75% of tensile strength. Rounding radius under head of screws was consistent with the rule. Loaded screws did not exhibit signs of hydrogen embrittlement for 200 hours because all screws are resistant to crack formation. The test was repeated using a tightening torque corresponding to the force of 100% of strength. Screws were loaded by torque according to DIN 898/1. But neither using these conditions has not resulted hydrogen embrittlement. Subsequently worse conditions were chosen to induce hydrogen and therefore the rounding radius under the head of screws was modified to 0.215 mm. Even these conditions do not lead to the formation of hydrogen embrittlement for all loaded screws. Based on the results obtained from the wedge test we can conclude that pickling in 10% H₂SO₄ does not cause hydrogen charging at the critical level.

3 RESULTS AND DISCUSSION

3.1 Tensile test

Tensile tests were carried out at Zwick 1488 tensile machine in order to investigate the effect of hydrogen on the change of mechanical properties of screws. For each type of screws was created separate set of tensile samples. Each set contained four samples - two samples without hydrogen charging and two samples after hydrogen charging by pickling in 10% H₂SO₄ at elevated temperature of 60°C. Pickling time was 30 minutes. The measured values are shown in Table 2. Based on the values obtained by the tensile test can be concluded that a significant change in mechanical properties, between samples exposed to pickling and samples that were not exposed to pickling, was not observed. But a slight decrease of strength R_m and yield

strength $R_{p0.2}$ was observed in all cases in relation to hydrogen charging samples.

3.2 Fractographic analysis of fracture surfaces after tensile test

Obtained fracture surfaces were subjected to fractographic analysis after the tensile tests. This analysis consisted of macroscopic and microscopic evaluation of generated fracture surfaces after tensile test.

3.2.1 Macroscopic evaluation

Based on macroscopic evaluation of hydrogen charging samples and samples without hydrogen charging we can conclude that for all samples was observed ductile cup fracture. Macroscopic deformation is highest for samples 10.9 and smallest for samples 14.9, which corresponds to the tensile strength values of screws. Significant differences between condition without hydrogen charging and hydrogen charging condition were not found. Simultaneously the milled shape of fracture was observed in all of the samples, which is documented in Figures 2 and 4. Metallographic evaluation showed that the observed milled shape of fracture is unrelated with hydrogen but is related to the heterogeneity of the microstructure.

3.2.2 Microscopic evaluation

Microscopic observation of fracture surfaces of hydrogen charging samples and samples without hydrogen charging was performed using a JEOL JSM 7600 SEM and was focused on the

assessment of the fracture micro mechanism changes of individual samples.

Fracture micromorphology of hydrogen charging samples and samples without hydrogen charging of type M16x60 10.9 is composed almost exclusively by transgranular ductile fracture with dimpled morphology (TDD) on the central regions, as well as on the sides of milled shape of fracture. Dimples are bigger and deeper around larger inclusions in hydrogen charging samples than samples without hydrogen charging, Figures 3 and 5. Only the surface of the inner walls of dimples in relation to pickled samples has the special microrelief reminding the hairlines, Figure 6. Both of these manifestations could be assigned to the action of hydrogen. But embrittlement of the material is not caused by the hydrogen - typical intergranular cleavage or transgranular quasi-cleavage facets were not observed. Similar findings were demonstrated for screws with higher strength values. Samples M10x85 F 130 V contained a specific microrelief reminding hairlines, Figure 7. The results of fractographic analysis showed that the material of all samples was suitably heat treated. The dominant fracture micro mechanism is TDD fracture. Observed milled shape fracture is not related to negative effects of hydrogen from pickling, but with the initial heterogeneity (streakiness) of microstructure. Pickling of samples has not resulted to the embrittlement of the material, or only with a minimal extent.

Table 2 Measured mechanical values of tensile test

No. m.	Designation	Material	Environment	$R_{p0.2}$ [Nmm ⁻²]	Average	R_m [Nmm ⁻²]	Average
1	12.9	42CrMo4	-	1226.17	1231.30	1304.61	1311.57
2	12.9	42CrMo4	-	1236.44		1318.54	
3	12.9	42CrMo4	H ₂ SO ₄	1206.12	1213.11	1285.71	1293.89
4	12.9	42CrMo4	H ₂ SO ₄	1220.11		1302.08	
5	10.9	42CrMo4	-	1118.54	1120.33	1183.49	1189.61
6	10.9	42CrMo4	-	1122.12		1195.73	
7	10.9	42CrMo4	H ₂ SO ₄	1112.19	1115.87	1178.04	1183.67
8	10.9	42CrMo4	H ₂ SO ₄	1119.55		1189.31	
9	F 130 V	37Cr4	1	1366.84	1326.85	1407.2	1396.98
10	F 130 V	37Cr4	2	1286.87		1386.77	
11	F 130 V	37Cr4	H ₂ SO ₄	1275.91	1266.34	1390.47	1375.42
12	F 130 V	37Cr4	H ₂ SO ₄	1256.77		1360.38	

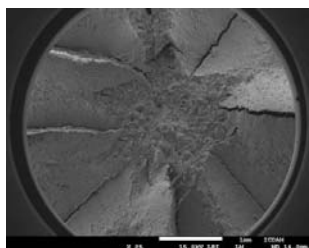


Figure 2: Milled shape of fracture

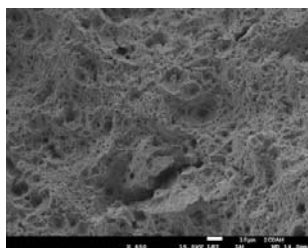


Figure 3: Central region - TDD fracture

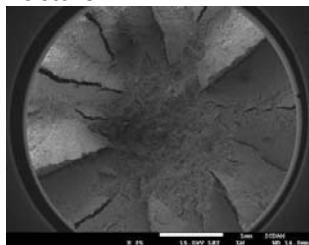


Figure 4: Milled shape of fracture

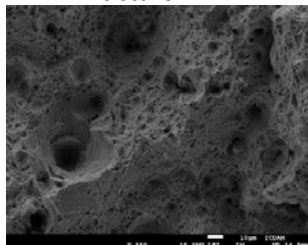


Figure 5: Central region - TDD fracture

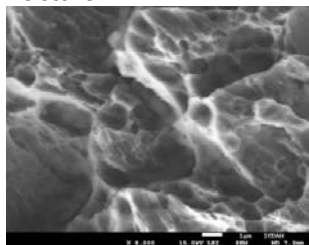


Figure 6: Micro morphology of fracture

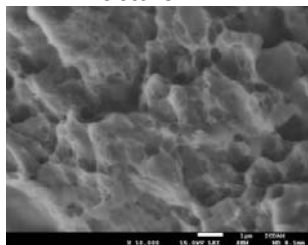


Figure 7: Micro morphology of fracture

4 CONCLUSION

Based on the conducted experiments, we have reached to the following findings:

- 10% H₂SO₄ reacted with the surface of the screws intensively than 15% HCl during pickling process. This reaction associated with the formation of atomic hydrogen, was much more pronounced with the usage of an elevated temperature of 60°C. Evaluation of hydrogen embrittlement using a wedge test did not demonstrate a measurable embrittlement of screws for all analyzed samples which were tightened to the recommended tightening torque. Similarly, reduction of radius under the screw head, in order to increase stress during the

wedge test does not result to the embrittlement of screws.

- Tensile tests conducted on hydrogen charging samples and samples without hydrogen charging did not show a significant change of mechanical properties. Typical characteristics of hydrogen embrittlement formation were not demonstrated by using a fractographic analysis of fracture surfaces. It has been proven that pickling operation is not the primary cause of hydrogen charging in relation to the analyzed types of high strength steels. In the future, investigation could be focused on the influence of electroplating, respectively combination of electroplating and pickling, in the relation to the hydrogen embrittlement formation of these steels.

Acknowledgements: This publication was created in the frame of the project "Centre of excellence for ceramics, glass, and silicate materials" ITMS code 262 20120056, based on the Operational Program Research and Development funded from the ERDF.)

5 REFERENCES

1. Sojka, J.: Odolnost ocelí vůči vodíkové křehkosti, Ostrava: Vysoká škola báňská - Technická Univerzita, 2007, s. 108
2. Bezecný J., Šopíková Z.: Control of Hydrogen Process of Screws after Surface Treatment. In: ACTA METALLURGICA SLOVACA CONFERENCE. Vol.1, No.2 (2010), p.94-98.
3. Firemné materiály Bolzano. Přehled vlastností oceli 42CrMo4, [online]: http://www.bolzano.cz/cz/technicka-prirucka/tycoveoceliuhlikovekonstrukcnialegovane/oceli/kzuslechtovanipodleen100831/prehledvlastnostioceli42crmo4?searched=42CrMo4&advsearch=oneword&highlight=ajaxSearch_highlight+ajaxSearch_highlight1
4. Material specification sheet: *Saarstahl – 37Cr4, 37CrS4*, [online]: http://www.saarstahl.com/fileadmin/saarstahl_extranet/images/04_produkte/walzstahlsorten/english/7034_7038_37Cr4_37CrS4.pdf
5. ISO/DIS 10587 Kovové a iné anorganické povlaky – Skúšky pre zvyškovú krehkosť pre kovové a povlakované skrutky so závitom, spojovacie skrutky a tyče – Metóda šikmého klina

VPLYV VYBRANÝCH PARAMETROV MORENIA NA VZNIK VODÍKOVEJ KREHKOSTI

Článok sa zaoberá vplyvom vybraných parametrov morenia na vznik vodíkovej krehkosti vysokopevných ocelí. V práci bol pozorovaný vplyv dvoch rozdielnych kyselín, rozdielnej teploty a rôzneho času morenia na vznik vodíkovej krehkosti dvoch vysokopevných ocelí. Po aplikácii vyššie uvedených parametrov morenia boli vzorky hodnotené pomocou klinovej skúšky za účelom preukázania vzniku vodíkovej krehkosti. Následne boli vykonané ťahové skúšky na namorených a nenamorených vzorkách, ktoré boli následne vyhodnotené fraktograficky a metalograficky.

COLOR CHANGE MEASUREMENT ON DIGIEYE

P. Gilewicz¹, J. Rutowicz², I. Frydrych¹ and A. Cichocka¹

¹Lodz University of Technology, Institute of Architecture of Textiles, Department of Clothing Technology and Textronics

²Institute of Leather Industry, Research Laboratory of Products, Processes and Environment
800159@edu.p.lodz.pl

Abstract: In the paper there is presented a trial of application of new measurement principle of color change with the use of DigiEye device. The measurements were done for PES fabrics destined on the outer layers of clothing. Samples for the color change were first aged in the Xenotest 150. Ageing process of fabrics was done according to the method of blue scale. Results obtained before and after the ageing test during exposing the examined samples on the light are presented. Results of color change obtained in the color system CIE L*a*b* are discussed.

Keywords: color change, DigiEye, ageing test, method of blue scale.

1 INTRODUCTION

Color measurement seems to be trivial; however, there are many different phenomena, which influence the perception of color. It should be kept in mind that the color is a psychophysical impression caused by light. Electromagnetic radiation falling to the eye is reflected from nontransparent surfaces and dispersed going through the transparent body. The impression of color is a subjective color sense of the observer [1]. The perception of color depends on the observer's experience and his knowledge about the use of the sense of sight. Color determination depends on: the spectral light radiation, the amount of the light energy and the presence of the other colors close to the chosen one [2]. The important event during the color determination is a metamerism phenomenon. Metamerism relies on the different color perception of the same object dependably on the kind of light, by which the object is lighted [3]. Color measurement is affected by the type of light, which is called an illuminant. Illuminant D is an average daylight from different time of the day based on the actual measurement of spectral light with the color temperature 6.504 K marked as the illuminant D65.

All kinds of clothing change the color during their usage. The change of color is affected by many factors such as the properly selected dyeing method, textile ageing process or different chemicals used during the maintenance. Consumers pay an attention to the color quality and uniformity of final products. Therefore, it is important to have a suitable system enabling the

objective color assessment. Measurement of color change of textile is generally performed in a wavelength range of 400 nm to 700 nm, because for the majority of people the range of visible radiation is in the following interval of wave length – $\lambda = 400\div 700$ nm.

Application of color measurement devices in the industry allows making the process objective. Nevertheless, it was dealt with occurring the problems concerning parameter differences of the measurement device. Models of color space such as RGB, or CMYK commonly known in the computer graphics are dependent on a kind of apparatus used for the color determination. These models belong to the group dependent on the measurement principle (device). It was necessary to create a system, which allows for an univocal color determination and its changes, i.e., to create the system independent on the measurement device. Modification of color systems allow for creating the CIE L*a*b* system [3]. CIE L*a*b* system is based on three color attributes: the lightness, chroma and hue. Hue is the main color feature, which is changed with the change of visible light wave length. Chroma is the percent content of shadow in the color, and the lightness is the percentage of achromatic color (white, black and grey color). The assumptions of system CIE L*a*b* are coordinates describing the color space. Two axes described by symbols *a* and *b* are crossed perpendicularly to each other. The third axis perpendicular to the plane *ab*–*L* axis designates the lightness. The advantage of this system is an easiness of color comparison, which is very important during the production of textile articles

of combined color patterns [3]. The color difference ΔE in the system CIE L*a*b* is determined according to the following standards: PN-EN 105-J01:2002 and PN-EN105-J03:2009.

2 METHODOLOGY

2.1 Color measurement devices

In order to study the color change in the textile industry there are used devices with an integration sphere. The operation idea of the spectrophotometer is reflecting light inside the sphere. The device Macbeth 2020 diffused the light inside the sphere with the geometry $d/8^\circ$. It means that the reflected from the sample beam is collected at the angle 8° [4, 5]. Measurements made on the spectrophotometer are characterized by a high precision, but they need more time than the visual assessment [6]. Difficulties can be caused by the complicated small patterns on the surface of examined fabric. The examined sample is folded a few times in order to eliminate the errors caused by the spaces between threads, which can cause the light transmission. Next, sample is put in the spectrophotometer jaws into the window of one inch diagonal [7, 8].

Creating a new technique of touchless measurement allows for making the photo and measuring on this photo the color coordinates. Such a technique enables the touchless measurement in a few seconds. Results of measurements are obtained on the basis of indicating on the computer monitor a point on the sample or marking the whole area of measured object. Shown result is an average value from the marked area. DigiEye enables also to obtain the picture of area with the luster and texture. The whole analysis and obtaining the results of measured sample are done virtually. Option used for the measurement acts according to the principle of chromatic adaptation. It is the brain ability, which relies on the color perception dependably on the light. Sample is placed in the lighted cabin equipped in a specially designed light sources. The source of light is bulbs placed at both sides of cabin. To fulfill the requirement of standard ISO 23603:2005 the special light contains the mixture of fluorescent D65 illuminant and the light of LED [9].

2.2 Object of measurement

Two chosen polyester fabrics destined for the outer layer of clothing were tested before and after the ageing test.

Table 1 Characteristics of tested fabrics

Kind of fabrics	Symbol of fabrics	Mass per square meter g/m^2	Thickness mm
Woven fabric	P1	166.8	0.39
Knitted fabric	P2	328.2	2.26

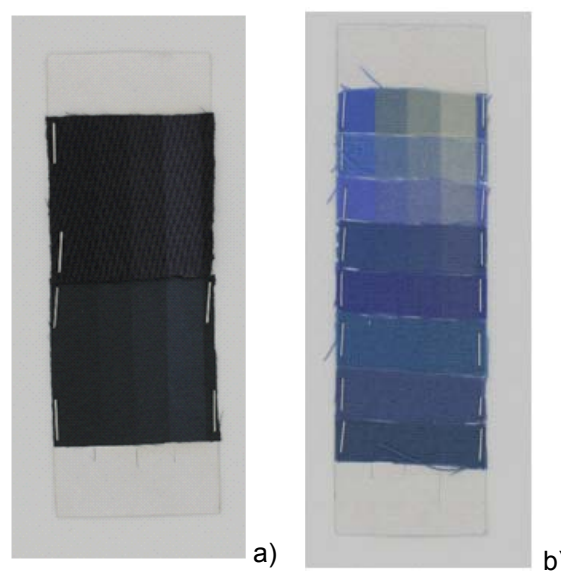


Figure 1 Photos of examined samples done by the DigiEye after all diaphragms: a) PES samples; b) blue scale

2.3 Sample irradiation procedure

The chosen samples were exposed on the xenon light in the Xenotest 150 (of firm Herau) according to the standard PN-EN ISO 105-B05:2013, method 2. Samples were lighted in the normal conditions in four steps. The first step – the sample was lightened with a diaphragm I covering $\frac{1}{4}$ part of examined area. The color change obtained on the pattern No 4 should correspond to the grade 4 according to the grey scale. Next, the diaphragm covering $\frac{1}{2}$ part of examined area was applied; the lightening has been performed up till obtaining the change on the pattern No 6 corresponding to the grade 4 according to the grey scale. The last diaphragm covered $\frac{3}{4}$ parts of the area of examined samples. The light exposure should be carried out to obtain the change on the pattern No 7 corresponding to the grade 4 (Figure 1).

3 RESULTS & DISCUSSION

On the basis of spectral characteristics the color coordinates in CIE L*a*b* system, are calculated, thanks to which in a simple way, the color differences between not lighted samples and aged in the Xenotest can be calculated. Research was done to verify the possibility of testing the color changes on the DigiEye device. Both devices (DigiEye and Macbeth) have different methods of sample illumination, what can cause different values of ΔE . The comparison of color coordinates was performed for unexposed samples and after changes of all diaphragms, one by one (Tables 1 and 2). Samples were illuminated by the illuminant D65.

The analysis of results was performed in two different ways: comparison of characteristics of color coordinates in the CIE L*a*b* system for each sample (Tables 1 and 2) and the comparison of sample color change to the unexposed sample (pattern) on both devices

(Table 3). Results obtained by the first way on presented tables 1 & 2 show that the obtained values are different. Big differences for the sample 2 result from its structure. Sample 2 is a knit of Polartec type, for which the direction of arrangement of covering fibers during the measurement influences the results.

Second way relies on the comparison of exposed samples to the pattern, which was unexposed one. In this case it can be observed that the values of color change ΔE obtained for the same sample by different measurement devices are similar. It results from the fact that the colorimeter DigiEye has a wider application in the color difference measurement for one kind of sample than in the case of determination the precise absolute values of color coordinates in CIE L*a*b* system. DigiEye device equipped in a digital camera, which is not predicted for colorimetric application, can influence the spectral sensitivity, and due to this fact the values can differ from the standardized sensitivity of colorimetric observer.

Table 2 CIE L*a*b* coordinates form the spectrophotometer and colorimeter

	Spectrophotometer Macbeth			Colorimeter DigiEye		
	L	a	b	L	a	b
P1 unexposed	19.13	1.91	-4.66	18.69	1.96	-4.37
P1 - I diaphragm	19.36	1.87	-4.74	18.69	1.96	-4.37
P1 - II diaphragm	19.61	2.06	-5.72	19.06	2.89	-7.65
P1 - III diaphragm	20.54	2.34	-7.95	20.55	2.87	-8.23

Table 3 CIE L*a*b* coordinates form the spectrophotometer and colorimeter

	Spectrophotometer Macbeth			Colorimeter DigiEye		
	L	a	b	L	a	b
P2 unexposed	13.53	0.45	-1.14	12.97	-2.74	-0.68
P2 - I diaphragm	14.47	0.25	-0.90	12.97	-2.74	-0.68
P2 - II diaphragm	15.75	-0.16	-0.76	14.61	1.53	-0.29
P2 - III diaphragm	18.05	-1.37	-0.90	16.32	-2.72	1.94

Table 4 Color difference between unexposed and after 3rd diaphragm obtained from both devices

Sample	Spectrophotometer Macbeth										
	Unexposed sample			Sample after diaphragm III			Differences				
	L	a	b	L	a	b	ΔL	Δa	Δb	ΔE	
sample 1	19.13	1.91	-4.66	20.54	2.34	-7.95	1.41	0.43	-3.29	3.6	
sample 2	13.53	0.45	-1.14	18.05	-1.37	-0.9	4.52	-1.82	0.24	4.9	
Sample	Colorimeter DigiEye										
	sample 1	18.69	1.96	-4.37	20.55	2.87	-8.23	1.86	0.91	-3.86	4.4
	sample 2	12.97	-2.74	-0.68	16.32	-2.72	1.94	3.35	0.02	2.62	4.3

4 CONCLUSIONS

After analysis of measurement results there can be stated the influence of using different measurement devices, recalculating software, and applied technical solutions as well as the structure of examined area of each sample. Considering the results of color coordinates for the same sample obtained from two different measurement devices we obtained the small differences for sample P1. Sample P2 reaches bigger changes because of structure.

Relatively smaller differences in results of color change obtained from both devices were obtained for the sample 1, which seems to be characterized by the high light resistance. Due to structure of knitted fabric (sample P2) can be observed differences color determination between devices as well. In the case of measurement of color changes ΔE for one sample before and after lightening the results obtained from both measurement devices are similar. The differences between the value of ΔE obtained for both equipment cannot be noticed by the human eye.

After this experiment right seems to be a statement about a possibility of using the DigiEye device for measuring the color changes. Research confirming this assumed thesis is necessary to determine a correlation between results from both devices is in the process.

5 REFERENCES

1. Williams S.: Practical colour management, Optics & Laser Technology 38, 2006, pp. 399-404
2. Collective work, Textile Metrology, Scientific-Technical Editor, Warsaw 1973
3. Tarasiuk J.: Problem of Colour, <http://home.agh.edu.pl/~tarasiuk/didactics/doc/GFK/S/03.pdf>, access 04.09.2013
4. Lau L.N., Kan C.W., Yuen Marcus C.W., Lau Robert K.W.: Study of the correlation between solid colors measured by spectrophotometer and DigiEye, The First International Conference on Interdisciplinary Research and Development, 31 May - 1 June Thailand, 2011
5. Mielicki J.: Overview information about color; Foundation for Development of Polish Colors, Lodz 1997
6. Pietrzykowski J.: Geometries of measurement applied in colorimetry spectrophotometry of reflected optical radiation and their notation, Research of Electrotechnics Institute, booklet 237, 2008
7. Adamczyk P., Frydrych I., Rutowicz J.: Comparative Analysis of the CIELab System Obtained from Devices: Macbeth & DigiEye, 19th International Conference STRUTEX, 3-4.12.2012, Liberec, Czech Republic
8. Adamczyk P., Frydrych I.: Analysis of color changes carried on spectrophotometer Macbeth 2020 & digieye devices, III Visiting Lodz University of Technology, PhD Scientific Session, 22-24.04.2013, Rogow, Poland
9. DigiEye user guide, Version 2.51 (rev a)

MERANIE FAREBNEJ ZMENY NA PRÍSTROJI DIGIEYE

V práci je prezentovaný proces aplikácie nového stanovenia farebnej zmeny použitím zariadenia DigiEye. Merania boli robené na PES tkaninách určených pre vonkajšie vrstvy oblečenia. Starnutie vzoriek určených na stanovenie zmeny farby bolo vykonané na prístroji Xenotest 150. Proces starnutia tkanín bol hodnotený pomocou modrej stupnice. V práci sú prezentované výsledky získané pred a po teste starnutia, pri ktorom sú skúmané vzorky vystavené pôsobeniu svetla. Sú diskutované výsledky zmeny farby vo farebnom systéme CIE L*a*b*.

DESIGN OF DMA EXPERIMENTS FOR POLYMERS

Ivan Kopal

Alexander Dubček University of Trenčín, Faculty of Industry Technologies in Puchov, Slovakia
ivan.kopal@fpt.tnuni.sk

Abstract: A two-level full factorial design of experiments has been used to improve the measurement process utilised in a dynamic mechanical analysis procedure for the characterisation of viscoelastic properties of polymeric materials. The measurement process has been analysed in a systematic way, which allows the identification of outputs of the dynamic mechanical analysis tests characterizing viscoelastic properties of examined polymeric material with a high effectivity. By applying the randomized two-level full factorial design methodology, the main factors that influence properly chosen outputs of dynamic mechanical analysis tests by a statistically significant amount, as well as the combination of the levels of main factors that make the measurement process least influenced by them have been obtained.

Keywords: design of experiments, full factorial design, dynamic mechanical analysis, viscoelastic properties of materials.

1 INTRODUCTION

The dynamic mechanical analysis (DMA) represents one of the most powerful methods for the research of viscoelastic properties of polymers. Some of the most important applications of DMA are the measurement of polymers dynamic module, as well as its loss factor on various temperatures of material and frequencies of dynamic mechanical loading, the possibility to study the relationships between the structure of the polymers and its basic properties such as glass transition and melting point, the identification of temperature, intensity and activation energy of relaxations, etc. [1].

The results of DMA are typically provided as a plot of storage modulus E' , loss modulus E'' and loss factor $\tan \delta$ versus temperature, time or frequency. However, the outputs of DMA tests depend also on the number of others factors involved in the measurement process [2]. The simultaneous influence of several input factors on the experimental results can be identified via a properly chosen design of experiments (DOE) [3], what is able to improve the process of measurement ultimately. Generally, at a lower number of examined input factors, the two-level full factorial design of experiments is highly effective [4]. The objective of this work is to identify the outputs of DMA characterizing the viscoelastic properties of examined polymeric materials with a very high effectivity, to find out, by applying the two-level full factorial design of experiments methodology, the main factors influenced these outputs by a statistically

significant manner and to search out the combination of the main factors levels that make the measurement process least influenced by main factors.

2 EXPERIMENTAL PROCEDURE

In this study, the DMA measurements of viscoelastic properties were taken on a sample of high-density polyethylene (HDPE) with 956 kg.m⁻³ value of density and 75% degree of crystallinity, using a Perkin Elmer PYRIS Diamond Dynamic Mechanical Analyzer, within the temperature interval from 16°C to 157°C determined by a surroundings temperature and by a melting point of tested material. In the first step of experimental process, a multifrequency DMA screening test was carried out in order to observe a viscoelastic behaviour of the sample under investigation in the given temperature interval and applied frequencies 1, 2, 5, 10, 20 Hz standardly used in the multifrequency DMA testing of polymers. The rectangular shape specimen of HDPE 4.3 mm wide, 20 mm long and 1.2 mm thick has been tested at constant heating rate 3°C.min⁻¹. The experimental results of screening test in the form of multifrequency DMA scan is shown in the Figure 1.

From the Figure 1, it is evident that all three viscoelastic parameters E' , E'' and $\tan \delta$ markedly depend on temperature and frequency, but they are influenced also by a number of other DMA input factors. The complete list of these factors can be found, for instance, in the study [2]. They

can be divided into two categories: control factors and noise factors.

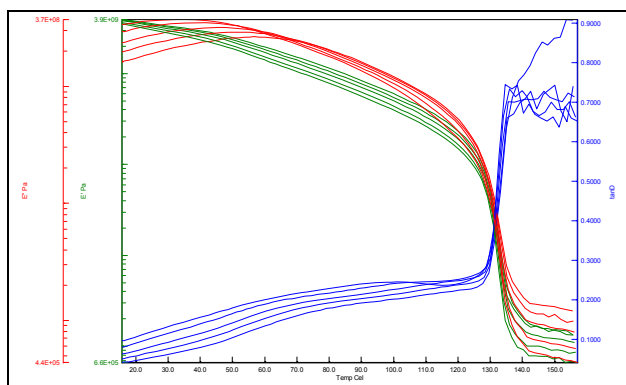


Figure 1 The multifrequency DMA screening test scan of HDPE

Heating rate of sample V , frequencies of mechanical loading F and sample width W have been chosen as effect control factors for the subsequent two-level full factorial design of DMA experiment whereas all the others control as well as noise factors were kept at constant value. The selection of effect control factors has been determined by economic demands and by demands of DMA response stability, which has been measured at all combinations of minimal and maximal values of these two-level effect factors. The low levels of factors V and W were $2^{\circ}\text{C}\cdot\text{min}^{-1}$ and 4.315 mm and its high levels $4^{\circ}\text{C}\cdot\text{min}^{-1}$ and 8.13 mm. The low level of factor F is represented by a frequency band 0.05, 0.1, 0.2, 0.4 and 0.8 Hz whereas the high level by the frequency band 1, 2, 5, 10 and 20 Hz. From the Figure 1 it is also evident that the temperature dependence of $\tan \delta$ is the most sensitive to the variations in frequency F from all of the registered viscoelastic parameters. Therefore, just $\tan \delta$ was the selected DMA output of HDPE testing by DOE procedure. Nevertheless, in connection with the large number of experimental data acquired from measuring at all selected frequencies in the given temperature interval, the maximum value of loss factor $\tan \delta_{max}$ appears as the high effective viscoelastic parameter for the next DOE analysis. Namely, the temperature of reaching $\tan \delta_{max}$ enables to identify the regions of relaxation transitions as well as its activation energy calculation.

3 RESULTS AND DISCUSSION

The analysis of experimental data registered in the realized DOE procedure has shown that for

frequencies higher than 1 Hz the extremum of $\tan \delta_{max}$ does not exist in the given temperature interval from 16°C to 157°C for both levels of factors V and W . Therefore, the frequency 1 Hz was regarded as the high level and 0.8 Hz as the low level of F factor in the next DOE data analysis. Subsequently, a sign method [3] has been used in order to evaluate effects of input factors V , W and F as well as its interactions on the $\tan \delta_{max}$ value (Figure 2). From the Figure 2, where a plot of effects is presented, one can see that absolute values of V and F factors effects are much greater than absolute values of W factor effect and effects of all interactions. Hence, the variations in V and F factors values have a main effect on $\tan \delta_{max}$, factor W and interactions VF and VFW have a much smaller effect on $\tan \delta_{max}$, while interactions VW and FW have no effect on $\tan \delta_{max}$ practically. From the plot of effects, presented on figure Figure 2, it is evident that the influence of particular monitored input factors on $\tan \delta_{max}$ will be minimal in case the heating rate of HDPE sample V and its width W will be setting up in the low level, whereas the frequency of dynamic mechanical loading F in the high level. In the event of DMA multifrequency measurement, it is optimal the frequency band of dynamic mechanical loading of tested sample to select from a neighbourhood of F factor high level.

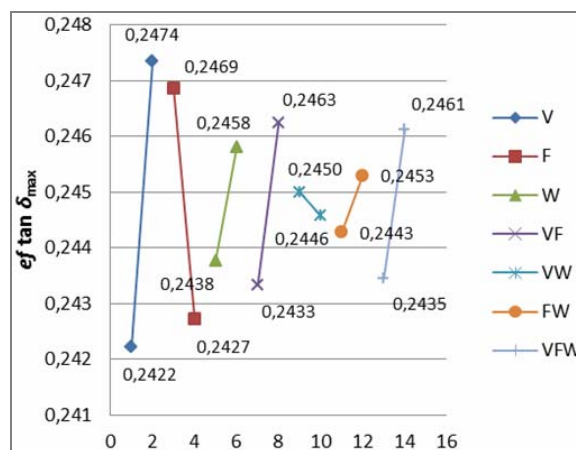


Figure 2 The plot of factors and interactions effects

Afterwards, a normal probability plot of effects and effects interactions has been designed for the purpose of its statistical significance estimation (Figure 3) [5].

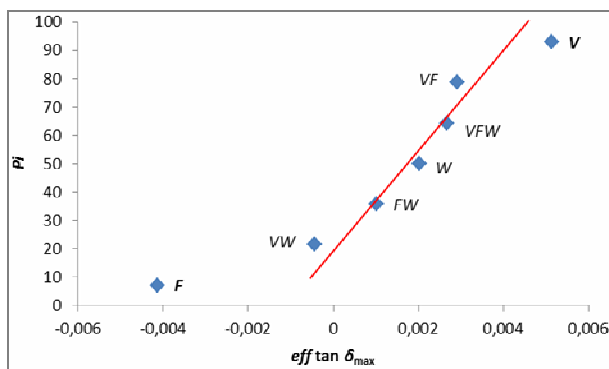


Figure 3 The normal probability plot of effects

As one can see from Figure 3, outside a normal distribution guideline, presented on the normal probability plot by straight line, nothing but effects of F and V factors are situated. It comes to this, that factors F and V influenced $\tan \delta_{max}$ by the statistically significant manner, while the influence of factor W and of all monitored input factors interactions are statistically irrelevant under the given conditions of DMA experiment.

4 CONCLUSIONS

The two-level randomized full factorial design of DMA experiment has been used to improve the measurements of viscoelastic properties of polymeric materials in this study. DOE experiment has been realized on the sample of high-density polyethylene in the multifrequency mode of DMA. The maximum of loss factor has been selected as the monitored DMA response. It has been shown that the statistically significant influence on DMA response have only the heating rate of sample and frequency of its mechanical loading that were

chosen, much like the sample width, as input factors of DMA tests in DOE experiment. Influence of sample width as well as of all monitored input factors interactions are statistically irrelevant under the given conditions of DMA experiment. The influence of particular input factors on monitored DMA response will be minimal in case the heating rate of HDPE sample and its width will be setting up in the low level, while the frequency of dynamic mechanical loading in the high level. In the event of multifrequency measurement, it is optimal the frequency band to select from a neighbourhood of high level of frequency factor.

Acknowledgments: The present work is sponsored by the research project VEGA 1/0385/14

5 REFERENCES

1. Menard K. P.: Dynamic Mechanical Analysis: A Practical Introduction to Techniques and Applications, CRC Press, Boca Raton, 1999
2. Rodríguez-Pérez M. A., Almanza O., del Valle J. L., González A., de Saja J. A.: Improvement of the measurement process used for the dynamic mechanical characterisation of polyolefin foams in compression, Polymer Testing Vol. 20, 2001, pp. 253-267
3. Montgomery D. C.: Design and Analysis Experiments, John Wiley & Sons, Inc., New York, 2001
4. Bolboaca S. D., Lorentz Jäntschi L.: Design of Experiments: Useful Orthogonal Arrays for Number of Experiments from 4 to 16, Entropy Vol. 9, 2007, pp. 198-232
5. Altman D. A.: Statistics with Confidence, GBR: BMJ Publishing Group, London, 2000

EXPERIMENTÁLNY DIZAJN DMA POLYMÉROV

Práca sa venuje dvojúrovňovému faktoriálnemu dizajnu DMA experimentu, ktorý bol navrhnutý na zlepšenie procesu merania viskoelastických vlastností polymérnych materiálov. Analýza skríningových experimentálnych dát z multifrekvenčných DMA meraní realizovaných na vzorkách HDPE umožnila identifikovať maximálnu hodnotu dynamického stratového činiteľa ako výstupu DMA, ktorý vo zvolenom frekvenčnom rozsahu a sledovanom teplotnom intervale charakterizuje viskoelastické správanie skúmaného materiálu s vysokou efektivitou. Zistené boli hlavné faktory a interakcie, ktoré štatisticky významným spôsobom ovplyvňujú výsledok DMA, ako aj navrhnuté také kombinácie úrovni sledovaných vstupných faktorov, pri ktorých je ich vplyv na výsledky DMA skúmaného polymérneho materiálu za daných podmienok minimálny.

TEMPERATURE DEPENDENCY OF DC ELECTRICAL CONDUCTIVITY OF HARDENED POLYURETHANE BASED CARBON NANOCOMPOSITES

Ivan Kopal and Karol Kováč

*Alexander Dubček University of Trencin, Faculty of Industry Technologies in Puchov, Slovakia
ivan.kopal@fpt.tnuni.sk*

Abstract: *The study of electrical properties of hardened polyurethane filled by single walled carbon nanotubes is presented in this paper. The objects of the research are nanocomposites made out of a hardened polyurethane matrix filled by single walled carbon nanotubes with different amount and different purity. Temperature dependencies of dc electrical conductivity were measured in a temperature range from 25°C up to 100°C. It has been shown that electrical dc conductivity of hardened polyurethane have an increasing character in dependence on temperature. The results have shown that higher amounts of nanotubes increase dc electrical conductivity. Nanotubes with purity of 90% increase electrical conductivity more than nanotubes with 60% purity.*

Keywords: *electrical conductivity, electrical percolation, single walled carbon nanotubes, hardened polyurethane.*

1 INTRODUCTION

Polyurethanes are the polymers synthesized from diisocyanates and polyalcohols and belong to a polyester-amides group. We can get these polymeric materials with a wide range of desired properties. This is reason, why they are more used as matrix in nanocomposites. Carbon nanotubes used in these nanocomposites are usually multi-walled or the more expensive single-walled [1]. Electrical properties such as electrical conductivities are the most important characterizations of all engineering materials. Nowadays we make new materials which should be used, for example, as biomaterials or semiconductors from polymers. Information about influence of carbon nanotubes on a percolation behavior is one of the most important for practical application. In the work [2] researchers examined influence of multi-walled carbon nanotubes on percolation behavior in different types of hard segments in the used polyurethane. They identified percolation threshold in the material at amount of nanotubes under one percent. Very similar work [3] concludes the percolation threshold under amount one percent of multi-walled carbon nanotubes, which have been filled in polyurethane matrix. In our work we study the dc electrical conductivity of hardened polyurethane filled by single-walled carbon nanotubes with a different amount and different purity.

2 EXPERIMENTAL

2.1 Materials

Polyurethane has been synthesized from PX 522/HT POLYOL and PX 521-522 HT ISO ISOCYANATE. Our investigated poly-urethane carbon nanocomposites were prepared in two stages. Single-walled carbon nanotubes with purity 90% and 60% were stirred in the reaction component PX 522/HT POLYOL for approximately two minutes by the ultrasound mixer WELDER. These nanotubes are produced by the company NanocylTM and they were filled to the matrix in three different amounts: 0.5, 1 and 1.5 wt%. The mixing was implemented in a vacuum chamber to degas the polymerization mixture in the next ten minutes. After adding the isocyanate with trade name PX 521-522 HT ISO ISOCYANATE the mixture was stirred by an ultrasound for two minutes. Next the process of curing was carried out for 4 hours at 80°C and 16 hours at 100°C. Each sample was pressed by the displacement speed of 2 mm/min to a force value of 100 kN. The pressure modulus and the coefficient of compressibility was in the range of tension of 20 - 60 MPa [4]. From basic material were prepared by cutting thin discs with thickness about 1.2 mm with diameter 30 mm. Samples were coated with a conductive graphite layer DAG 580 on the contact surfaces.

2.2 Methods

After the evaporation of isoamyl alcohol samples of tested carbon polyurethane nanocomposites

were subjected to measurement by using a direct method of thermal dependence of the dc electrical conductivity measuring. For determination of the dc conductivity, the dc electric current was measured at a constant voltage of 10 V using a Novocontrol Concept 90 equipment, in the temperature range from 25°C up to 100°C. The current was determined by a Picoammeter Keithley 6517B. The temperature was measured by using a Pt 100 temperature sensor, with an accuracy of $\pm 1^\circ\text{C}$. A connection scheme for the temperature dependency of the dc electrical conductivity measuring according to direct method we have shown in the Figure 1.

The experimental equipment is shown on the Figure 2.

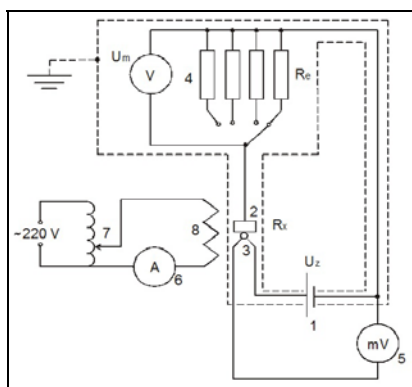


Figure 1 The connection scheme for measurement of temperature dependency of dc electrical conductivity according to the direct method (1-source of dc voltage, 2-sample, 3-thermocouple, 4-Voltmeter, 5-milivoltmeter, 6-ampmeter, 7-autotransformer, 8-heating windings)



Figure 2 Experimental equipment for dc electrical conductivity measurement

3 RESULTS AND DISCUSSION

In the Figure 3 it is shown the temperature dependency of dc conductivity for pure polyurethane, nanocomposites with 90% purity of

nanotubes and nanocomposites with 60% purity of nanotubes.

The temperature dependency of dc conductivity shows a significantly increasing character for hardened polyurethane and nanocomposite with 0.5 wt% of nanotubes with the 60% purity. At this amount does not occur major changes of electrical dc conductivity. Influence of amount of nanotubes is significant at nanocomposites with nanotubes of 60% purity, but these nanocomposites do not achieve as high values of electrical conductivity as nanocomposites with nanotubes of 90% purity.

The amount 1.5 wt% of nanotubes with purity 90% increases electrical dc conductivity 7.7×10^{11} times in comparison with the pure hardened polyurethane at temperature 25°C.

Nanotubes with the purity 90% cause percolation already at amount 0.5 wt%. Nanotubes with the purity 60% cause percolation at amount 1.5 wt%, but these nanotubes are cheaper. Temperature dependencies of electrical dc conductivity for nanocomposites with 90% purity of nanotubes do not have a significantly increasing character.

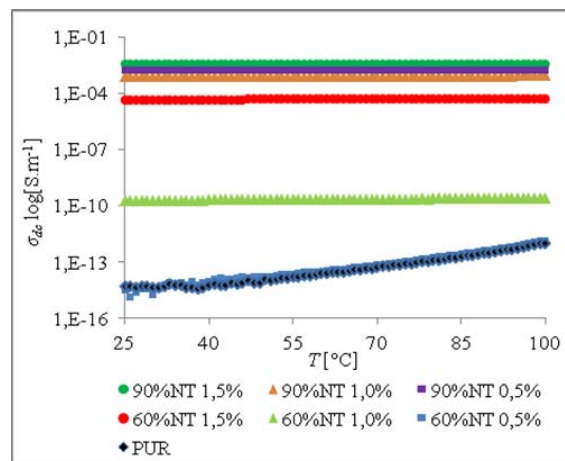


Figure 3 Temperature dependency of dc conductivity for hardened polyurethane, nanocomposites with 90% purity of nanotubes and nanocomposites with 60% purity of nanotubes

4 CONCLUSIONS

The paper presents the results of our study of the temperature dependence of electrical dc conductivity of nanocomposites with polyurethane matrix filled by single-walled carbon nanotubes with different amount and different purity of nanotubes in a temperature range from 25°C to 100°C. Adding single walled carbon nanotubes with 90% purity causes percolation of electrical dc conductivity already at amount 0.5 wt%, but

adding 1.5 wt% of carbon nanotubes with 60% purity causes percolation of electrical dc conductivity accordingly. The amount 1.5 wt% of nanotubes with 90% purity increases the electrical dc conductivity 7.7 x 10¹¹ times in comparison with the pure hardened polyurethane at temperature 25°C.

Acknowledgments: *The present work is sponsored by the research project VEGA 1/0385/14.*

5 REFERENCES

1. Drobny J. G.: Handbook of Thermoplastic Elastomers: 9 - Thermoplastic Polyurethane Elastomers, Elsevier, 2007, pp. 215-234
2. Yun S., Im H., Kim J.: The effect of different hard segments in polyurethane on the electrical conductivity of polyurethane grafted multi-walled carbon nanotube/polyurethane nanocomposites. Synthetic Metals, 2011, Vol. 161 (13-14), pp. 1361-1367
3. Bouchard J., Cayla A., Devaux E., Campagne C.: Electrical and thermal conductivities of multiwalled carbon nanotubes-reinforced high performance polymer nanocomposites, Composites Science and Technology, 2013, Vol. 86, pp. 177-184
4. Lалуha d.: Elektrické vlastnosti polymérnych materiálov, In Diplomová práca, Trenčín, Slovenská Republika: Trenčianska univerzita Alexandra Dubčeka v Trenčíne, Fakulta priemyselných technológií, 2012, 49 p

TEPLOTNÁ ZÁVISLOSŤ JEDNOSMERNEJ ELEKTRICKEJ VODIVOSTI UHLÍKOVÝCH NANOKOMPOZITOV NA BÁZE MATRICE Z TVRDENÉHO POLYURETÁNU

Práca je venovaná štúdiu elektrických vlastností tvrdého polyuretánu plneného rôznym množstvom jednodenných uhlíkových nanorúrok s rôznou čistotou. Skúma vplyv množstva nanorúrok s čistotou 60% a 90% na perkolačný jav jednosmernej elektrickej vodivosti testovaného polyuretánového uhlíkového nanokompozitu pri teplotách v intervale od 25°C až do 100°C, s krokom 1°C. Závislosť jednosmernej elektrickej vodivosti bola zisťovaná priamou metódou, resp. meraním pretekajúceho jednosmerného elektrického prúdu pri konštantnom napätí 10 V pomocou zariadenia Novocontrol Concept 90 a prístroja Keithley 6517B. Získané výsledky preukázali, že perkolačný jav je pri jednosmernej elektrickej vodivosti spôsobený pridaním uhlíkových nanorúrok s čistotou 90% do polyuretánovej matrice už v množstve 0.5 hm%. K takmer rovnakému zvýšeniu elektrickej vodivosti dochádza aj pri pridaní 1.5 hm% nanorúrok s čistotou len 60%, čo je výborným zistením z hľadiska ceny použitého nanoplňiva. Najvyšší nárast jednosmernej elektrickej vodivosti pri teplote 25°C bol nameraný pri nanokompozite s obsahom 1.5 hm% čistých nanorúrok, v ktorom sa v porovnaní s čistým tvrdým polyuretánom jednosmerná elektrická vodivosť zvýšila až 7,7 x 10¹¹ násobne.

FTIR SPECTROSCOPY MEASUREMENTS OF ORIENTED POLYPROPYLENE FILMS

Ivan Kopal and Leoš Polka

*Alexander Dubček University of Trencin, Faculty of Industry Technologies in Puchov, Slovakia
ivan.kopal@fpt.tnuni.sk*

Abstract: *In the study we are focusing on altering specific properties of bi-axially oriented isotactic polypropylene films with temperature applied during annealing of these films. Fourier transform infrared spectroscopy (FTIR) method is used for investigation of material changes. Several structural changes occur during this process like reorganization of polymeric macromolecules in the time and a decrease in the defect concentration, which cause an increase in crystalline to amorphous ratio called crystallinity. Changes in crystallinity degree of polypropylene have been qualified based on deconvoluted infrared absorption spectra registered in transmission setup of FTIR-8601PC spectrometer at the room temperature of 23°C. Experimentally it was proven that higher temperature applied during annealing causes greater increase in crystallinity degree of polypropylene. We also found out that registered spectra are highly dependent on an orientation of a sample during the main measurement. These features were also observed on mechanical analysis of iPP samples.*

Keywords: *FTIR, dynamic mechanical analysis, polypropylene films, polymers.*

1 INTRODUCTION

Polypropylene is one of the most common and most used synthetic polymers. Thanks to its favorable chemical, physical and mechanical properties it can be found in wide range of industrial and commercial applications. The properties can be easily modified using different additives or altering a manufacturing process itself. The most frequently used form of polypropylene (PP) is isotactic polypropylene (iPP). Fourier Transformation Infrared Spectroscopy was used as an analytic method for study of bi-axially oriented iPP foils. This method is characteristic for relatively very simple sample preparation and main measurement process. FTIR spectroscopy is highly efficient technique based on absorption of infrared (IR) beams by studied samples. It causes changes in rotation and vibration states of molecules and altering their dipolar momentum [1]. Infrared beams react with whole molecules, parts of molecules or functional groups depending on its energy and these interactions are registered in a form of peaks in absorption spectra at a specific wavenumber [2]. IR spectra analysis allows us to identify organic and inorganic compounds with high accuracy. There are 3 main FTIR techniques: transmission, reflectance and attenuated total reflectance [3]. Mechanical analysis of iPP revealed that mechanical

properties are highly dependent on a temperature applied during annealing of iPP foils and also whether the loading is applied in a stretching direction or in upright direction. The transmission FTIR technique is used in this study for further investigation of this phenomenon.

2 EXPERIMENTAL

Bi-axially oriented PP foils were used during the experiment. Samples were fixed in frame with stretching direction noted on it. In a process of manufacturing the thin iPP film with a thickness of 400 μm , from which the specimens were prepared, the extruded sheet was drawn firstly in machine direction and then in transverse direction with draw ratio of 4 x 7. The temperatures of 120, 140, 150, 160, 170°C were applied during annealing of the material. After stretching the material obtained a considerably greater tensile strength and lower elongation at break in stretching direction, what was proven using dynamic mechanical analysis via a Perkin Elmer Pyris Diamond Mechanical Analyzer 8000 [4]. IR absorption spectra for iPP films prepared in a room temperature 23°C and relative humidity of 60% were registered. The transmission method of FTIR on FTIR-8601PC Shimadzu spectrometer, a wavenumber range of 4000-700 cm^{-1} , step of a 2 cm^{-1} and resolution of 2 cm^{-1} was used for IR spectra analysis of tested specimens. The

machine was calibrated by polystyrene calibration foil. IR spectra were processed in SigmaPlot software in this study. We were also testing for differences in registered IR spectra between measurements in horizontal orientation and vertical orientation of a material sample in spectrometer chamber according to the stretching direction of iPP foils.

3 RESULTS AND DISCUSSION

On a Figure 1 there are registered infrared spectra of bi-axially oriented polypropylene foils in a range of 2800-700 cm^{-1} .

Samples are labeled in TB x/10_y °C_z pattern, where x – elongation ratio, y – annealing temperature and z – horizontal (H) or vertical (V) arrangement towards IR source and IR detector in a spectrometer. As one can see on a Figure 1 there are noticeable differences between the registered spectra in horizontal and vertical arrangement of the sample towards IR source and IR detector. We can see a main difference in an area around 1450 cm^{-1} and around 1380 cm^{-1} . The area around 1450 cm^{-1} is characteristic for $-\text{CH}_2-$ bending and $-\text{C}-\text{H}$ scissoring and area around 1380 cm^{-1} is characteristic for $-\text{CH}_3$ bending. In the fingerprint region of IR spectra one can see at wavenumber of 973 cm^{-1} absorbance peaks typical for CH_3 rocking and C-C chain stretching vibrations of iPP amorphous phase and at 998 cm^{-1} peaks characteristic for CH_3 rocking, CH_2 wagging and CH bending of the crystalline phase consisting of α -helix short PP chains. Absorbance intensity A_{998} at 998 cm^{-1} of crystalline phase and absorbance intensity A_{973} at 973 cm^{-1} of amorphous phase were used to count the crystalline to amorphous phase ratio for iPP samples as A_{998}/A_{973} . We also found out that measurement of degree of crystallinity is not dependent whether we use horizontal or vertical arrangement of the sample towards IR source and IR detector. For a resolution enhancement registered IR spectra were deconvoluted to single components. This band-narrowing process of IR spectra was done by the Fourier self-deconvolution method.

Deconvolution spectra of iPP sample for temperature 23°C is presented on Figure 2. The same process was applied for other samples as well and they are not listed. Variations between horizontal and vertical arrangement in certain areas of IR spectra can be further analysed using polarized IR beams as it may seem that iPP foils react differently accordingly to the stretching

directionity. Polarized IR beams could provide better view on these areas.

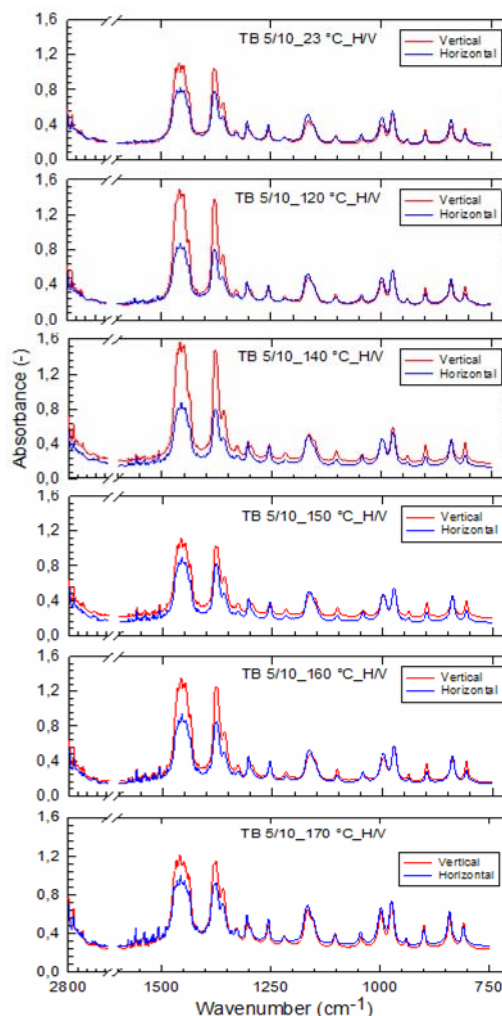


Figure 1 FTIR spectra of bi-axially oriented polypropylene film

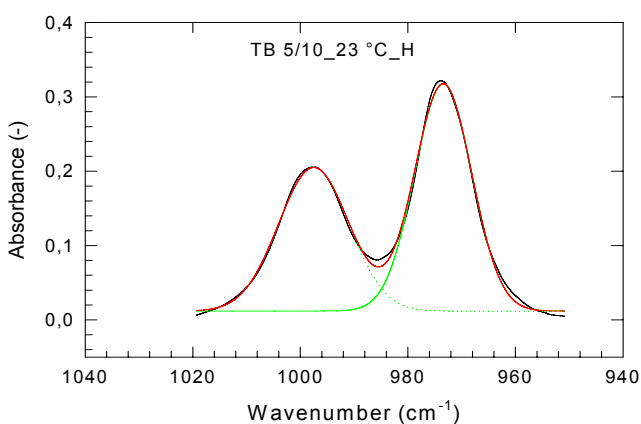


Figure 2 Deconvolution spectra of PP film for 23°C

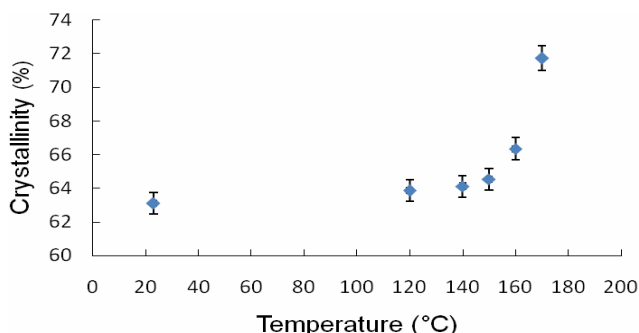


Figure 3 Crystallinity to temperature relativity for PP samples

Absorbance intensity ratio A_{998}/A_{973} in crystalline and amorphous phase for all applied temperatures during annealing of examined PP samples as well as for the temperature of 23°C is presented in Figure 3 in the form of functional dependency of crystallinity versus temperature. In a Figure 3 there is a noticeable increase in crystallinity with rising temperature applied during the annealing iPP film. This can be explained with changes in a structural orientation of polypropylene after exceeding the temperature over the glass transition point.

4 CONCLUSIONS

Study of bi-axially oriented polypropylene foils by means of FTIR spectroscopy proved that applying high temperature (annealing) on a fixed iPP foils

can be used as a suitable method for increasing degree of crystallinity in these samples. By applying temperature exceeding a glass transition point in iPP we can achieve significantly higher ratio between crystalline and amorphous phase of isotactic polypropylene.

Acknowledgments: The present work is sponsored by the research project VEGA 1/0385/14.

5 REFERENCES

1. Lee S. H.: Rheological and electrical properties of polypropylene/MWCNT composites prepared with MWCNT masterbatch chips, *European Polymer Journal*, Vol. 44, Issue 6, 2008, pp. 1620-1630
2. Kang J., Yang F., WU, T.: Polymerization control and fast characterization of the stereo-defect distribution of heterogeneous Ziegler–Natta isotactic polypropylene, *European Polymer Journal*, Vol. 48, 2012
3. Tan H. P., Ling S. K., Chuah C. H.: One- and two-dimensional Fourier transform infrared correlation spectroscopy of *Phyllagathis rotundifolia*, *Journal of Molecular Structure*, Vol. 1006, Issues 1–3, 2011, pp. 297-302
4. Subrananaian N.: FT-IR, FT-Raman spectra, density functional computations of the vibrational spectra and molecular conformational analysis of 2,5-di-tert-butyl-hydroquinone, *Spectrochimica Acta Part A: Molecular and Biomolecular Spectroscopy*, Vol. 83, Issue 1, 2011, pp. 165-174

FTIR SPEKTROSKOPIA ORIENTOVANÝCH POLYPROPYLENOVÝCH FILMOV

V tejto práci je kvantifikovaná zmena stupňa kryštalinity biaxiálne orientovaného iPP filmu na základe analýzy dekonvolučných infračervených absorpčných spektier registrovaných v transmisnom móde na IR spektrometri FTIR-8601PC pri teplote okolitého prostredia 23°C. Bolo preukázané, že v teplotnom intervale 120 – 170°C s rastúcou teplotou žihania skúmaného biaxiálne orientovaného iPP filmu sa podiel kryštalickej fázy oproti amorfnej fáze zvyšuje, teda, že stupeň kryštalinity narastá. Meraním biaxiálne orientovaných iPP filmov v horizontálnom, ako aj vo vertikálnom usporiadaní vzhľadom na smer dĺženia vzoriek skúmaného materiálu boli zistené rozdiely aj v týchto spektrách. FTIR spektroskopickou analýzou boli potvrdené zmeny mechanických vlastností meraných na DMA zariadení Perkin Elmer Pyris Diamond Mechanical Analyzer 8000. Môžeme teda usudzovať, že polymérne reťazce amorfnej fázy a kryštalografická os v kryštalickej fáze sa orientujú prednostne v smere dĺženia iPP.

BIKE TIRE WITH TEXTILE REINFORCEMENT – EXPERIMENT AND COMPUTATIONAL MODELING

Jan Krmela and Mário Vančo

*University of Alexander Dubček in Trenčín, Faculty of Industrial Technologies
I. Krasku 491/30, 020 01 Púchov, Slovak Republic
jan.krmela@fpt.tnuni.sk; jan2.krmela@post.cz*

Abstract: *The paper deals with the bike tire with textile reinforcement from view experiment and computational modeling by Finite Element Method. The special static test machine called static adhesor was used for experiments. Results from experiments are radial deformation characteristics and contact patches for different inflation pressures of selection bike tire. The radial stiffness value of concrete bike tire is obtained from the radial deformation characteristics. Knowledge about stiffness and experiment results is necessary for the verification analyses between results from computational modeling and experiment data. The approach to creation of computational model of bike is presented in this paper.*

Keywords: *bike tire, textile, experiment, computational model, radial stiffness, contact patch.*

1 INTRODUCTION

The paper deals with experiments and approaches to computational modeling of a selected bicycle tire Maxxis High Roller 2.5 26". This tire is widespread and popular among downhillers for its good traction and low rolling resistance. Compared to conventional bicycle tires, he includes technological and material improvements [1].

The carcass is formed of two textile - reinforcement of Nylon. The tire has reinforced sidewalls. The tread is using a special soft compound elastomer. The tread has sharp edges and tread elements are chamfered on one side in order to reduce rolling resistance.

This issue was solved within diploma work [1] and this paper presents the selected results.

2 EXPERIMENT ON STATIC ADHESOR

The measurements were performed on a modified static test machine (Figure 1), called static adhesor [2, 3]. By measurements can be simulated the static load of bicycle tires. The wheel is connected to a device using a special axis. It is possible to overload the tire.

By the tests is possible to determine radial deformation characteristics, size and shape of the contact patches with the analysis of the contact pressure for the specific conditions of load and inflation pressure of the tire. The result is the radial stiffness of the tire, which is an important

parameter, because it is possible to replace the entire tire for bicycle simulations as a whole.



Figure 1 Static adhesor for experiments bicycle and car tires

During the load simulation the tire is pressed against the glass by the press arms. Under glass are placed strain-gate sensors of forces. Radial deformation is measured by potentiometric sensor. Sensors are connected to on-line recording and monitoring of measured data to the notebook through the data logger.

Bicycle tires were tested at three different inflation pressures 180, 280 and 380 kPa. On the Figure 2 are shown the tire deformation at inflation pressure of 180 kPa reflecting a load from 0 to 200 kg.

The radial deformation characteristic, what is the dependency radial deformation of tire out of the radial load, for inflation pressure 180 kPa is shown on the Figure 3.

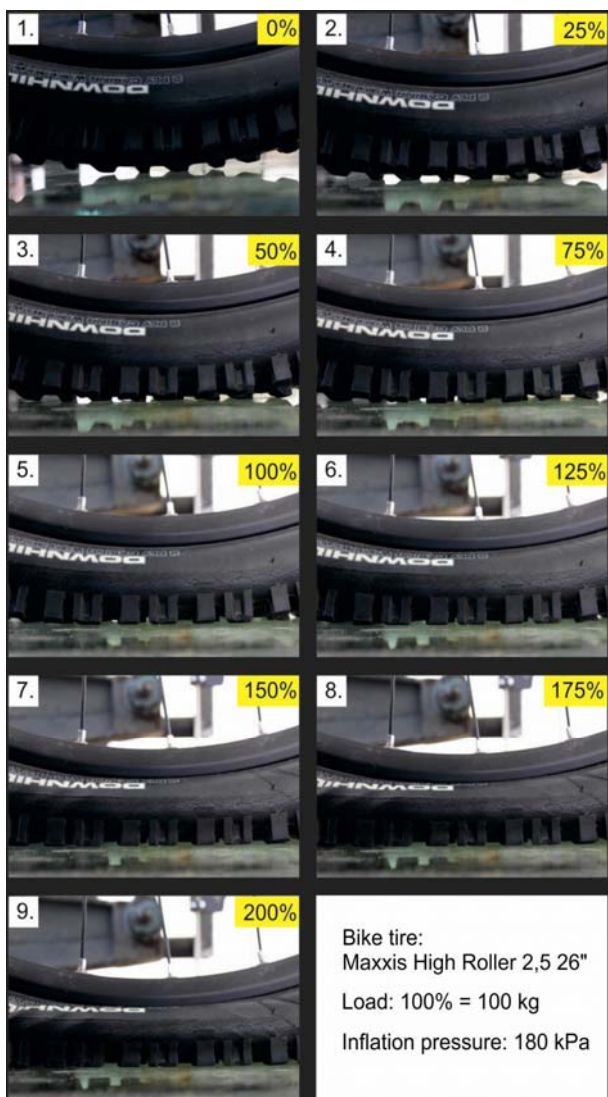


Figure 2 Radial deformation of bicycle tire at a given load for the inflation pressure 180 kPa

The determined values of the radial stiffness of the tire according to [4] are shown in the Table 1 and very depending on inflation pressure of tire.

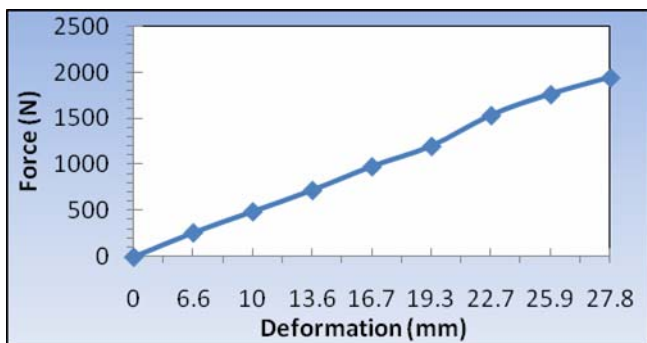


Figure 3 The radial deformation characteristic at inflation pressure 180 kPa

Table 1 The radial stiffness of bicycle tire for given inflation pressures

Pressure (kPa)	Radial stiffness (N/mm)
180	84.0
280	96.5
380	120.0

With the application of a pressure - sensitive film is able to analyze the contact pressure distribution, which is in color spectrum, as shown on the Figure 4.

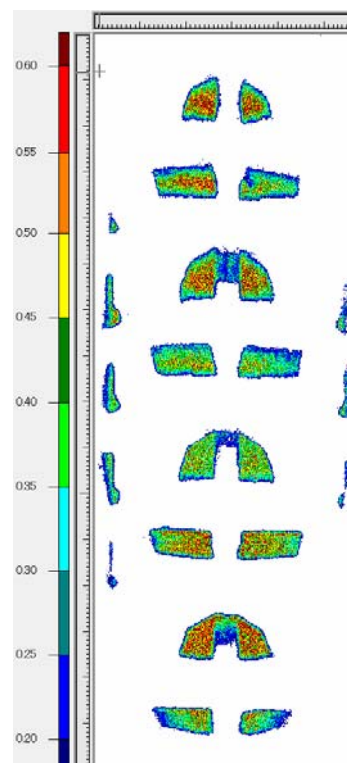


Figure 4 Distribution of contact pressure in the contact patch by inflation pressure 180 kPa and load 100 kg

3 APPROACH TO COMPUTATIONAL MODELING

The precise geometry of cross section of the tire is needed for create a three-dimensional model of segment of bicycle tire. Tire was installed on the rim and inflated to 180 kPa.

The external dimensions of tire were measured. Tire was subsequently dismantled and erupted in order to set up the internal geometric dimensions. In this way was created technical drawing of tire (Figure 5), which is necessary for creating solid model (Figure 6).

The quarter of solid model of tire was imported into the FEM program system. The meshing of computational model is shown on the Figure 7.

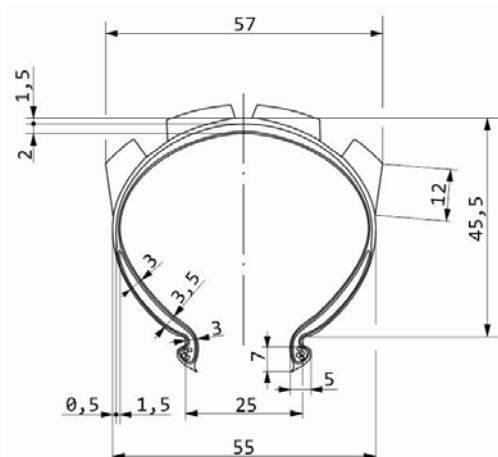


Figure 5 Cross section of given bicycle tire

The reinforcements are not included in the computational model because this model serves as a debugging model. The material parameters were specified by one type of material only, with modulus of flexibility 90 GPa and Poisson number 0.45.

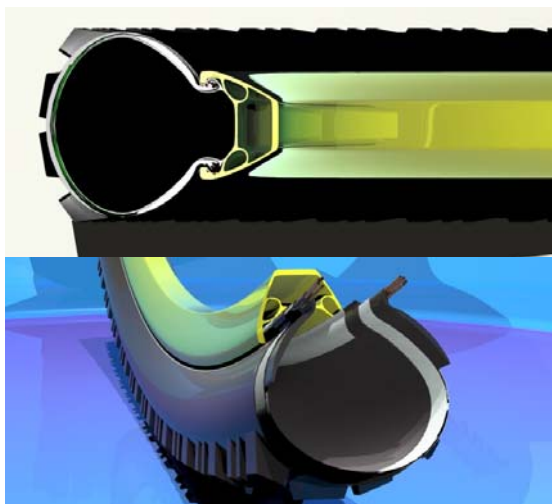


Figure 6: Geometry of bicycle tires Maxxis High Roller 2.5 for import into FEM program

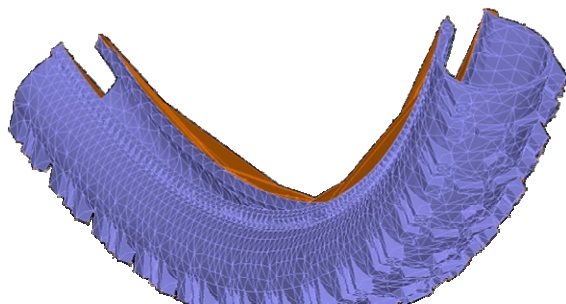


Figure 7 Meshing of quarter of computational model in FEM program

In this model can be the radial load force simulated. It is the strain - stress analysis. The deformation of tire as sample from computation is on the Figure 8.

For further calculations it is necessary to enter into the computational model of reinforcement materials such material parameters, which can be obtained from experiments - for example standards prescribed static tests in tension.

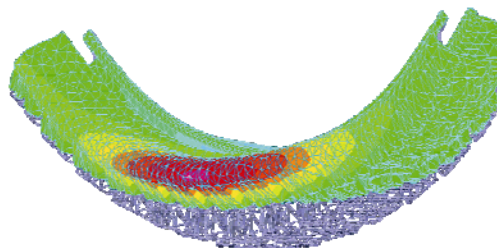


Figure 8 Deformation of tire

After entering the material parameters the computational model will be used for detail contact analyses between tire and road or unevenness for given inflation pressure. The contact patches, radial deformation characteristics and radial stiffness will be compared with data from the experiment.

Based on verification analyzes could be to refine the computational model of view of boundary conditions and material parameters. The construction and material changes in the housing will be proposed to achieve better performance, these are required from downhill tires.

4 CONCLUSION

Based on a comparison of experimental data and results of computational modeling is possible to propose modification to the tire tread design to achieve better traction when cornering without increasing rolling resistance with respect to a given application in mountain biking - downhill.

High demands are required from these bicycle tires. They must be resistant to sharp-edged obstacles, they must have adequate deformation and slip characteristics and high adhesion and low rolling resistance.

It is necessary to specify next material parameters to computational model. It is then possible to solve computing also load states which would be difficult to simulate experimentally.

The approach to computational modeling can be applied also to automobile tires as is indicated in the diploma work [5] as sample.

Recommendations for further research:

- create the detail computational model of bike tire in all reinforcements with concrete material parameters,
- computationally simulate such conditions that may occur during the operation of tires and can be described as critical,
- static testing device modified so that the tire can be loaded with a wheel camber angle,
- propose modification of tread and tire construction, which would increase the possibility of used bicycle tires for demanding applications.

5 REFERENCES

1. Vančo M.: Konštrukcia bicyklových plášťov z pohľadu ich deformačných stavov (The construction of the bicycle tire - casing and their deformation states). Diploma work. University of Alexander Dubček in Trenčín, Faculty of Industrial Technologies, Púchov, Slovak Republic, 2014 (in Slovak)
2. Krmela J.: Systems Approach to the Computational Modeling of Tyres - I. Part. Brno, Czech Republic, 2008, 102 p. (in Czech)
3. Krmela J., Beneš L., Krmelová V.: Statical Experiments of Tire as Complex Long-Fibre Composite for Obtaining Material Parameters and deformation Characteristics, Materials Engineering 19 (3), Slovak Republic, 2012, pp. 124–135
4. Krmela J., Pastorek M.: Determination of Radial Stiffness of Tire from Experiments on the Static Test Device Called Static Adhesor. Metallurgical Journal (Hutnické listy) 65 (7), Czech Republic, 2012, pp. 81–84
5. Horný E.: Prístup k navrhovaniu nových plášťov pneumatík (The approach to design of new tire casing). Diploma work. University of Alexander Dubček in Trenčín, Faculty of Industrial Technologies, Púchov, Slovak Republic, 2014 (in Slovak)

BICYKLOVÁ PNEUMATIKA S TEXTILNÍ VÝZTUŽÍ – EXPERIMENT A VÝPOČTOVÉ MODELOVÁNÍ

Článek se zabývá bicyklovou pneumatikou s textilní výztuží z pohledu experimentu a výpočtového modelování metodou konečných prvků. Pro experimenty bylo použité speciální statické testovací zařízení nazývané statický adhezor. Experimenty lze získat radiální deformační charakteristiky a kontaktní plochy pro různé tlaky huštění pláště pneumatiky. Z radiálních deformačních charakteristik vybrané pneumatiky lze získat hodnoty statické radiální tuhosti. Znalosti o tuhosti a experimentálně získané výsledky jsou důležité pro verifikační analýzy výsledků z MKP výpočtů s experimentálními údaji. V článku je uvedený návrh přístupu k výpočtovému modelování dané bicyklové pneumatiky.

CATIONIC ESTERS OF HYDROXYETHYLCELLULOSE: SYNTHESIS, CHARACTERIZATION AND PROPERTIES

V. Krmelová¹, M. Halaj¹, J. Pleváková¹, I. Sroková¹ and V. Sasinková²

¹University of Alexander Dubček in Trenčín, Faculty of Industrial Technologies
I. Krasku 491/30, 020 01 Púchov, Slovak Republic

²Slovak Academy of Sciences, Institute of Chemistry, 845 38 Bratislava, Slovak Republic
vladimira.krmelova@fpt.tnuni.sk

Abstract: The paper deals with the preparation of amino esters of hydroxyethylcellulose (HEC) and their characterization. Modification was carried out by method of ring-opening of lactam of type N-methyl-2-pyrrolidone (NMP) under catalyse by tosylchloride and pyridine in homogenous reaction medium NMP. The prepared derivatives were characterized by FT-IR spectroscopy and according to this determination, it can be concluded that HEC amino esters have been prepared. Cationic esters of HEC were studied by testing of surface-active and solution properties. In relation to the properties, the most interesting fact is based on complex formation of cationized HEC with CMC anions in the solution and it can be utilized for drug or enzyme encapsulation in future.

Keywords: cationized hydroxyethylcellulose, ring opening reaction, surface-active properties, polyelectrolyte formation.

1 INTRODUCTION

Cationic polysaccharide derivatives have unique properties for which can be used in a wide range of applications. The combination of polysaccharides containing an amino group with anionic active agents can lead to the formation of complexes, aggregates or nanoparticles. Unlike cationic polymers, such as amino functionalized acrylates or methacrylates, cationic polysaccharide derivatives are biocompatible and biodegradable, and therefore are better for use in medicine. Functionalization of polysaccharides is a universal transformation as it provides easy access to prepare a variety of new biomaterials with tailor made properties. Some methods for the synthesis of amino group containing polysaccharide derivatives are described in literature [1–3]. In this study the cationic esters of hydroxyethylcellulose prepared by ring opening reaction of N-methyl-2-pyrrolidone which is reactant and solution was investigated. The structural and solution properties were characterized.

2 EXPERIMENTAL PART

2.1 Materials and methods

Hydroxyethylcellulose-1 (HEC-1, MS=2.5; DS=1.0) was from HOECHST (Frankfurt, Germany), hydroxyethylcellulose-2 (HEC-2, MS=2; DS=1.0; Mw= 250.000 g/mol),

carboxymethylcellulose (CMC, DS=0.7), pyridine and ion exchange resin Amberlite were from Sigma Aldrich (Steinheim, Germany). The HEC were dried before use. N-methyl-2-pyrrolidone (NMP) and p-toluenesulphonic acid chloride (TosCl) were from Alfa Aesar (Karlsruhe, Germany). Sodium dodecyl sulfate (SDS) was obtained from Lachema (Brno, Czech Republic). *Fourier-transform infrared (FT-IR) spectra* were obtained on the Nicolet 6700 spectrometer with an ATR extension piece (Smart orbit diamond) with using 128 scans at a resolution of 4 cm⁻¹ at the Institute of Chemistry, SAS (Bratislava, Slovak Republic).

Synthesis of cationic esters of hydroxyethylcellulose: In a typical experiment, 1.0 g (3 mmol) dry hydroxyl-ethylcellulose was dissolved in 40 ml NMP for 2 h at 120°C under stirring. The HEC dissolved completely after stirring overnight at room temperature. Subsequently 1.2 ml pyridine (16.5 mmol, 5 mol/mol AGU) was added to the HEC solution followed by stirring for 10 min. Then 2.8 g (16,5 mmol, 5 mol/mol AGU) TosCl was added and mixture was allowed to react for 5 h at room temperature. Then 10 ml of water was added dropwise and stirring continued 30 for 30 min. The polymer was isolated by precipitation with 800 ml acetone/ethanol (1:1). The solid was filtered off, washed five times with acetone (50 ml) and dried in vacuum at 40°C. In addition, the sample was dissolved in 40 ml of distilled water

and dialyzed for 5 days against 1 l of distilled water. Distilled water was changed 3 times per day. Activated ionic exchange resin Amberlite (20 g) was added to the polymer solution and the mixture was stirred overnight. Finally, the sample was isolated by centrifugation and subjected to lyophilisation.

2.2 Surface-active properties of HEC-CA derivatives

Emulsifying efficiency was tested for emulsion of the 'oil in water' (O/W) type. The emulsion was prepared by mixing 9 ml water containing 0.05 g of the tested derivative and 1 ml of paraffinic oil dyed with SUDAN IV using the laboratory mixer (Heidolph DIAX 600) at 20 500 rpm for 1 min. The stability of the emulsion was estimated at three time intervals after the emulsions had been prepared, i.e. 5 min (h_1), 1 h (h_2) and 24 h (h_3), and expressed in terms of the height (mm) of the oil and cream layers were formed on the surface of the emulsion.

Surface tension was measured at 25°C using the Du Nouy ring apparatus. The surface tension data were plotted against the logarithm of the polysaccharide concentration in water in the concentration range 0.019–2.5g/l. From the inflection point of the plot, the critical micelle concentration (c.m.c.) and minimum surface tension (γ_{\min}) were derived [4].

2.3 Preparation of polyetectrolyte complexes

According to the Zarth C. [5] procedure was used for the preparation of the complexes. HEC-AE were dissolved in water (1% w/v), and 0.5 M NaCl (polycation in the complex formation) and added to an aqueous solutions of carboxymethyl-cellulose (1% and 0.25% w/v, polyanion in the

complex formation) dropwise using a syringe. Complex formation was assessed visually.

3 RESULTS AND DISCUSSION

Cationic ammonium acid esters based on hydroxyethylcellulose were synthesized via ring-opening reaction of N-methyl-2-pyrrolidone (NMP). According to Zarth C. [1], the HEC-1 and 2 reacted with 5.5 mol TosCl and 5.5 mol pyridine per mol AGU in homogenous reaction medium NMP at room temperature for 5 hour. The reaction conditions, yields and results from surface-active measurements are shown in Table1.

The FT-IR spectra were used to structure characterization (esterification extent) of HEC-AE derivatives. As illustrated in Figure 1, the spectral patterns of the derivatives were similar to those of the starting HEC. The broad OH signal at 3438 cm^{-1} indicated the presence of hydroxyl groups in both derivatives. The absorption band at $\sim 1726\text{ cm}^{-1}$, slightly varying in intensity was attributed to the $\nu(\text{C}=\text{O})$ vibration of the ester groups of both HEC-AE derivatives. By comparing of the height and area of the ester bands can be concluded that were prepared derivatives with different degree of substitution, which are also reflected in the performance evaluation.

The round absorption band at $\sim 1640\text{ cm}^{-1}$ is attributed to the adsorbed water.

The surface-active properties of the HEC-AE derivatives were characterized by surface tension (γ_{\min}), critical micelle concentration (c.m.c.) and emulsifying efficiency. The results are summarized in Table 1.

Table 1 Reaction conditions of HEC-AE derivatives prepared in NMP medium at room temperature, yields and surface-active properties (emulsifying efficiency, minimal surface tension and critical micelle concentration)

Sample	CMC : TosCl : Py	Time (h)	Yield ^a (g/g)	γ_{\min} (mN/m)	c.m.c. (g/l)	Oil / cream layer ^b (mm/mm)		
	(Molar ratio)					h_1	h_2	h_3
HEC-AE1	1 : 5.5 : 5.5	5	0.625	50.6	0.38	0/0	0/0	0/9
HEC-AE2	1 : 5.5 : 5.5	5	0.840	52.1	0.64	0/0	0/2	0/10
HEC-1	-	-	-	53.5	0.34	0/0	0/0	0/9
HEC-2	-	-	-	59.1	0.60	0/0	0/0	0/10
SDS	-	-	-	32.0	1.25	-	-	-
Tween 20	-	-	-	-	-	0/0	0/0	0/11

^a Expressed as g of the recovered derivative per g HEC (on dry mass basis);

^b Height of the oil and cream layers formed on the surface of the emulsion after 5 min (h_1), 1 h (h_2) and 24 h (h_3).

The HEC-AE derivatives are able to moderate decrease the surface tension of water from of 72.8 up to ~50.6 mN/m. The effect was lower in comparison to that of the surfactant SDS (γ_{\min} 32.0 mN/m), but higher when compared to the unmodified HEC possessing γ_{\min} of 59.1 mN/m. The c.m.c. values of modified derivatives were similar as unmodified HEC (~0.34-0.64 g/l) and lower than SDS (1.25 g/l). It has to be noted that the unmodified HEC show surface-active properties due to its nonionic surfactancy imparted by the hydroxyethylene substituent and its high molar substitution [6, 7].

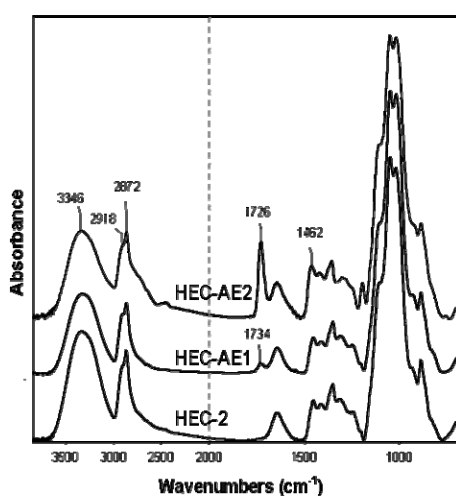


Figure 1 FT-IR spectra of unmodified HEC-2 and HEC-AE1 and 2 derivatives

The tested derivatives exhibited excellent emulsifying efficiency (Table 1), comparable to that of the commercial emulsifier Tween 20. Many polymeric surfactants have been reported to have good emulsification ability but to reduce only moderately the surface and interfacial tension [6, 8]. As seen, the ability of the unmodified HEC to stabilize O/W emulsions was not affected by introduction of amino group. This can be explained by the emulsification mechanisms of polymeric surfactants differing from those of classical low molecular-mass surfactants [9].

The complex formation of cationized amino esters of polysaccharides like cellulose, dextran and HEC with CMC anions in the solution is known from literature [5]. Aqueous solution of cationized polysaccharides was dripped into an aqueous solution of anionic polysaccharide (CMC) and comparatively soft particles were formed by the electrostatic interaction between the ammonium groups of polysaccharides and the carboxyl moieties of CMC. We wanted to know, if HEC-AE derivatives will have same behaviour. Figure 2

shows HEC-AC1 derivative dissolved in water (1%, w/v) dripped into CMC solutions (1%, w/v). The beads were formed, too. But in the case of lower concentration of CMC (0.25%, w/v), the beads had tend to collapse after few minutes.



Figure 2 Complex particles formed from carboxymethylcellulose solution and aqueous solution of derivative HEC-AE1

4 CONCLUSION

Water soluble cationic ammonium acid esters based on hydroxyethylcellulose were prepared by ring-opening reaction of N-methyl-2-pyrrolidone in the presence of TosCl in homogenous reaction media NMP using mild reaction conditions (room temperature, time 5 h and recommendation molar ratio). The FT-IR spectra of HEC-AE derivatives confirmed the presence of ester absorption bands at ~ 1726 cm⁻¹. HEC-AE derivatives exhibited very positive surface-active properties. They lowered surface-tension of water from 71.8 mN/m to ~ 50.6 mN/m and exhibited excellent emulsifying properties comparable to that of the control - the synthetic emulsifier Tween 20. The preparation of the amino esters was indirect confirmed by forming polyelectrolyte complexes, too. The subject of the future investigations will be film formation of HEC-AE derivatives and study of contact angle on different surfaces.

Acknowledgement: This research has been supported by the Slovak grant agency Vega, project No. 2/0085/13.

5 REFERENCES

1. Zarth C., Koschella A., Pfeifer A., Dorn S., Heinze T.: Synthesis and characterization of novel amino cellulose esters, *Cellulose* 18 (5), 2011, pp. 1315–1325
2. McCormick CL., Dawsey TR.: Preparation of cellulose derivatives via ring-opening reaction with cyclic reagents in lithium chloride/N,N-dimethylacetamide, *Macromolecules* 23, 1990, pp. 3606–3610

3. Petzold-Welcke K., Michaelis N., Heinze T.: Unconventional cellulose products through nucleophilic displacement reaction. *Macromolecular Symposia* 280, 2009, pp. 72–85
4. Tomanová V., Pielichowski K., Sroková I., Žoldaková A., Sasinková V., Ebringerová A.: Microwave-assisted synthesis of carboxymethylcellulose - Based polymeric surfactants, *Polymer Bulletin* 60(1), 2008, pp. 15–25
5. Zarth C.: Novel Cationic Esters derived from Cellulose and Dextran: Synthesis, Structure Analysis and Properties, Dissertation at Friedrich-Schiller-Universität Jena, 2012, pp. 1–141
6. Akiyama E., Kashimoto A., Fukuda K., Hotta H., Suzuki T., Kitsuki T.: Thickening properties and emulsification mechanisms of new derivatives of polysaccharides in aqueous solution, *Journal of Colloid and Interface Science* 282(2), 2005, pp. 448–457
7. Sarkar N.: Structural interpretation of the interfacial properties of aqueous solutions of methylcellulose and hydroxypropyl methylcellulose, *Polymer* 25(4), 1984, pp. 481–486
8. Holmberg K., Jönsson B., Kronberg B., Lindman B.: *Surfactants and Polymers in Aqueous Solution*, Wiley, 2002, pp. 1–562
9. Kang H.S., Yang S.R., Kim J.D., Han S.H., Chang I.S.: Effects of Grafted Alkyl Groups on Aggregation Behavior of Amphiphilic Poly(aspartic acid). *Langmuir* 17(24), 2001, 7501–7506

KATIONOVÉ ESTERY HYDROXYETYLCELULÓZY: PRÍPRAVA, CHARAKTERIZÁCIA A VLASTNOSTI

Práca je zameraná na prípravu, charakterizáciu a štúdium vybraných povrchovo-aktívnych a komplexotvorných vlastností amino esterov hydroxyetylcelulózy (HEC-AE). Na ich prípravu sa použila metóda otvárania kruhu N-metylpyrolidónu (NMP) v prítomnosti tosylchloridu a pyridínu v homogénnom reakčnom prostredí NMP. Kde NMP je rozpúšťadlom a zároveň aj reaktantom. Pripravené HEC-AE deriváty sa charakterizovali FI-IR ATR spektroskopiou. Hodnotili sa vybrané povrchovo-aktívne vlastnosti ako povrchové napätie, kritická micelárna koncentrácia, emulgačná účinnosť. HEC-AE deriváty znižovali povrchové napätie vody a vykazovali výborné emulgačné účinnosti porovnateľne so štandardným emulgátorom Tweenom 20. Taktiež je zaujímavá tvorba komplexov aminoesterov HEC s anionovými polysacharidmi vo forme gélov, ktoré sa v budúcnosti môžu využiť v liekových formách. Predpokladá sa i tvorba filmov a posúdenie ich hydrofobicity meraním kontaktných uhlov zmáčania bude predmetom ďalšieho štúdia.

MODEL CALCULATION OF THE THERMAL CONDUCTIVITY AND THERMAL RESISTANCE FOR THE LAYERED LAMINATED TEXTILE FABRICS

Jela Legerská

*Alexander Dubček University of Trenčín, Faculty of Industrial Technologies in Púchov
I. Krasku 491/30, 020 01 Púchov, Slovakia
jela.legerka@fpt.tnuni.sk*

Abstract: *The main aim of the work was to evaluate the thermal transfer through the layered laminated textile fabrics which are applied for the production of car seat covers. The investigation was based on parallel and series model calculation of the thermal resistance and the thermal conductivity and subsequently, the values obtained by the given parallel and series model calculation were compared with real experimental measurements which were measured with help of special devices, such as: Alambeta, Tci and PSM. On the basis of the theoretical model calculations which were compared with the experimental results, it can be concluded that there is the possibility to replace the experimental measurement values by those values which are based on model calculation. Moreover, the influence of compressibility of car seat cover on the change of the thermal-insulating properties was also confirmed.*

Keywords: *thermal conductivity, thermal resistance, porosity, car seat cover, layered laminated textile fabrics.*

1 INTRODUCTION

From the aspect of the increasing requirements relating to the preservation of the customers safety as well as comfort, the high attention is also paid to the car seats and car seat covers. The mentioned high requirements can be described from two specific aspects. The first aspect is connected with the active safety and it means that in the case of any collision, the car seat and safety belts are required to provide maximum protection of all passengers. The second aspect or passive aspect is closely connected with requirements to dissipate the heat and humidity by car seat because it is connected with the good comfort of all passengers [1]. The high heat capacity and low thermal conductivity are the main disadvantages of the car seat covers and this means that long time is desired to be warmed up in the winter and when they are warmed up, they keep the heat for long time and it can be problem in summer. This paper is focused on the calculation of the thermal conductivity and thermal resistance of layered laminated textile fabric used for car seat covers. The mentioned calculation is based on the suitable selection of the model. The input data which were used for calculation involve thickness, mass per unit area, specific density, packing density and porosity. The model calculations have been compared with experimental measurements

thermal resistance. The influence of the thickness on the thermal transfer referring to heat passing through car seat cover was also monitored. The model calculation of the thermal conductivity of the layered laminated textile fabric without air phase was made to simulate the compressibility in the car seat.

2 THEORETICAL PART

2.1 The model calculations

Theoretical calculation of thermal resistance and thermal conductivity is based on parallel and series model. The three phase model was used. These models included the thermal conductivity of the given textile components and it was $K_{s(1,3)}$. Furthermore, it also included the thermal conductivity of the foam which was $K_{s(2)}$ and air with the thermal conductivity for this model was K_a . The relative ratio of the air phase is equal to porosity p_o and the relative part of the fibre phase is equal to $1-p_o$ [5]. Model calculation of thermal conductivity was made according to the equations (2) and (3). Before calculating the thermal conductivity was calculated packing density and porosity according to the equation (1) separately for each component layered laminated fabric. The individual layers of laminated fabric were separated in a specific way one from another during the process of the measurement. This delaminating caused that a little part of the

polyurethane foam was caught on the upper layer of the textile fabric (n.1) and it led to pores clogging. According to the mentioned fact and based on the equations standing for (2) and (3), the limit value of polyurethane thermal conductivity ($K_{pur} = 0.1 \text{ Wm}^{-1}\text{K}^{-1}$) was used instead of the air thermal conductivity (K_a) for calculation of thermal conductivity of the upper layer of the textile fabric using the parallel and serial model.

$$\mu = \frac{\rho_v}{\rho} \quad [0-1] \text{ or } p_o = 1 - \mu \quad (1)$$

Parallel model thermal conductivity:

$$K_{1(2,3)} = p_o \cdot K_a + (1 - p_o) \cdot K_{s1(2,3)} \quad (2)$$

Series model thermal conductivity:

$$K_{1(2,3)} = \frac{K_a K_{s1(2,3)}}{p_o K_a + (1 - p_o) K_{s1(2,3)}} \quad [\text{Wm}^{-1}\text{K}^{-1}] \quad (3)$$

where:

μ - packing density of components of 1, 2, 3 [0...1]

ρ_v - specific density of components of 1, 2, 3 calculated from the ratio of mass per unit area ρ_s [$\text{g}\cdot\text{m}^{-2}$] and thickness h [mm]

p_o - porosity of components of 1, 2, 3 [0...1]

ρ - density of components of 1, 2, 3 (components 1 and 3 = $1.33 \text{ g}\cdot\text{cm}^{-3}$)

$K_{1(2,3)}$ - thermal conductivity of components of 1, 2, 3 [$\text{W}\cdot\text{m}^{-1}\text{K}^{-1}$]

K_a - thermal conductivity of air $K_a = 0.026 \text{ W}\cdot\text{m}^{-1}\text{K}^{-1}$

$K_{s1(2,3)}$ - thermal conductivity of components of 1, 2, 3 where $K_{s1(3)} = 0.218 \text{ W}\cdot\text{m}^{-1}\text{K}^{-1}$ and $K_{s2} = 0.033 \text{ W}\cdot\text{m}^{-1}\text{K}^{-1}$.

It is necessary to point out that the density of foam component of 2 was measured by picnometric method and its values are: $\rho_{A2} = 0.596 \text{ g}\cdot\text{cm}^{-3}$, $\rho_{B2} = 0.541 \text{ g}\cdot\text{cm}^{-3}$, $\rho_{C2} = 0.84 \text{ g}\cdot\text{cm}^{-3}$.

The thermal resistance individual components were calculated according to the equation (4) and the final thermal resistance to the equation (5).

$$R_{ct1(2,3)} = \frac{h_{1(2,3)}}{K_{1(2,3)}} \quad [\text{W}^{-1}\text{m}^2\text{K}] \quad (4)$$

$$R_{ct} = R_{ct1} + R_{ct2} + R_{ct3} \quad (5)$$

where:

$R_{ct1(2,3)}$ - thermal resistance of components of 1, 2, 3 [$\text{W}^{-1}\text{m}^2\text{K}$]

$h_{1(2,3)}$ - thickness of components of 1, 2, 3 [m]

Because the calculation of thermal conductivity and thermal resistance component was made according to the parallel and serial model as the resulting values of is take the average values.

3 EXPERIMENT

3.1 Materials

Car seats are composed of approximately 4 basic parts (if only standard equipment is taken into account). The given 4 parts include metal frame, padding, car seat cover and head rest [2]. This presented study is mainly devoted to car seat covers made in variant A, B, C (Table 1). They are made as layered laminated textile fabrics and they are composed of upper, middle and lower part. Synthetic polyester woven fabrics or knitted fabrics are the materials which are used for manufacturing of the upper part or layer (Figure 1). The middle layer of the car seat cover is made of polyurethane polymeric foam. The thermal or electrical conductivity of the introduced foams is lower in comparison with conductivity of any other textile materials [3]. The fine polyester knitted fabric is used as the third layer. In Table 1 there is the basic information on the monitoring of layered laminated textile fabrics.

Table 1 Experimental data of thickness, mass per unit area, specific density, density and percentage ratio of the components 1, 2, 3

s	h_1 [mm]	h_2 [mm]	h_3 [mm]	ρ_{v1} [$\text{g}\cdot\text{cm}^{-3}$]	ρ_{v2} [$\text{g}\cdot\text{cm}^{-3}$]	ρ_{v3} [$\text{g}\cdot\text{cm}^{-3}$]	comp.1 [%]	comp.2 [%]	comp.3 [%]
A	3.0	3.28	0.70	0.081	0.080	0.080	43	47	10
B	2.97	1.63	0.35	0.112	0.112	0.126	60	33	7
C	1.9	0.43	0.25	0.180	0.174	0.180	74	16	10

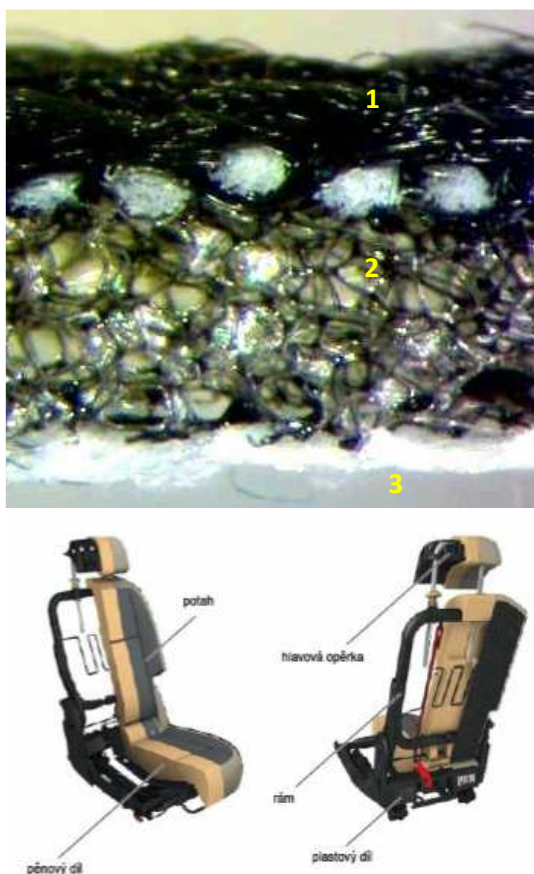


Figure 1 The cross section of layered laminated textile fabric (1 is woven fabrics, 2 foam, 3 knitted fabrics) and the cross section of car seat covers in Škoda Roomster [4]

4 RESULTS AND DISCUSSION

In Table 2, there are model values of the thermal resistance for individual components and for car seat cover as the whole. The calculation of the thermal conductivity of the car seat cover was also made (it was also according to equations (2) and (3)) but it has to be pointed out that the amount of the air in the car seat cover was not taken into account. The air leaves the car seat cover in consequence of compressibility during sitting and it causes the growth of thermal conductivity and decrease of thermal resistance. Table 3 shows that the air in car seat cover

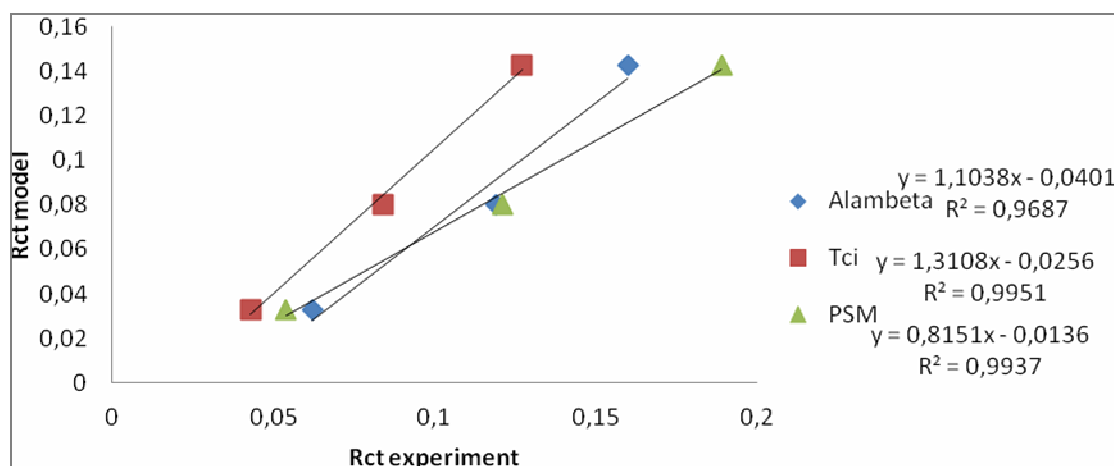
increases its thermal insulation by 30-71%. Table 2 shows that there is the decrease in thermal resistance with the decrease in the thickness of the car seat cover and it means that there is the faster transfer of heat to the environment and therefore, laminated textile fabrics with the lower thickness are more suitable for higher environment temperatures but it is important to emphasize that there is commonly the polyurethane padding of car seat under the layered laminated textile fabric and thus, the process of transfer of heat is markedly slower. On the other hand, the foam padding ensures impact resistance, damping vibrations. From the physiological aspect, the foam with minimum thickness is more suitable but in comparison with the foam with the maximum thickness, the foam with minimum thickness is not suitable from the safety aspect. It was necessary to compare model calculations of thermal conductivity with those one which were obtained in an experimental way because only this comparison could confirm that the model calculations are real. Table 3 shows the results of experimental measurements of thermal resistance and the measurement procedures were performed with help of the special devices including Alambeta, Tci and PSM [7]. The results show a relatively high variability of the measurements. Each of the devices simulates the conditions of thermal transfer between the skin, clothing and environment. However, the technical measurement procedures for the mentioned devices are different and therefore, the measured parameters are also different. The facts about different result obtained by different measuring devices are also based on previous measurements performed by the author of the paper [6] and therefore, simpler model calculations of thermal conductivity and thermal resistance are more suitable to be used. The correlation confirmed high tightness between model and experimental values representing thermal resistance (Figure 2).

Table 2 Model values of thermal resistance for individual components and units

s	R_{ct1} [W ⁻¹ m ² K]	R_{ct2} [W ⁻¹ m ² K]	R_{ct3} [W ⁻¹ m ² K]	R_{ct} average values [W ⁻¹ m ² K]	R_{ct} parallel model [W ⁻¹ m ² K]	R_{ct} series model [W ⁻¹ m ² K]
A	0.019	0.099	0.022	0.140	0.146	0.1396
B	0.019	0.049	0.0097	0.078	0.083	0.077
C	0.013	0.013	0.006	0.032	0.034	0.032

Table 3 Values from experimental measurement of thermal resistance using Alambeta, Tci, PSM devices and values of thermal conductivity

s	K with air [W.m ⁻¹ K ⁻¹]	K without of air [W.m ⁻¹ K ⁻¹]	R [%]	R _{ct} Alambeta [W ⁻¹ m ² K]	R _{ct} Tci [W ⁻¹ m ² K]	R _{ct} PSM [W ⁻¹ m ² K]
A	0.0298	0.009	30	0.160	0.127	0.189
B	0.032	0.015	47	0.119	0.084	0.121
C	0.039	0.028	71	0.062	0.043	0.054

**Figure 2** Correlation of dependency between experimental and model values of the thermal resistance of layered laminated textile fabric

5 CONCLUSIONS

The main aim of the paper was to make the model calculation of the thermal resistance and conductivity for layered laminated textile fabrics. The given models were based on theoretical values of thermal conductivity and density for the individual components of layered laminated textile fabrics. The experimental measurements of thickness and mass per unit area for each one component were necessary for the calculation of porosity for individual components of layered laminated textile fabrics. Based on the literature resources, it is important to point out that the density of foam is in the range 0.4 – 0.8 g.cm⁻³. The picnometric method was used for measurement of foam density in order to verify or specify the mentioned literature data in relation to the foam density. The value of thermal resistance was calculated according to the model equations (2-5). According to the obtained results, it can be concluded:

1. The results of the model calculation for thermal resistance are comparable with experimental values which were obtained with help of special measuring devices including Alambeta,

TCI PSM (Figure 3). The correlation confirmed high tightness between model and experimental values representing thermal resistance. The models calculation based on the simple method can be used as an indicator which indicates what exactly should be measured by help of different measuring devices.

2. It was confirmed that the measurements of thermal resistance are variable and they are also dependent on the type and setup condition of the devices.
3. The layered laminated fabric with an air has greater thermal - isolation properties than the layered laminated fabric without air.
4. The thermal conductivity of car seat is greater in areas where the pressure is caused by passenger because there is the higher concentration of heat and air leaves these pressed areas.
5. Thermal resistance increases with thickness but it decreases with increase of specific density of the car seat cover. This phenomenon can cause that there will be the accumulation of the heat between the layered laminated textile fabrics and padding of the car

seat covers. It is not enough to look for any appropriate solution in relation to car seat cover because the solution and changes have to be carried out also for car seat padding. There are some of changes which can be carried out:

- to replace foam with 3D knitted fabric,
- to install the special ventilation in the car seat,
- to make the holes into the foam of the car seat.

It can be concluded that monitoring of changes in the thermal properties of the textile car seat cover can be good choice for decrease of the production costs.

Acknowledgment: *This work was supported by the project KEGA n. 003 TnUAD-4/2014.*

6 REFERENCES

1. Website:http://www.tyden.cz/rubriky/auta/auto-tema/automobilove-sedacky-racte-se-posadit_88254.html
2. Website Faurecia : <<http://www.faurecia.com>
3. Legerská J., Kopal I.: Thermal properties of laminated materials, International conference TEXCI, December 2013, TU Liberec, p. 32
4. Skoda Auto: study materials: Passive security, internal training document, 2006, p. 36
5. Militký J., Kremenaková D.: Selected topics of textile and material science, Thermal Conductivity prediction of textile materials, TU Liberec, ZČU NTC Plzeň, 2011, pp. 368-374
6. Legerská J.: Study of thermal transmittance, depending on the structure of the fabric, Dissertation thesis, TuAD Trenčín, FPT Púchov, 2010, pp. 81-83
7. Uričová S., Lizák P.: Analysis of thermal properties of car set cover using various pressure, Technolog 5(4), VTS ŽU Žilina, pp. 244-246

MODELOVÝ VÝPOČET TEPELNEJ VODIVOSTI A TEPELNÉHO ODPORU POŤAHU AUTOMOBILOVÉHO SEDADLA

V práci sa zameriavame na hodnotenie prechodu tepla cez poťah automobilového sedadla. Hlavným zámerom bolo vyskúšať paralelný a sériový model výpočtu tepelnej vodivosti a tepelného odporu. Modelové výpočty boli porovnané s experimentálnymi meraniami tepelného odporu na týchto prístrojoch: Alambeta, Tci a PSM. Hodnotil sa tiež vplyv stlačiteľnosti poťahu na sledované vlastnosti. Z teoretických výpočtov a experimentálnych výsledkov vyplýva možnosť nahradit' experimentálne merania vyskúšanými modelmi. Potvrdil sa aj vplyv stlačiteľnosti poťahu auta na zmenu tepelno - izolačných vlastností.

PREPARATION OF BLENDED YARNS WITH MULTIFUNCTIONAL PROPERTIES

Jaroslav Ligas and Kamila Huljaková

VÚTCH-CHEMITEX, spol. s r.o., Rybníky 954, 011 68 Žilina, Slovak Republic
vutch@vutch.sk

Abstract: Today, textile products with added value should be offered on the market in order to obtain competitive advantage. Therefore, this work focuses on preparation of yarns connecting basic characteristics with unique properties e.g. thermoregulating, magnetical, electrical, optical, mechanical, elastic properties and offering, thanks to this combination, wide application possibilities in various fields. These yarns were prepared using a new technology of twisting various types of functional filaments on multifunctional twisting device DirecTwist 2B. Filaments with special functional properties were combined to obtain new special blended yarns with final multifunctional effect. These special properties were subsequently evaluated and a new assortment of textile fabrics with multifunctional properties was prepared using the blended yarns.

Keywords: blended yarns, multifunctionality, thermoregulation, flammability reduction, antimicrobial activity.

1 INTRODUCTION

Today research and development in the field of blended yarns focuses mainly on yarns with multifunctional properties, with improved qualitative parameters, performance characteristics and protective properties and with higher added value. Source materials for their manufacture are mainly special fibre types which are able to ensure not only so-called standard protective function but also to meet more exacting requirements concerning wearing comfort and enhanced protective function. Multifunctionality of textile materials involves integration of at least two and more properties which become even necessary from a viewpoint of final product and its purpose. A basis for achievement of the multifunctional effect of textile materials are mainly special fibre and yarn types incorporated into the textile construction. Special fibre types with multifunctional properties include mainly:

- fibres with reduced flammability, based mostly on aramide fibres and/or blends of aramide and non-flammable viscose fibres ensuring besides protection against heat and fire also high strength and good chemical resistance;
- electroconductive fibres based on metal and/or carbon showing excellent antistatic properties, high strength and abrasion resistance and in dependence on used metal also antimicrobial properties;
- antimicrobial fibres which are able already on a level of bacteriostatic efficiency to prevent

growth and reproduction of various types of microorganisms, inhibit unpleasant odour and increase this way wearing comfort and health protection against dermal diseases;

- fibres with protective function against ultraviolet radiation offering due to additives based on TiO₂ and SiO₂ nanoparticles, incorporated in mass of the textile fibre, protection against adverse effects of solar UV radiation, maintaining at the same time high wearing comfort.

2 EXPERIMENTAL

Experimental part of the work focuses on preparation of multicomponent multifunctional blended yarns using the unique multifunctional twisting device DirecTwist 2B with subsequent evaluation of properties of the special multifunctional yarns prepared this way.

2.1 Preparation of multifunctional yarns

The yarns were prepared on DirecTwist 2B multifunctional twisting device. It is an automatic twisting device with two independent twisting heads (units), with programmable adjustment, designed for preparation of various types of blended yarns from standard (cotton, polyester, polyamide, polypropylene) and special (electroconductive, antimicrobial, non-flammable etc.) staple fibres and filaments.



Figure 1 DirecTwist 2B

At present, highly flexible fibres are applied using doubling technology from independent bobbins in combination with standard textile fibres during technological process of textile manufacture (woven fabrics, knitted fabrics).

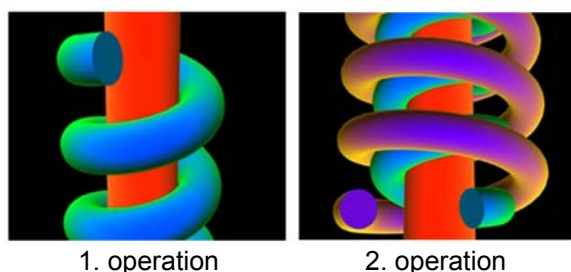


Figure 2 Covering yarn preparation

Highly flexible blended yarns with variable flexibility and physico-mechanical properties for a wide range of applications were manufactured using the new technology of preparation of

blended yarns on DirecTwist 2B multifunctional twisting device. Properties of non-elastic fibres and properties of fibres with high elasticity are linked together in one yarn this way. The new technology of yarn preparation uses a covering type process where diamond yarn is prepared in two subsequent operations.

3 RESULTS AND DISCUSSION

The basic physico-mechanical properties – strength, elongation (Table 1) and workability of the yarn was improved and special properties e.g. antistatic (metal, metallized fibres), antimicrobial (fibres containing silver particles) and transport (profiled fibre) properties were imparted to the yarn. In order to enhance added value it is possible to use also other filament types with special properties (Table 2) and/or to combine optimally the above-mentioned fibres in the yarn shell using wrapping technology. The yarns can be used in a wide range of applications; they are suitable for instance for manufacture of highly functional sportswear for active sportsmen, leisurewear, underwear, swimwear, socks, clothing for pregnant women etc.

An advantage of the multifunctional yarn with reduced flammability and with antimicrobial efficiency is integration of non-flammability (Figure 3), antistatic properties and EMI shielding properties into one, highly multifunctional yarn. The yarn shows excellent properties such as strength, non-flammability, antistatic properties, abrasion resistance, high wearing comfort etc.

Table 1 Twist of specific yarn types, measured and calculated yarn fineness, strength, elongation

	Material used	Number of twists to meter / twist direction	Draft	Calculated fineness [dtex]	Calculated fineness with draft [dtex]	Actual fineness [dtex]	Strength [N]	Elongation [%]
1	1x100 % PES with AM efficiency, 167 dtex 1 x 100% elastane 44 dtex	500 / Z	1.50	222	332	230.08	6.250	38
2	1x100 % PES with AM efficiency, 167 dtex 1 x 100% elastane 44 dtex	500 / Z	2.00	222	443	237.73	6.225	37
3	1x100 % PES with AM efficiency, 167 dtex 1 x 100% elastane 44 dtex	500 / Z	2.50	222	554	230.37	6.763	38
4	1x100 % PES with AM efficiency, 167 dtex 1 x 100% elastane 44 dtex	500 / Z	3.00	222	665	234.36	6.432	35

Table 2 Material composition of a knitted fabric and bacterial reduction

	Material composition of knitted fabric	Bacterial reduction [%] (Staphylococcus aureus)
1	PES with antimicrobial efficiency 167 dtex + elastane 44 dtex, draft 1,5	99.37
2	PES with antimicrobial efficiency 167 dtex + elastane 44 dtex, draft 2	99.23
3	PES with antimicrobial efficiency 167 dtex + elastane 44 dtex, draft 2,5	99.31
4	PES with antimicrobial efficiency 167 dtex + elastane 44 dtex, draft 3	99.29

The yarn is designed for various applications including manufacture of protective clothing for firemen and soldiers as well as workwear. The clothing provides multifunctional protection of the user.



Figure 3 Vertical flammability test, limited flame propagation

4 CONCLUSION

This work was aimed at research evaluation and preparation of a new assortment of blended yarns with multifunctional effect. The new yarn types were prepared using technology of twisting various types of functional filaments on the unique multifunctional twisting device DirecTwist 2B. This way suitable combination of special properties of the yarns was achieved. Special functional properties (e.g. antimicrobial, antistatic, non-flammable) imparted to the blended yarns were evaluated in the frame of the works.

Construction of the blended yarns was improved on the base of the achieved results in order to obtain final multifunctional and/or even synergic effect of the new special types of blended yarns. An assortment of textiles (woven fabrics, knitted fabrics) with multifunctional properties and with higher added value of final products was prepared using the blended yarns. Basic structural and physico-mechanical properties as well as performance characteristics of the prepared fabrics were evaluated and their parameters were optimized.

Acknowledgement: This contribution was worked out in the frame of solution of the project „Multifunctional yarns for clothing and technical applications – MULTIPROTECH“ with financial support of Slovak Research and Development Agency on the base of contract No. APVV-0267-11.

5 REFERENCES

1. Li Z.: Multifunctional differential synthesize air textured yarn, CN 201400743 (Y)
2. Xiaoming L.: Multifunctional silver-fibre fabrics, CN 2898070 (Y)
3. Nobutada Y., Toshiyuki, M.: Stretchable Fancy Yarn Having Antimicrobial Property, JP 2004115954 (A)
4. Zhizhong Q., Ping Z., Zhong L. Chuanxiang Q.: Anti-flaming and anti-static polyester filament yarn and preparation method thereof, CN 101962817 (A)

PRÍPRAVA ZMESNÝCH PRIADZÍ S MULTIFUNKČNÝMI VLASTNOSŤAMI

V dnešnej dobe v textilnej oblasti je potrebné na získanie konkurenčnej výhody na trhu ponúkať výrobky s pridanou hodnotou. Preto táto práca sa zaoberá prípravou priadzí, ktoré v sebe spájajú nielen základné vlastnosti, ale aj vlastnosti ktoré sú unikátne ako napr. termoregulačné, magnetické, elektrické, optické, mechanické, elastické a svojou kombináciou ponúkajú široké možnosti aplikácie v rôznych oblastiach.

Tieto priadze boli pripravené za použitia novej technológie zosúkania rôznych typov funkčných vlákien na multifunkčnom zariadení DirecTwist 2B. Vlákna so špeciálnymi funkčnými vlastnosťami boli kombinované pre získanie nových špeciálnych zmesných priadzí s multifunkčnými vlastnosťami. Tieto špeciálne vlastnosti boli následne hodnotené a nový sortiment textilných tkanín s multifunkčnými vlastnosťami bol pripravený s použitím zmesných priadzí.

TEXTILE DESIGN AS SYMBIOSIS OF TECHNICAL AND ARTISTIC ASPECT

Pavol Lizák

*Alexander Dubček University of Trenčín, Faculty of Industrial Technologies
I. Krasku 491/30, 0201Púchov, Slovakia
pavol.lizak@fpt.tnuni.sk*

Abstract: *Textile design represents a specific and internally differentiated professional activity, combining the elements of technical and artistic creation, which are used in order to shape the different aspects of the world and human communication positively. Design arose from the base of art and architectural activities synthesized in them more and more scientific, technical and artistic disciplines. The aim of the design as a creative professional activity is to achieve a comprehensive quality of objects, processes, services and systems for the duration of their performance and thus contribute to the quality of life. Despite of the fact that the design as a type of creative activity arose from the base of art and architectural activities synthesized in themselves more and more scientific, technical and artistic disciplines, its output affects very diverse spheres of human activity, economy, starting and ending art.*

Keywords: *design, technical aspect, textile design, artistic.*

1 INTRODUCTION

Human skills are at the foundation of value creation and innovation and fashion design adds distinctive added value to the textile product and clothing. Euratex, the European Apparel and Textile Confederation, suggests that 'non-technological' innovation in the textile and clothing sector could represent up to twenty per cent of the turnover invested in product development per annum.

The aim of this paper is to consider the current context of textiles from the perspective of design, manufacture, technological development and product application. The interconnections between these areas are described through discussion of historic and current developments as well as suggested future directions. Textile design is a complex field of practice which operates in a competitive, global industry. Textile designers are often unacknowledged in the process of design, obscured by the names of companies, brands and fashion designers. This contribution attempts to bring clarity to the subject by revealing some of its hidden structures and interrelationships. It also seeks to capture the diversity of textile design through documenting technical and aesthetic considerations together with some of the traditional craft and advanced digital approaches currently applied by different sectors of the industry.

This paper I have divided into the following three sections - Fabric construction approaches to

textile design; Surface approaches to textile design and Applications and advances.

2 FABRIC CONSTRUCTION APPROACHES TO TEXTILE DESIGN

Fabrics are made from yarns and fibres. Fabrics may be made by a variety of processes including weaving, knitting, knotting and twisting yarns together and by bonding fibres together. Yarns are made from fibres (Figure 1), and fibres may be natural such as cotton and wool, or man-made such as acrylic and polyester. Textile fabrics are structures that are made up of yarns or fibres in the form of a plane (essentially a flat or level surface) that is a structure which has a much greater surface area in relation to its thickness.

Yarns and fibres [1] are structures that are for the most part cylindrical and that are very long in relation to their diameter. The performance of any textile structure depends on its properties and characteristics. These are dependent upon a combination of factors including component properties (fibres and yarns), as well as the geometrical arrangement of fibres in yarns and of yarns in fabrics.

Different end uses will require different levels of performance from fibres, yarns and fabrics in terms of resistance to deformation (stress and strain), elongation and extensibility, elastic recovery (degree of return to the initial state after extension), stiffness, abrasion resistance, flexibility, moisture regain (the weight of moisture

in a material expressed as a percentage of the oven-dry weight), heat resistance, combustibility, resistance to light, etc.

Weave designers in industry require a different approach to design creation and development, even though their education may have been identical to that of the craft weaver. Tight deadlines, cost and productivity demands, coupled with performance requirements all have to be taken into account, and this necessitates a more considered approach to the design process. Re-invention of classic fabrics, a trawl through the archives, or interpretations of trend predictions are the most likely routes to a design collection for an industry-based designer; requiring a decisive focused approach. Designs are easily sent electronically to the weaving facility, enabling quick turnaround and ease of editing a design as necessary. Fabrics can be simulated and mapped onto realistically generated garments, bodies or other three dimensional forms giving a good indication of how a given fabric will look in situ (Figure 2).

Simulation of woven fabrics may not, however, always be executed by a specialist weave designer. Lectra Product Lifestyle Management systems include dobby weave design based on a library of weaves and yarns, which can be used in combination to mock-up fabric designs. This type of software does not rely on specialist knowledge of weave structures or how they are formed, but does give the designer a visual tool with which to communicate their ideas.

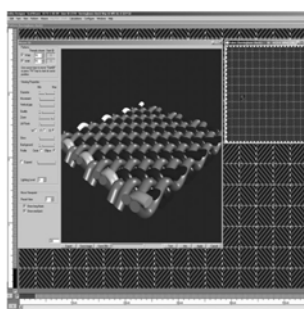


Figure 1 Structure of Yarn **Figure 2** Fabric simulation

Current CAD packages cannot entirely replace the physical weaving of a cloth, as they are cannot easily simulate the physics of weaving; the effect of yarn twist, for example, or the dimensional changes between one weave structure and another. Spider weaves, whose distorted threads are a result of using a combination of long warp threads surrounded by tight plain weave, are one example of this.

3 SURFACE APPROACHES TO TEXTILE DESIGN

For textile design is very important areas of surface design, printed textiles (Figure 3), embroidered textiles, colour and dyeing and finishing, which are considered from the perspective of current commercial practice and future developments. 'Surface design' focuses on the disparate approaches and processes which can now be applied to a broad range of surfaces as well as the potential coatings and finishes available to the designer. These developments have in themselves led to new designing strategies where links between science, technology, art and design are shifting previously held preconceptions about materials, applications and the role of the designer.

As designers and manufacturers make more use of digital systems, so the exploration of the technology will increase. Previous changes in printing technology did alter styles of design, but not fundamentally the methods by which they were created. As noted before, within the last fifteen years, the typical design process has gone from hand drawn or painted to the use of Photoshop® and Illustrator®, both programmes from Adobe's® Creative Suite® package. Although this software does offer designers a very rich range of possibilities, it is perhaps worth noting that a very high percentage of the creative industries are operating within a framework defined by a single corporate entity.



Figure 3 Printed surface

Although the underlying technology is very complex, a uniquely digital printing path from design to manufacture offers the opportunity of a significantly simplified and quickened workflow. There have been many cost and efficiency savings with the advent of digital printing; however, they only demonstrate one half of the story; where inkjet printing can make a real contribution is in relation to design and the

environment. From a design perspective the ability to print full-colour, detailed designs using any scale using repeat or non-repeating elements, engineered printing gives this method plenty of scope to have an impact.

4 APPLICATIONS AND ADVANCES

Today colour [2] forecasting is a fundamental element in the creation of textile and garment collections, and a tool employed by manufacturers, designers and retailers in the development of their apparel collections. It is used in the initial stages of the design process, so has to be available considerably earlier than other trend information, typically two years ahead of the season under development. Colour forecasting involves the systematic evaluation and synchronisation of past seasonal colour influences, socio-cultural and economic factors, fashion trends and the forecasters' intuition, to create several colour palettes applicable to a variety of market sectors each season. As illustrated in Figure 4, all these factors combined result in the final developed colour forecast.



Figure 4 Factor influencing colour forecast

The design and development of textiles for interiors has become more directly linked to fashion cycles as the lifespan of the textile product becomes shorter due to faster changes in trends for interior fashions and the demand for innovation. Consequently the role of the textile designer in the new product development process is far more exciting and challenging. The initial design stage often starts with a created concept on paper, referred to as a moquet, which can be a finished piece of creative artwork or an inspirational idea, with the suggestion of a repeat or layout and colour placement. Textile designers often become specialists in particular areas of design and methods of manufacture, as it is such a complex field and difficult to keep abreast of all of the technical advances from design through to manufacture considering the many different processes that are available today. A design concept can be adapted by CAD and the repeat and layout can be experimented with to achieve the most practical but also the most creative

interior textile. CAD has reduced the overall development time of a product and reduced costs in many ways, for example by reducing the samplings and trials produced on bulk machines and consequently reduced the costs of 'down time' on the machines, that is time not engaged with actual manufacture of bulk goods. One of the most successful advances in CAD is the ability to visualise a design concept for a textile or interior made up and seen as a final application in a room set or superimposed onto a piece of furniture (Figure 5), for example, long before any manufacturing process has even begun.

This advance has enabled textile designers to develop a concept through to the final interior or end application and to experience the overall impression that the product will make. This concept is becoming more popular in all areas of the market including retail, contract and domestic markets.

The work of a designer could be described, in academic terms, as an iterative and creative research methodology; building on known practice. However, the designer's role in a commercial fashion company was (and largely remains) to follow and interpret the existing trends and keep the seasonal fashion cycle operating in high gear. He or she is a democratic actor in the creative team, accorded respect but not autonomy and subservient to the brand values.

Commercial designers are employees, team leaders with executive powers, but rarely business partners. Most are aware that they are 'only as good as their last collection', and easily replaced, so the pressure to deliver profits, without the risk of identifying a personality is intense. Universities and colleges expanded and accredited courses for fashion (Figure 6) and textile design and a wave of art school educated, independent freelance designers and youth orientated brands followed and challenged the hegemony of the elite couture system and stranglehold of dull high street stores [3].

Technical textiles are currently used in agriculture, transport, building industry, furniture industry, shoemaking industry, automotive industry, in hydraulic engineering, products for sport and leisure time.

Inside the structure of flexible (elastomeric) fibers (Fig. 7) are built delicate conductive metal particles. These particles are in original condition distant from one another and the fibers are non-conductive. When the fiber is stretched, twists, compressed, etc. particles closer together. This

reduces the electrical resistance of the fibers to a state of conductivity.



Figure 5 Interior design



Figure 6 Fashion design



Figure 7 Jacket with IPOD

5 CONCLUSION

The structure of a fabric, whether knitted, woven or part of a composite, forms the cornerstone of the material's performance and aesthetic. With the growth of technological advances on all levels we are seeing these structures inspire new designs and even whole new products not previously imagined. Knitted and woven fabrics

can combine a vast array of yarns and be used to create both two- and three-dimensional fabrics as well as eliminate the need for seams. Composites are where two or more materials are brought together to create a third new material with enhanced capabilities. Within this we are seeing embroidery used for its structural rather than decorative qualities alongside innovative fiber laying techniques for yacht sails and other large-scale products. Surface treatments range from coating to finishing and are used either to enhance existing capabilities or to provide the entire performance with the fabric element acting as a carrier for the technology.

All of these developments combine to see textiles used in unexpected areas, as we see them used in medical implants and to make car and truck bodies. Increasingly they are replacing heavier materials such as metals or even concrete, a move influenced by environmental concerns as well as international legislation. This is a trend that looks set to continue well into the future, transforming both the textile industry and the world around us.

Acknowledgment: This work was supported by the project KEGA n. 003 TnUAD- 4/2014.

6 REFERENCES

1. Lizák, P.: Evaluation methods of materials structure. Krakow: Towarzystwo Słowaków w Polsce, 2011. ISBN 978-83-7490-384-4, 86 s
2. Mete, F.: The Creative Role of Sources of Inspiration in Clothing Design, *International Journal of Clothing Science & Technology*, Vol. 18, Issue 4, 2006, pp. 278–293
3. Fletcher, K.: Sustainable Fashion and Textiles: Design Journeys, Earthscan, London, 2008

TEXTILNÝ DIZAJN AKO SYMBIÓZA TECHNICKÉHO A UMELECKÉHO HĽADISKA

Textilný dizajn predstavuje špecifický a vnútorne diferencovanú profesionálnu činnosť, kombinujúcu prvky technickej a umeleckej tvorby, ktoré sa používajú, aby sa pozitívne vytvárali rôzne aspekty ľudskej komunikácie. Cieľom dizajnu ako tvorivej odbornej činnosti je dosiahnutie komplexnej kvality objektov, procesov, služieb a systémov počas ich výkonu, a tým prispievajú ku kvalite života, kde môžu krásu kombinovať s inteligenciou. Dizajn preto je kľúčovým faktorom na začiatku 21. storočia pri inovácii a humanizácii technologických procesov a je významným prvkom v kultúrnych a hospodárskych zmenách. Cieľom tejto práce je ďalej posúdiť aktuálny kontext textílií z pohľadu dizajnu, výroby, technologického rozvoja a použitia výrobku.

IMPACT OF FIBER MACROSTRUCTURE ON TRANSPORT PROPERTIES OF TEXTILE FABRICS

Pavol Lizák¹, Sayed Ibrahim² and Anton Schlosser¹

¹Alexander Dubček University of Trenčín, Faculty of Industrial Technologies
Department of Material Engineering, Púchov, Slovak Republic

²Technical University of Liberec, Faculty of Textile,
Department of Textile Technology, Liberec, Czech Republic
pavol.lizak@fpt.tnuni.sk

Abstract: The cross sectional shape of fibers highly influences the heat and mass transfer through textile clothing. Four polyester fibers of different cross sectional shapes namely trilobal and triangular, plain and air and frictional texturized were used in this work. A relationship between the called shape factors for the different fibers was established. The air permeability and the water vapor transfer were analyzed. It was found that the size of the surface area has an impact on process of processing fibres, determines the penetration of gases or liquids, sorption and diffusion in the fibres.

Keywords: fibres, the specific surface area, transport properties, yarn, heat transfer.

1 INTRODUCTION

1.1 Specific surface area of fibers:

Fiber is the basic structural element of all textile fibrous assemblies [1]. Fiber is sufficiently long and thin configuration. It is characterized by many properties such as length, fineness, diameter, aspect ratio, cross-sectional shape, surface area, specific surface area, strength, breaking elongation, etc. Figure 1 illustrates a fiber of length l , mass m_f , volume V_f , and surface area A_f .

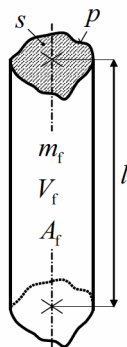


Figure 1 Fiber

Let us assume a homogenous fibrous assembly contains N number of such identical fibers. If L , m , V , A represent length, mass, volume, and surface area of all fibers in the assembly, respectively; then we can write. Values of fiber density are given in Table 1.

Table 1 Fiber density values

Fiber	Fiber density (ρ) [kg/m ³]
Cotton	1520
Linen, jute	1520
Wool	1310
Natural silk	1340
Viscose	1500
Acetate	1320
Polyester	1360
Polyamide	1140
Polypropylene	910

Fiber fineness (t): In practice, it is often necessary to specify the fineness characteristic of fibers. The fiber fineness is usually defined by fiber mass per unit length; in other words, it is called "linear density". The fiber fineness can be expressed as follows:

$$t = \frac{m}{l} = \frac{s l \rho}{l} = s \rho \quad s = \frac{t}{\rho} \quad (1)$$

If a fiber has circular cross section s of diameter d , the value of the diameter d can be easily calculated from equation (2):

$$s = \frac{\pi d^2}{4} \quad d = \sqrt{\frac{4s}{\pi}} = \sqrt{\frac{4t}{\pi \rho}} \quad (2)$$

Let us now consider a fiber with noncircular cross-sectional shape, such a fiber is presented in $P/(\pi d) = 1$ a classical geometrical way without

any defined diameter (Figure 2b). The variable d calculated from Eq. (2) expresses the diameter of an equivalent circular cross-sectional area, which is shown also in Figures 1 and 2b, and this diameter is known as equivalent fiber diameter. The correct value of fiber cross-sectional area can be calculated without considering the real shape of the fiber. Let a fiber with of cross sectional area s and perimeter P , for circular shape it is valid. For all other cases, the value of $P/(\pi d) > 1$.

K. Malinowska [2] established the so-called shape factor as follows:

$$A_f = P * l \quad (3)$$

Accordingly, the perimeter of any fiber can be calculated as:

$$P = \pi d(1+q) \quad (4)$$

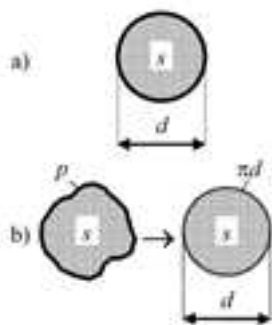


Figure 2 Cross-section fibre

Table 2 Values of shape factor according to Malinowska [2]:

Shape of fiber cross-section	q
Circle – ideal (O)	0
Circle – real fiber	0 to 0.07
Triangle – ideal (Δ)	0.29
Triangle – real fiber	0.09 to 0.12
Mature cotton	0.20 to 0.35
Irregular saw	> 0.60

Fiber specific surface area (a): The fiber surface area is expressed by $A_f = P.l$, and the fiber specific surface area is expressed by surface area per unit mass of fiber. From equations (3) and (4) we can write the following expression for fiber specific surface area:

$$a = \frac{Pl}{\frac{\pi d^2}{4} l \rho} = \frac{\pi d(1+q)}{\frac{\pi d^2}{4} \rho} = \frac{4(1+q)}{\rho d} \quad (5)$$

The surface area of fibers affects significantly many textile properties such as sorption, handle, etc. These in turn affect the physiological, hygienically and thermal comfort parameter of clothing.

1.2 Transport of sweat

Transport properties of water vapor, liquids and energy in textile materials [2], are function of fiber surface properties, contact places between fibers, and capillary spaces between fibers. Macrostructure modification of textile fibers by physical processes affects mainly the transport properties of fibers. Transport properties are heat transfer, transport of water vapor and air permeability are main physiological properties of textiles. Here we will investigate the effect heat on sweat flow through textile fabrics. Sweat occurs on human skin, transport though clothing to environmental sphere. The resistance to water vapor transportation through textile fabrics is given as:

$$R_e = (p_s - p_a).a/H_e \quad (6)$$

where: R_e – resistance of water transport [$\text{m}^2.\text{Pa}.\text{W}^{-1}$].

At higher values of R_e less thermal resistivity against water vapor transport.

R_e has its maximum value in still state. At moving state, this value decreases, due to the heat balance in human body:

$$R_e = \sum R_{et} + \sum R_{eL} \quad (7)$$

R_e – resistivity of water vapor transport of all textile layers including air between layers.

R_{et} – resistivity of water vapor transport in one textile layer

R_{eL} – resistivity of water vapor transport in one air layer.

In single textile clothing layer, the resistance of water vapor is given by following equation:

$$R_e = R_{cL'} + R_{et} + R_{cL''} \quad (8)$$

$R_{eL'}$ – resistance of water vapour transport i.e. the air layer in micro climate under the cloth;

$R_{eL''}$ – resistance of water vapor transport where the air layer is found over the outside layer of the cloth.

2 EXPERIMENTAL

The experimental part deals with evaluation the effect of macrostructure of PE textiles on water vapor permeability. Table 2 shows the cross

section of the PE fibers, with the different fiber data: linear density t , shape factor q and the specific surface area a .

Table 2 Profile of used fibers

Profile of fibers					
t [dtex]	1.3	2.3	4.9	4.9	7
q	0.058	0.18	0.15	0.097	0.13
a [$m^2 \cdot kg^{-1}$]	281	233	156	148	129

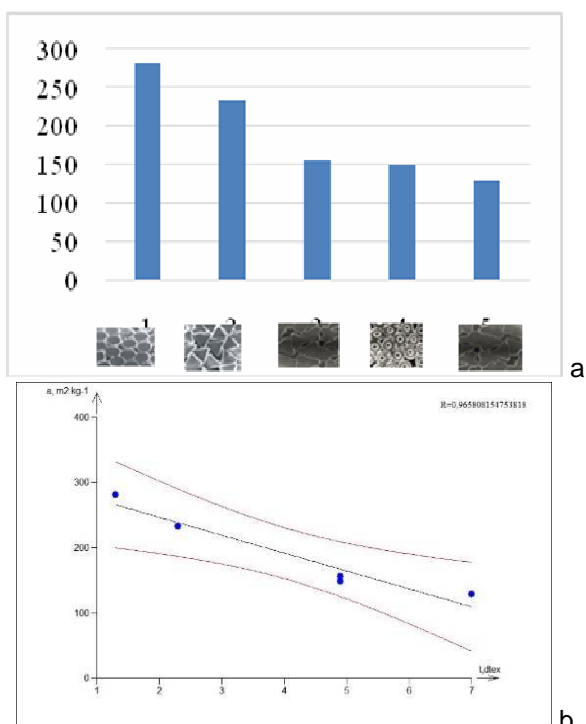


Figure 3 Relationship between (a) specific surface area and profile of fiber, (b) surface area and fiber linear density t

3 RESULTS AND DISCUSSIONS

Figure 4 illustrates the relative humidity of fibers of different cross sectional shapes, namely trilobal and the triangular cross sectional shape, frictional and airtexturized. It is interesting to compare the time needed to reach 100% relative humidity. The fibers of trilobal shape texturized air technology, posses the least time, which is 183 s. Quick transfer of water vapor for textile layer is very important from the point of view of high physical loading to reach the surrounding condition of the micro climate. This phenomena is supported by the capillary absorptivity of the profiled fibers.

Fibers of double T shape show better transport of water to the fabric surface as shown in Figure 4. Fibers texturized by air method obscure better thermal isolation properties compared to fibers texturized by friction method.

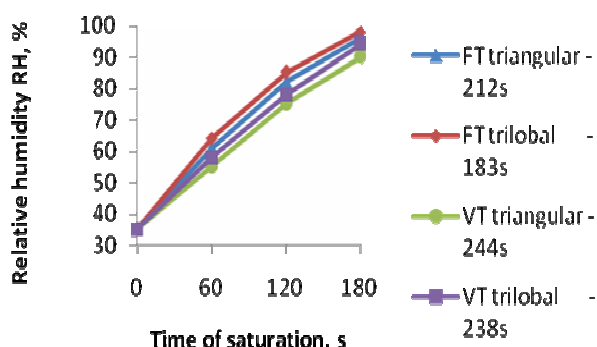


Figure 4 Relative humidity RH versus time of saturation for different PE textile fiber with different profile

The interaction of linear densities of fibers and the cross sectional shape of fibers leads to different pores structure, with different geometrical voids [3, 4], which in turn affect the transfer values of vapor water. Increasing the porous structural parameter, decrease R_{et} and this results in increasing transfer of water vapor.

Figure 5 shows the effect of porosity of blended fabrics PES/CO on the water vapor permeability, which is estimated by about 18.8%. The testing installation consists of porous metal disk have numerous channels which simulates the human skin. The metal disk is heated to a temperature near human skin temperature. The water vapor resistivity can be measured by this method R_{et} [5].

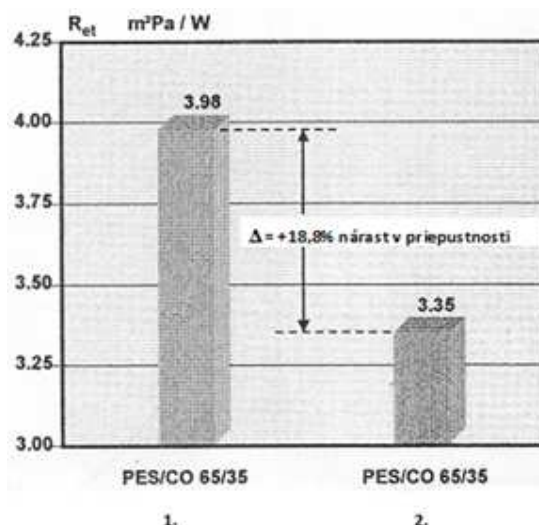


Figure 5 Effect of textile construction with different pore size on relative humidity resistivity

4 CONCLUSION

In the group of evaluated PE fiber profiled laterally, with the cross sectional shapes trilobal and the triangular cross sectional shape, frictional and airtextrized, it was found that the fiber prepared by frictional texturized FT with the trilobal cross sectional shape has the highest capacity to the transport of moisture and high comfort.

The fiber with the trilobal cross sectional shape exhibits a better migration of water across the surface in comparison with the triangular cross sectional shape (Figure 4).

Fiber air textured fabrics provide better thermal insulation properties compared with fibers shaped frictional. The fineness of the fibers in the interaction with the cross sectional shape produces a different porous structure, with different pore geometry, as reflected by the values of moisture. Increasing the pore structural

modifications change is reduced R_{et} and flow of water vapour increases.

Acknowledgment: This work was supported by the project KEGA No. 003 TnUAD- 4/2014.

5 REFERENCES

1. Lizák P.: Evaluation methods of materials structure, Krakow: Towarzystwo Słowaków w Polsce, 2011, p. 86
2. Malinowska K.: Prace Inst. Włok., 29, Lodź 1979
3. Suprun N.: Dynamics of moisture vapour and liquid water transfer through composite textile structures, In: 1st International textile, clothing and design conference, October 6-9 2002, Dubrovnik, Croatia
4. Onder E., Sarier N.: Improving thermal regulation functions of textiles, In: World textile Conference 4th Autex Conference, June 22 – 24, 2004, Roubaix
5. Lizák P., Murárová Z.: Komfort odevov, Krakow, Towarzystwo Słowaków w Polsce, 2013, p. 129

VPLYV MAKROŠTRUKTÚRY VLÁKIEN NA TRANSPORTNÉ VLASTNOSTI TEXTILNÝCH VLÁKNOVÝCH ÚTVAROV

Vlákná sa líšia tvarom povrchu, ktorý je výrazne ovplyvnený priečnym rezom. Všetky vlákna zďaleka nemajú tvar valca, ale vykazujú rôzne profily s tým, že sa tento priečny rez vlákna môže v rôznych miestach meniť. U syntetických vlákien ovplyvňuje tvar povrchu predovšetkým proces ich výroby a tvarovania. Tvar povrchu postihuje mimoriadne mechanické procesy spracovania vlákien. Veľkosť povrchu má vplyv na procesy spracovania vlákien, podmieňuje prenikanie plynov alebo kvapalín, sorpciu a difúziu vo vláknach. Vnútorňý povrch vlákien súvisí s existenciou pórov vo vlákne. Dôležitou charakteristikou povrchu vlákna je merný povrch. Vplyv makroštruktúry na úrovni vlákien, priadzí a textílií je významný na transportné vlastnosti, pričom smerom k vyšším vláknovým sústavám sa zvyšuje. Zvyšovaním jemnosti a členitosti profilu v súbore hodnotených vlákien sa zvyšuje transport vlhkosti. Transportné vlastnosti sú spojené s transportom energií, kvapalných a plyných látok, pričom sa využívajú povrchy elementárnych vlákien, miesta kontaktov medzi vláknami a kapilárne priestory medzi vláknami. Makroštruktúra vlákien modifikovaná fyzikálnymi spôsobmi je hlavným nositeľom transportných vlastností vlákien. Transportné vlastnosti – prestup tepla, prestup vodnej pary a priepustnosť vzduchu podporujú hlavne fyziologické vlastnosti textílií.

EFFECT OF DLC-COATED NEEDLE ON SEWING PERFORMANCE

Adnan Mazari, Antonin Havelka and F. Buyuk Mazari

*Technical University of Liberec, Department of Textile Clothing, Liberec, Czech Republic
adnanmazari86@gmail.com*

Abstract: DLC (diamond-like carbon) coatings are well-known for the properties like protection against wear, low friction of coefficient and high hardness. In this research sewing needles are coated with DLC layer and then investigated for sewing performance. 3-6% less needle temperature is observed for the DLC-coated needle as compared to normal needle. Higher number of "cycles till breakage of thread" is observed for DLC coated needles.

Keywords: Sewing needle, needle temperature, sewing thread, lockstitch.

1 INTRODUCTION

In the sewing process, the sewing thread undergoes friction between fabric, guides, tension devices on machine, bobbin thread and the sewing needle. The performance of sewing thread in apparel industry has become extremely important. Every day, thousands of products ranging from shirts to automotive airbags are sewn. Hence, even small improvements may result in significant corporate benefits. Heavy industrial sewing, such as that used in the manufacture of automobile seat cushions, backs and airbags, requires not only high production but also high sewing quality (i.e. good appearance and long-lasting stitches)[1].

Needle heat-up is a major problem on the sewing floor [2]. In recent years, in order to increase production, high-speed sewing has been extensively used. Currently, sewing speeds range from 1000~4000 r/min. In heavy industrial sewing, typical sewing speeds range from 700~2000 r/min. Depending on the sewing conditions, maximum needle temperatures range from 100~300°C [1]. This high temperature weakens the thread, since thread tensile strength is a function of temperature, resulting in decreased production [12, 13]. In addition, the final stitched thread has 30 - 40% less strength than the parent threads [3, 11, 14]. As a result of improved understanding of the causes of sewing damage, many technical developments, such as improved needle design [4], fabric finishes [5, 6], thread lubrication and needle coolers [7, 8, 15], have taken place over the years.

DLC (diamond like coatings) possesses a small friction coefficient and high wear resistance. Therefore they have been used to improve the service characteristics of various metal parts [9].

In this research we coated the needles with DLC to examine the sewing performance which includes needle temperature and tensile properties of stitched sewing thread.

2 EXPERIMENTAL PART

In this research, needles (100 Nm) are coated with DLC layer by RF/PACVD/MS (radio frequency plasma assisted chemical vapour deposition/magnetron sputtering) method. The coated needles are further compared with the non-coated needles in terms of needle temperature during sewing, surface roughness and sewing performance.

2.1 DLC coating of sewing needles

During the last 20 years DLC coatings became a very attractive material in many industrial applications. In our research we coated the needles (Grozbeckert ,100 Nm, R type) using RF/PAVCD/MS method .The system consists of a cylindrical chamber 290 mm in diameter and 190 mm high, with water cooled bottom electrode connected through a feeder-box to the radio frequency of 13.56 MHz power generator. The magnetron equipped with 60 mm Ti-cathode is mounted in the centre of the chamber top cover. The parameters and steps of sample preparation are as below.

Sample cleaning:

The specimens (needles) were ultrasonically cleaned in methanol for 20 min before deposition. The base pressure of the reaction chamber is kept less than 10^{-3} Pa.

Etching:

The samples mounted on R.F electrode are etched in argon plasma for 10 min at self-bias

voltage = - 500 V, pressure = 4 Pa and Argon gas flow rate of 10 sccm.

Deposition of Ti coating:

Firstly the Ti layer is applied by magnetron sputtering for 5 min with pressure of 1.2 Pa, self-bias voltage of - 300 V, flow rate of Ar. was 10 sccm and power on Ti sputtered target was 1025 W.

Deposition of DLC coating:

The DLC layer synthesis is conducted by RF/PACVD process for 20 min with methane gas at a constant flow rate of 20 sccm, pressure of 20 Pa and self-bias voltage of - 600 V.



Figure 1 Needle after DLC coating

3 RESULTS

The DLC thickness was measured using AFM (Atomic force microscopy) and found to be 960 nm, whereas the Ti-gradient layer was found to be nearly 150 nm. The results (Table 3) from AFM shows that DLC-coated needles shows less average roughness parameters as compared to normal needles.

Figures 2 and 3 show the surface topography of normal needle and DLC-coated needle surface of 10*10 µm and Figures 4 and 5 show the surface image of DLC-coated and normal needles at surface 100*100 µm.

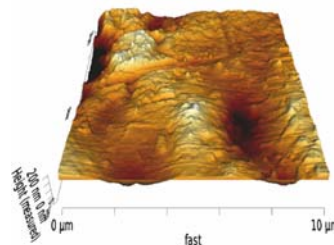


Figure 2 Surface image normal needle

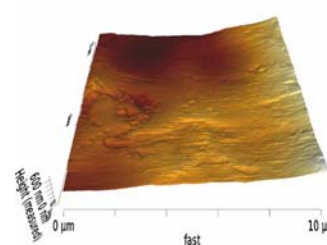


Figure 3 Surface image DLC-coated needle

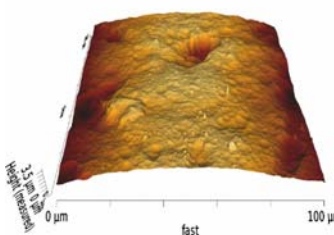


Figure 4 Surface image normal needle (100*100 µm)

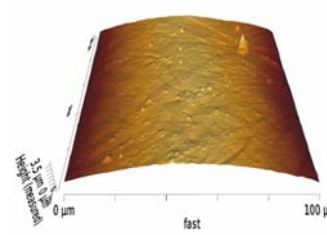


Figure 5 Surface image DLC-coated needle (100*100 µm)

Table 1 Sewing thread used for the experiments

Thread type	Company name/ product name	Fineness [tex]	Twist (t/m)	Twist direction (ply/single)	Coefficient of friction µ
Polyester–polyester core spun	AMANN/Saba C-80	40(20*2)	660	Z/S	0.20
Polyester–polyester core spun	AMANN/Saba C-50	60(30*2)	640	Z/S	0.23

Table 2 Fabric used for the experiments

Fabric type	Weave	Weight	Ends/cm	Picks/cm	Fabric Thickness
100%cotton Denim	2/1 Twill	257 g/m ²	25	20	0.035 cm

Table 3 Roughness properties of needles (100*100 µm)

	Normal needle	DLC-coated needle
Average roughness R _a	689.6 nm	657.7 nm
RMS roughness R _q	802.6 nm	763.2 nm
Peak to valley roughness R _t	3.864 µm	3.837 µm

3.1 Comparison of Tensile properties for DLC-coated and normal needles

Tensile properties of all sewing threads are tested before sewing and after sewing process. Sewing process is performed for 15 seconds and sewing thread is carefully removed from the seam by cutting the bobbin thread. Each thread is measured 10 times each for all thread types respectively.

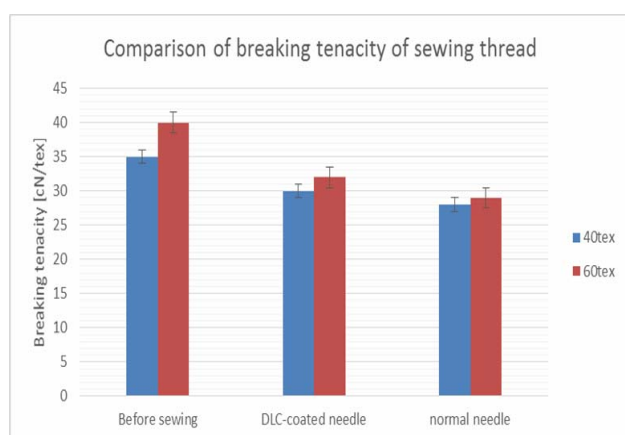


Figure 6 Breaking tenacity of sewing threads

This experiment is necessary to compare normal and DLC-coated needle for the effect of needle temperature and friction on tensile properties of sewing thread. It is visible in Figures 6 and 7 that the tensile properties of sewing thread with DLC-coated needles are 6% higher as compared to normal needles.

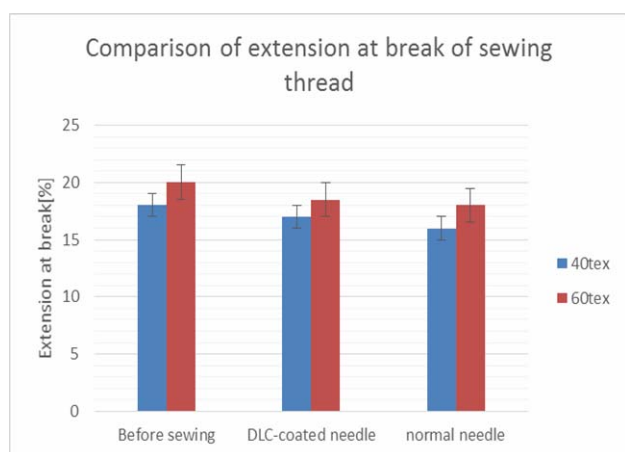


Figure 7 Breaking extension of sewing threads.

This is due to low friction properties of sewing needle coated with DLC and it might be due to the change of emissivity of needle, as the polished normal needle emissivity is 0.06 and for DLC-coated needles is 0.71, which allows more

energy to be radiated from the needle. This increase of emissivity causes the needle to release more energy in the form of radiation and less will be conducted to the sewing thread.

4 CONCLUSIONS

DLC-coating is getting popular rapidly and use for sewing needles can bring significant corporate benefits. Following is concluded from our research:

- DLC-coated needles show better roughness property as compared to normal needles by AFM measurement.
- Needle temperature is 12°C higher for normal needles as compared to coated needles for 40 tex thread and 8°C higher for 60 tex thread. It is due to better surface roughness and friction properties of DLC-coated needles.
- The tensile properties of sewing thread with DLC-coated needles are 6% higher as compared to normal needles. This is due to low friction properties of sewing needle coated with DLC and it might be due to the change of emissivity of needle, as the polished normal needle emissivity is 0.06 and for DLC-coated needles is 0.71, which allows more energy to be radiated from the needle. This increase of emissivity causes the needle to release more energy in the form of radiation and less will be conducted to the sewing thread.
- DLC-coated needles can be greatly useful for clothing companies which require high speed sewing with higher production and productivity.

5 REFERENCES

1. Qinwen Li, and Liasi E.: A study on the needle heating in heavy industrial sewing part-1, *Int. J. of Clothing Sc. and Technol.* Vol. 13(5), 2001, pp. 351-367
2. Hersh S. and Grady P.: Needle heating during high speed sewing, *Text. Res. J.* Vol. 39, 1969, pp. 101-120
3. Midha VK, Mukhopadhyay A, Chatopadhyay R, Kothari VK.: Studies on the changes in tensile properties of sewing thread at different sewing stages, *Text. Res. J* 79, 2009, pp.1155-1167
4. Lewis J.: Clothing finishing procedure for preventing sewing damage in wool and wool/synthetic fiber double jersey fabrics, *Clothing Res. J* Vol. 1(3), 1973, pp. 3-19

5. Poppinswimmer K.: Sewing damage in knit goods- What can be done, *Melliand and Textilberichte* (English edition) Vol. 9, 1980, pp. 1556-1559
6. Fan J.: The Effect of Throat Plate Design on Sewing Damage on an Overlock Sewing Machine, *Res. J. of Text. and Apparel* Vol. 1(1), 1977, pp. 112-116
7. Mazari A., Havelka A.: Optimizing vortex cooling time for Sewing needle of industrial lockstitch machine, *Int. J. of Text. and Fash. Techn.*, Vol 4(1), 2014, pp. 25-34
8. Gurada A., Yukseltan E., Kaplangiray B. and Kanik M.: The effects of various lubricants on the friction properties of sewing threads, *Text. Res. J*, 2013, DOI: 10.1177/0040517512470199
9. Batory et al.: The effects of deposition parameters on the properties of gradient a-C:H/Ti layers, *J. of Achievement in Mat. and Manufact. Eng.* 37(2), 2009, pp 381-386
10. Mazari A., Havelka A. and Hes, L.: Experimental techniques for measuring sewing needle temperature, *Tekstil ve konfesyon*, ISSN: 1300-3356, 2014 (1), pp 68-75
11. Gurada A., Kaplangiray B and Kanik M.: The effects of lubrication on properties and seam performance of sewing threads, *Tekstil ve Muhendis* Vol. 18, 2011, pp 19-25
12. Mazari A., Havelka A.: Influence of needle heat during sewing process on the tensile properties of sewing thread, *Tekstilec* 56(4), 2013, pp. 345-352
13. Yukseloglu M., Citoglu F. Catinkaya B.: A study on the needle heating in polyester blend upholstery fabrics, *Industria Textila* Vol. 63(5), 2013, pp 246-253
14. Sondhelm W.S.: Causes of seam damage: Needle heating, *Journal of Textile Institute* Vol. 44, 1953, pp 580-585
15. [Eryuruk S., Kalaoglu F.: The effects of different amounts of lubricant application on sewing thread performance properties, *Text. Res. J* Vol. 80(12), 2010, pp 1232-1242

VPLYV DLC NÁTEROV IHLY NA ŠIJACÍ VÝKON

DLC (diamond-like carbon) nátery sú dobre známe pre svoje vlastnosti, ako je ochrana proti opotrebeniu, nízkemu koeficientu trenia a vysokej tvrdosti. V tomto výskume boli šijacie ihly potiahnuté vrstvou DLC a následne bol pri šití skúmaný ich výkon. Ihla s povlakom DLC mala o 3-6% nižšiu teplotu v porovnaní s normálnou ihlou. Vyššia pevnosť v ťahu šijacích nití (jadrovej PES nite) je pozorovaná pri šití ihlou s DLC povlakom.

FUNCTIONAL ADVANTAGES OF 3D WOVEN GLASS NANOCOMPOSITES

Rajesh Mishra¹, Vijay Baheti¹, Jiri Militky¹, Dana Kremenakova¹, B.K. Behera²,
Mohanapriya Venkataraman¹ and Veerakumar Arumugam¹

¹Technical University of Liberec, Faculty of Textile, Liberec, Czech Republic

²Indian Institute of Technology, Textile Department, New Delhi, India

Abstract: An exploratory work has been carried out in the field of three phase composites in which flyash nanoparticles were incorporated in addition with 2D and 3D glass woven fabrics while preparing composites. These flyash nanoparticles were prepared by high energy ball milling technique & its effect on functional properties of composites were observed. Functional properties of the nanocomposites were determined and compared with those of regular composites. In thermo-mechanical analysis, the composites with the 3D woven fabrics as reinforcement showed higher storage modulus. Further improvement in the storage modulus due to addition of flyash can be explained as the nanoscale dimension of flyash nanoparticles have got very large surface area which leads to interaction sites & hence efficient load transfer between reinforcing agent & matrix. Though the addition of flyash nanoparticles improved the mechanical properties of composites marginally, a significant improvement was observed in functional properties of composites. The concept of adding nanoscale filler in the matrix material with fabric reinforcement in a new three phase composite has been shown to be very successful.

Keywords: 3D woven fabrics, nanocomposites, DMA, knife penetration, electrical conductivity.

1 INTRODUCTION

Woven fabrics in 2D sheet form have many properties, such as drapability, flexibility, comfort and all of these make them suitable to be used as materials for clothing and other domestic end-uses [1]. However in case of composite applications, the main cause behind the failure is delamination failure of 2D woven laminates whose interface strength is determined by the bond strength between the matrix and multiple layers of fabrics. Also importantly, crimp in the 2D fabric as composite reinforcement significantly reduces in-plane stiffness and strength of composite [2]. These drawbacks of 2D fabrics as reinforcement material for composite demands a better integral structure with substantial thickness, possibly crimp-less & having better strength in through-the-thickness direction. Thus in its initial part, the research has been focused to investigate the thermo-mechanical properties of 3D woven fabrics of various structures in comparison with 2D fabrics [3].

2 MATERIALS AND METHODS

2.1 Specifications for 3D glass fabrics

Different structures of 3D woven fabrics e.g. orthogonal, angle interlock and warp interlock were developed with following specifications. Stuffer warps/m is 500, binder warps/m is 300

and wefts/m is 900. Areal density is 1350-1420 g/m².

2.2 Preparation of composite samples

All composites were prepared by *compression moulding technique*. LY556 Epoxy resin was used as a matrix component for all the fabrics. The principal advantage of compression moulding is its ability to produce parts of complex geometry in short period of time.

2.3 Test methods

Knife penetration test

To carry out this test, the testomic tester M350-10CT was used. This is a machine with an adjustable speed of the penetrating knife and a changeable type of stabbing knife. For the testing purposes of this experiment, a single sharp pointed knife was used.

Thermo-mechanical characterisation- DMA test

The dynamic mechanical analysis of the composite materials was performed on DMA DX04T RMI instrument. The test was performed in three point bending mode with gauge length and sample width of 30 mm and 10 mm respectively.

Characterization of electrical properties

Hewlett Packard (hp) 4339B high resistance meter was used to measure the surface resistance and volume resistance of the composites. The environmental condition for the

measurement was 220°C temperature and 29.5% relative humidity and voltage used was 100 V. Electromagnetic shielding was characterized by the attenuation of electromagnetic field power density by using a simple device.

3 RESULTS AND DISCUSSION

SEM of resin nanocomposite

The scanning electron microscope fractographs of the nanocomposites, are depicted in Figures 1a) and 1b) at two different resolutions. It can be found that the dispersion of fly ash particulates in the matrix for the composite is uniform and the fly ash particulates disperse easily in the matrix. This means that the fly ash particulates could distribute uniformly in the matrix due to their high dispersibility.

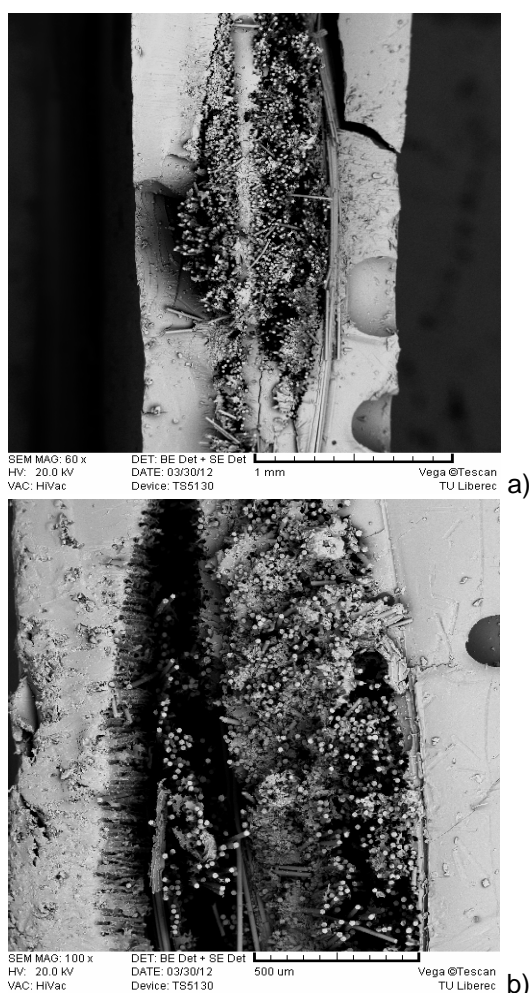


Figure 1 SEM fractographs of the nanocomposites

Knife penetration test

The breakdown strength & the work at breaking load are shown in Figure 2 respectively. 3D woven fabric reinforced composite shows higher

breaking load as compared to the 2D plain woven composite. The 3D orthogonal fabric shows lowest resistance, which may be because of less number of interlacement points in the structure giving chance to easily propagate the crack between the parallel threads when knife penetrates in the composite. The higher deformation of the plain woven composite while penetration of knife results into higher energy absorption & the case is similar for 3D warp interlock woven composite also.

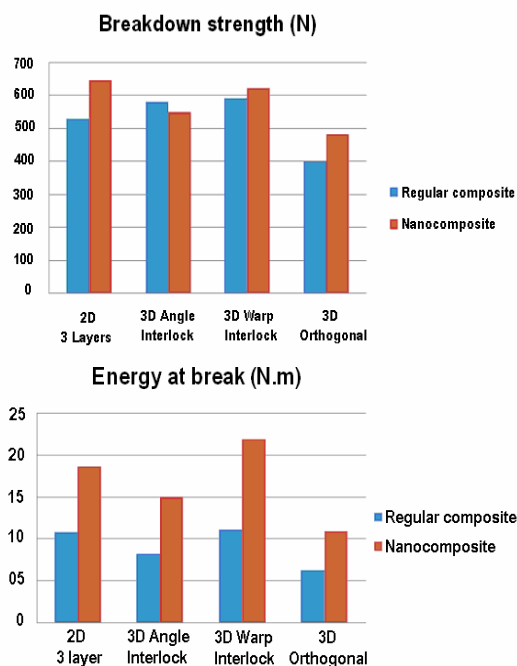


Figure 2 Breakdown strength and energy at break of composites and nanocomposites

The effect of flyash nanoparticles can be observed. The addition of nanoparticles improved the breakdown strength & energy by 30-40%. The uniform distribution of the nanoparticles on the surface as well as between the layers of plain woven fabrics while preparing the composites gave the highest change in the breaking strength.

Thermo-mechanical properties (DMA test)

Effect of fabric structure on thermo-mechanical behaviour of composites

Thermo-mechanical behaviour of the epoxy based composites with different reinforcement structures for regular composites & different loadings of nano flyash in case of nanocomposites has been investigated in this study.

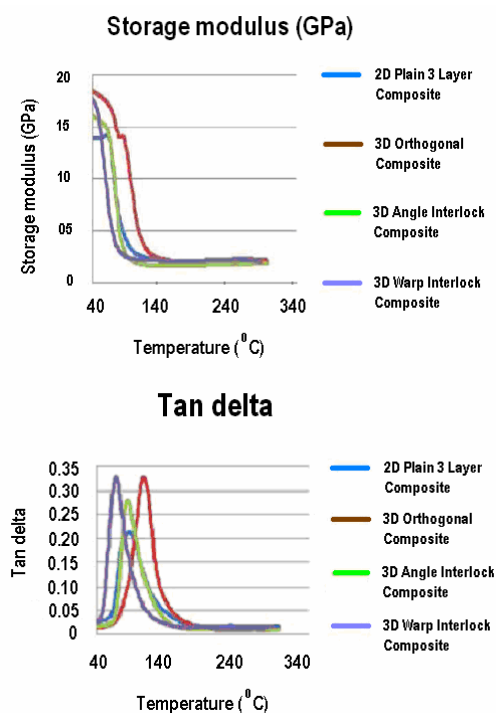


Figure 3 Thermo-mechanical properties of composites

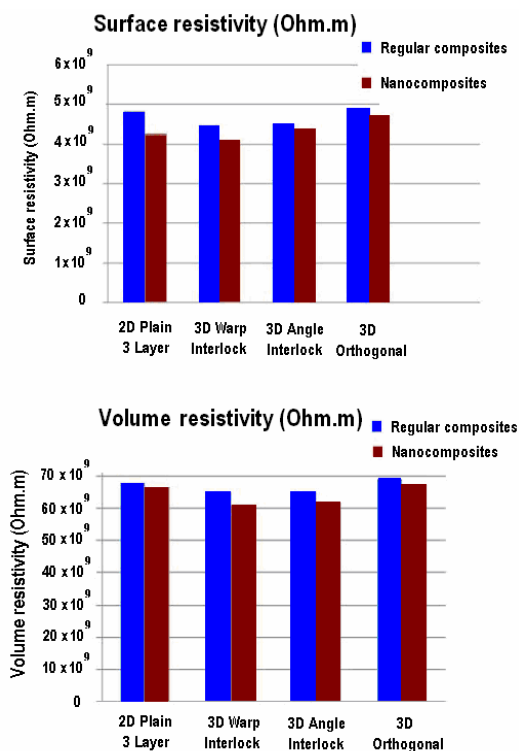


Figure 4 Resistivity of composites & nanocomposites

Electrical properties

As electrical conductivity is the property of material, so there is no significant effect of fabric structure on the electrical properties. All values of surface resistivity of the composites lie in a narrow range of $4.2 \times 10^9 \Omega.m$ to $4.8 \times 10^9 \Omega.m$. And the volume resistivity is also between $6.5 \times 10^{10} \Omega.m$ to $7.2 \times 10^{10} \Omega.m$.

4 CONCLUSION

The concept of adding nanoscale filler in the matrix material with fabric reinforcement in a new three phase composite has been shown to be very successful. The flyash nanoparticles needed for these composites were prepared by high energy ball milling technique. This method of preparation of flyash nanoparticles was found as universal & quick, giving mean particle size of 450 nm. Functional properties of the nanocomposites were determined and compared with those of regular composites. From DMA results, it is seen that storage modulus increased by significant amount while glass transition temperature remained almost unchanged for different composite samples determined by the peak in tan delta. Therefore, the changes in thermo-mechanical properties were due to the physical presence of the nanoclay as opposed to changes in the polymeric network structure. Improvement in the conductivity of nanocomposite is observed due to addition of flyash nanoparticles. This enhancement caused slight improvement in the shielding effectiveness of the nanocomposites. But both these changes are not so significant to be taken into consideration in related applications. This is attributed to properties of flyash particles. Conductive particles can be used for further enhancement of EM shielding.

5 REFERENCES

1. Mishra R., Militky J. and Behera B.K.: Modeling and simulation of 3D orthogonal fabrics, Journal of the Textile Institute, Vol. 103, 2012, 1255-1261
2. Mishra R., Militky J. and Behera B.K.: 3D woven green composites from textile waste: mechanical performance, Journal of the Textile Institute, Vol. 105, No. 4, 2014, 460-466
3. Mishra R., Militky J. and Behera B.K.: Novelties of 3D woven composites and nanocomposites, Journal of the Textile Institute, Vol. 105, No. 1, 2014, 84-92

PVD METHOD USED FOR DEPOSITION OF SILVER AND TUNGSTEN LAYER ON THE COTTON WOVEN FABRIC

Františka Pešlová, Pavol Lizák, Michaela Ďurovcová, Mariana Janeková, Adriána Pavúčková
and Daniela Košťaliková

*Alexander Dubček University of Trenčín, Faculty of Industrial Technologies in Púchov
I. Krasku 491/30, 020 01 Púchov, Slovakia
frantiska.peslova@fpt.tnuni.sk*

Abstract: *According to the fact that the textile surface is not smooth but it is rough and porous, the typical adhesion between basic or initial material (substrate) and coating layer is not able to be provided around the whole surface of the textile material and therefore, it is necessary to point out that the penetration of the pure metal (it was silver and tungsten in this case) into the textile material has to be used. The mentioned penetration provides penetration of nanoparticle into the textile material as well as particle binding to the surface of the fine fibers. The individual fine fibers are the part of the threads which are used for preparation of the cotton woven fabric with the specific thickness and this resulting textile product can be observed in a macroscopic way. Using the static tensile test, the characteristic features of the deposited or penetrated layer were revealed on the basis of the rupture of individual fibers as well as on the basis of the behavior of the cotton sample in its whole volume. The most often observed parameters of PVD layers include thickness, adhesion to the substrate, wear resistance or resistance of coating material to any mechanical loading. In relation to the textile material, the character and chemical composition of the coating layer can have significant influence on the physical properties of the selected substrate (initial or basic textile material). Textile material as a substrate has its own specific features which are based on the material structure. The fiber is the basic constituent or building unit of textile materials. The fine fibers are used for production of yarn and subsequently, the textile fabric is produced. If the textile material has to be used in a correct way, it is necessary to have knowledge on the characteristic features and material properties.*

Keywords: *PVD method, silver layer, tungsten layer, cotton woven fabric.*

1 INTRODUCTION

The submitted paper is focused on the whole complex of problems including the possibility to use new deposition method in order to deposit coating material on the natural material represented by cotton. Physical vapor deposition method (PVD) is the new method which could be used for deposition of special coating material on natural textile materials but it is important to emphasize that in relation to textile materials, there is not a lot of knowledge on this method in technical practice and moreover, the literature knowledge is also only sporadic.

According to the mentioned fact, the investigation was focused on investigation of the quality of the layer deposited on textile material while the microscopic methods were used for the observation. The given microscopic investigation was performed in order to determine the strengthening of the basic textile material and it was also connected with observation of material behavior occurring after the rupture. The

substrate or basic material was represented by cotton and therefore PVD method was selected as the most suitable method because of low temperature which is used during application of the given deposition method and by this way, there was not any thermal influence on the initial or basic material (cotton).

The given paper is devoted to the material problems which are closely connected with the coating material and its deposition on the textile material. In material engineering, the material properties are commonly improved with help of surface treatments – coating or deposition process. Nowadays, the research and development is focused on ordinary materials which have to fulfil the specific requirements in relation to the specific application and therefore, the surface modification or surface treatment can lead to enhancement of these ordinary materials to be used for specific purpose. The application of the metallic elements as coating materials can lead to utilization of the ordinary materials in the technical as well as biomedical practice [1].

2 EXPERIMENTAL

In the given paper, the attention was mainly paid to the investigation and observation of the selected plant-based textile material which was represented by cotton. The cotton weaving leading to preparation of the woven fabric was based on the basic plain weave where the warp threads and weft threads are arranged to form a simple criss-cross pattern [2]. The given prepared cotton woven fabric was used for surface treatment using metals as silver (Ag) and tungsten (W). The selected cotton properties which are needed for experiment performance can be seen in Table 1.

Table 1 The selected material cotton properties

Fiber length	10 – 60 mm
Fiber thickness	12 – 45 μm
Fineness (mass per unit length)	1 – 4 dtex
Moisture Absorption	7%
Strength at dry conditions	2 – 5 cN/dtex
Elongation at dry conditions	6 – 10%
Density	1520–1540 $\text{kg}\cdot\text{m}^{-3}$
Degree of elasticity	74% at overloading of 2% 45% at overloading of 5%

The technology of vacuum evaporation (PVD method) was used for deposition of metallic coating layers on the mentioned textile material while the temperature was 50°C and special coating device called FLEXICOAT 850 was used for the deposition process.

It is important to point out that the selection of the deposition method was closely connected with the selection of the natural material substrate. The given substrate is represented by cotton which has low resistance to the high temperatures [3].

On the basis of the theoretical study and previous investigations, the pure tungsten (W) was used as coating layer on the cotton substrate and subsequently, the given investigation was also extended by research of pure silver (Ag) coating which is the subject of many investigations in relation to the biomedical instruments and aids. Before the investigation was performed, the cotton samples (representing substrate) had been washed at temperature of 90°C because of the stabilization of their proportions.

The coating or deposition process was carried out for large number of samples which were exposed to different deposition or coating time interval in

order to obtain the different thickness of the deposited layer.

In the given work, the silver as well as tungsten layers reach the thickness of 250 nm in relation to the deposition on the cotton woven fabric. The characteristic features of the textile samples before and after deposition can be seen in the Figure 1.

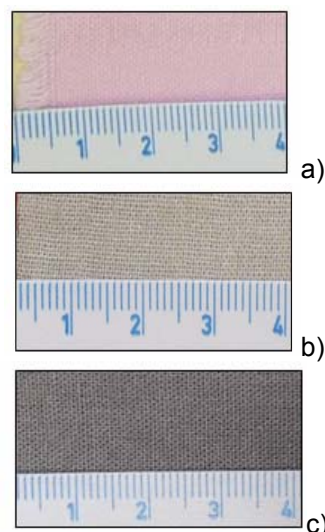


Figure 1 Cotton textile material: a) before any deposition, b) after deposition of the pure silver, c) after deposition of the pure tungsten

After the deposition of the silver layer, the appearance of the initial samples without coatings was changed in relation to the right and reverse sides. In relation to the silver layer, the silver color was observed on the right as well as reverse side and it means that silver coating was able to penetrate up to reverse side but the same effect was not observed in the case of tungsten coating. In the case of the both of investigated coating layers, the behavior corresponds to the physical properties of the pure silver and pure tungsten.

2.1 Textile structure (cotton woven fabric)

Evaluation of the structure was based on the knowledge relating to metallography of the samples which were prepared for microscopic investigation. The samples prepared from cotton woven fabric were observed in a microscopic way while the observation of these samples had been performed before the deposition of the silver layer and the tungsten layer. Subsequently, the pure silver layer and the pure tungsten layer were deposited on the given textile samples and observed in a microscopic way (see Figures 2 – 8). The initial or basic or substrate textile material

can be characterized as heterogeneous with the specific size of pores which represents the open sites between the individual points in the plain weave of the cotton woven fabric (see Figure 2a). In relation to the cotton woven fabric, the more detailed investigation showed (see Figure 2b) that the arrangement of thin fibers outgoing from twisted threads is not uniform.

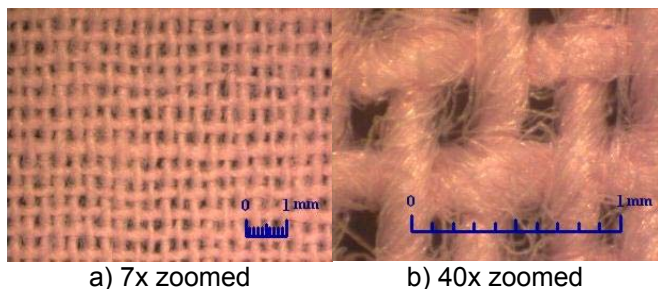


Figure 2 The cotton woven fabric without any coating

3 RESULTS AND DISCUSSIONS

On the basis of the detailed observation of the structure with coating (40x zoomed), it can be concluded that there is the higher compactness of the individual fibers but it is important to point out that the compactness does not mean that the individual fibers are stuck together.

The structure is still the same and surface morphology is smoother because of the absence of the individual thin fibers outgoing from the twisted threads.

In relation to the silver deposition, the individual fibers of the cotton woven fabric were covered with the coating layer (see Figure 5) but in relation to the tungsten deposition the coating layer was observed only on the surface of the substrate. The detailed view of the only one fiber (see Figure 6) exhibits the uniform thickness of the coating layer as well as the fineness of the relief.

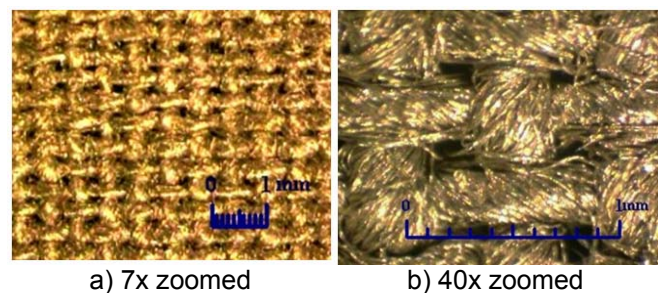


Figure 3 The cotton woven fabric with the silver coating

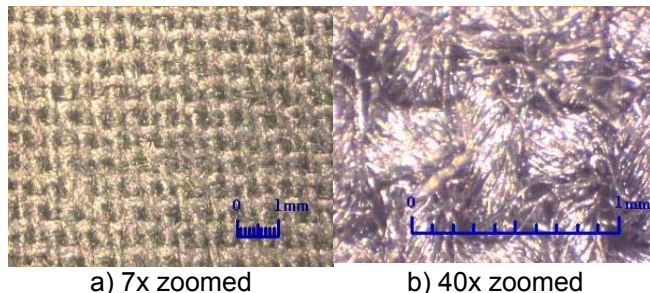


Figure 4 The cotton woven fabric with the tungsten coating

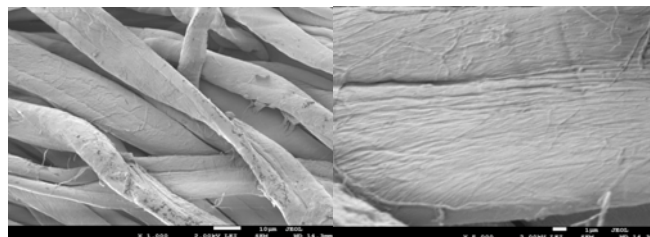


Figure 5 Detail of cotton fibres with metal coating

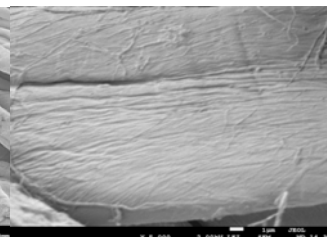


Figure 6 Relief of the cotton fibre surface with coating

After the deposition of Ag layer on cotton woven fabric sample, the given sample was torn and the surface was observed (see Figure 7). The results of this observation are similar to the results based on fractographic observation of the fracture area. It is important to emphasize that fracture behavior of the surfaces has to correspond to the fracture behavior which is characteristic for the given metallic elements (Ag, W) which are used as coating materials. The silver as well as tungsten layer deposited on substrate have very good adhesion ability (see Figure 8) and it can be proven by the fact that the deposition of silver or tungsten layer on the cotton substrate was not connected with the phenomenon representing the flaking of the silver or tungsten layer from the substrate but in the case of the rupture or damage of the coating layer, the whole ruptured or damaged layer was continuously attached to the substrate textile material.

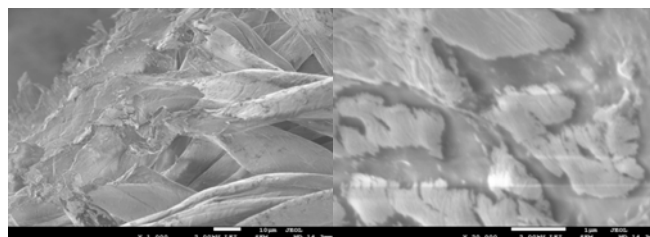


Figure 7 Torn cotton fibers with coating

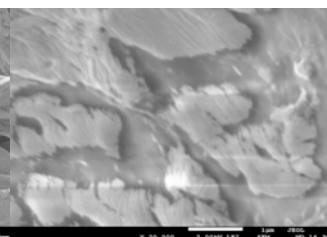


Figure 8 Detail of the cotton fiber surface with coating

3.1 Static tensile test

The samples with and without coating were subjected to the static tensile test in order to investigate the influence of the surface layer on the strength of the textile material. The strips of the same proportions were prepared in order to represent the samples and then, they were torn with help of INSTRON 6025H 1209 – the special tearing machine.

The graphic dependency of the deformation on the loading is the output material in relation to the static tensile test and the given graphic dependency can be seen in the Figure 9.

Based on the graphic dependency, it can be seen that application of coating process leads to the increase of the textile strength and it means that the force which is needed for the rupture or breakage has to be higher. Furthermore, it is necessary to say that there were not any enormous deformations of the cotton textile material because it is very important aspect in relation to the flaking of the coating from the surface. In relation to the tested samples, there was the difference in the force which was needed for the breakage of the textile sample with coating in comparison to the force which was needed for the breakage of the textile sample without coating in the Table 2.

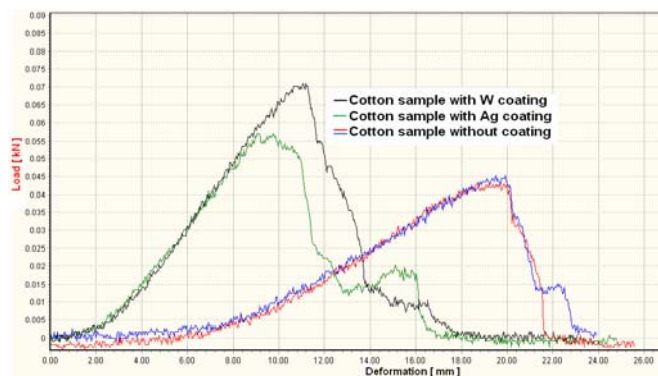


Figure 9 Graphic dependency of deformation on the loading

The investigation was connected with the observation of the characteristic features of the textile rupture (see Figure 10 a, b) and it can be concluded that the textile material with coating exhibited more compact structure of yarns in terms of the woven fabric structure and after the performance of the tensile tests, the given woven fabric structure was less ruptured. It means that individual fibers are more coherent in comparison to the fibers of sample without coating.

Table 2 Force (loading) needed for breakage of the sample with and without coating

Cotton sample	Force needed for the breakage of the sample
Cotton sample without coating	cca 42N
Cotton sample with Ag coating	cca 55N
Cotton sample with W coating	cca 70N

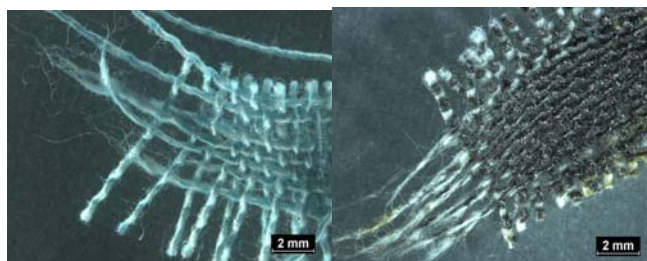


Figure 10 Torn samples of cotton textile material: a) without coating, b) with coating

4 CONCLUSION

According to the performed investigation, it can be concluded that selected metallic materials can be deposited on cotton because the original properties of cotton are not changed. Although the original properties of cotton are not changed, the silver or tungsten layer deposited on cotton caused that the given cotton woven fabric is strengthened and there are the diametric physical surface changes.

In the case of silver deposition on cotton, the new type of antibacterial material is formed while this new type of material is shapeable in various ways without any significant extension of wear or crumbling in relation to the silver coating layer. When the tungsten layer is used to be deposited on cotton, it is possible to use the given textile material at high temperatures – production of the fireproof clothes.

On the basis of the obtained results, it can be pointed out that deposition of the coating layers on the natural textile materials can lead to the production of new composite materials with the changed materials properties while the properties of basic or initial (substrate) material are preserved.

Acknowledgements: This work has been supported by KEGA č. 003TnUAD-4/2014.

5 REFERENCES

1. Lizák P., Legerská J., Ligas J., Uričová S., Drobny M.: The relationship between the pressure and the amount of fibers in the fiber structure, HUTNICKÉ LISTY Year. LXIV No. 7, 2011, pp. 112-114
2. Lizák P.: Evaluation methods of materials structure, Krakow, Towarzystwo Słowaków w Polsce, 2011, p. 86
3. Anisimov E., Pešlová F., Holec J., Horník J. s.l.: Microscopy and Non-destructive Materials Testing, 2010

PVD POVLAKOVANÁ BAVLNA STRIEBROM A WOLFRÁMOM

Predložená práca sa zaoberala problematikou, ktorej je v technickej praxi venovaná pomerne malá pozornosť. Jedná sa o možnosť aplikácie novej povlakovacej metódy PVD na prírodný materiál akým je bavlna. V literatúre sú len sporadické poznatky o povlakovaní textílií, preto úlohou tohto výskumu bolo využitie mikroskopických metód pre sledovanie kvality nanoseného povlaku. A to ako z pohľadu možného spevnenia základného textilného materiálu tak aj z pohľadu jeho správania pri porušení. Vzhľadom k tomu, že sa jedná o bavlnenú textíliu bola zvolená povlakovacia metóda PVD, ktorá nevyžaduje vysokú teplotu povlakovania, čím sa vylúčilo teplotné ovplyvnenie povrchu. Keď vychádzame z toho, že východiskový povrch textílií nie je rovinný ani hladký, ale pomerne veľmi drsný a pórovitý nebude sa jednať o typickú adhéziu povlaku k celkovému povrchu textílie, ale aj o penetráciu čistého kovu (v našom prípade striebra a wolfrámu) do vnútra textílie s následným uchytením nanočastíc, na povrchu jemných nití. Tieto kovom nasýtené nite sú súčasťou vlákna, ktoré je formované svojou väzbou do určitej hrúbky textílie tvoriacu následne jej makroskopickú rovinu. Charakter povlaku sa pri statickej skúške v ťahu prejavil nielen v porušovaní jednotlivých vlákien ale aj v správaní sa celého objemu bavlnenej vzorky. Je možno predpokladať, že sa povlakovanie prejaví aj na materiálových vlastnostiach zvolenej textílie.

COMPUTER GRAPHICS IN TEXTILE DESIGN

Pavol Rusko

*Catholic university in Ruzomberok, Pedagogical Faculty, Department of Art
Ruzomberok, Slovak Republic
p.rusko@centrum.sk*

Abstract: *Creativity is the guarantee of pushing the borders of quality further and the birth of new discoveries in all of the departments. The outstrokes between design and fine art bring the new inspiration in collaboration of the designer and the artist. Depending on the differences and similarities of the methods used in the work of graphic and textile designer we are able to allocate the application of computer graphics in textile design.*

Keywords: *Creativity, art, textile design, graphic design, computer graphics.*

The relationship between the fine art and design, but also art and design has existed eversince and these components of human activity are affecting each other. Art and craft weren't always divided into separate groups. There was only one, named "techné".

Craftsman was also an artist. A lot of workplaces for painters and sculptors existed that time. For example, big maestros as Leonardo da Vinci or Michelangelo Buonarotti reached more fields and affected painting, sculpting and architecture. Also a lot of other artists working in workplaces with their scholars created cartons for tapestries that were then produced by people in the tapestry manufactures. Also one of the best-known Flemish baroque painter Peter Pavol Rubens worked this way. In todays terminology we are able to say, that he was a tapestry designer, while thinking back, that time the tapestry was a woven picture representing historical topics or allegories. Fine art, design, architecture met again in Bauhaus, where artists like Kandinskij, Mondrian, Moholy Nagy, etc. were trying to integrate these departments into one under the leadership of Walter Gropius. The name of Bauhaus is formed by two german words: Bau - to build and Haus - house. Their goal was to build an imaginary house, where the architecture, the furniture and also the textice components and fine art products were connected. It needs a team work on a collective topic to get this result. The art school Bauhaus was formed and leaded by Walter Gropius in 1919 in Weimar, then in 1925 the school moved to Dessau, where it was leaded by Hannes Meyer and in the last year of its existence it moved to Berlin, where it was consciously leaded by Mies van der Rohe until the Hitlersdictature didn't close the school. The

references and tendencies of Bauhaus affected also a lot of different schools, just like the ŠUR – Škola umeleckých remesiel in Bratislava.

In the end of the last millenium there were lot of prognoses, that the 21st century will be the century of design and I guess it's true by watching changes in the car facelifts, fashion collections, new colour trends and clothes cuts. The improvement of digital technologies, the quality of computer programs and last, but not the least the access to the personal computers caused, that the working process of the designers has changed a lot during the past decades.

While in 80's, the textile designer designed a pattern, there were other people to work with the design then. We can recognize a new type of specialization, to which are all of the students of art academies led. For example the Department of Textile on Academy of Fine Arts and Design in Bratislava contains of three different sections. Section of textile in fine art, fashion design and textile design. (During the time of my studies /1981-1987/ there was only one section that included all of these three forms on the Department of Fine Arts).

There are two tendencies in these times, I mentioned the first: specialization and the other one is that lot of painters or sculptors feel the need to include design to the field of their activity. Interest in digital technologies and also work with computer programs (visualisations, 3D modelations, etc.) Also some of the designer products like T-shirt or cap prints start to become an interesting topic in both sections, graphic and textile design. So there's a similarity between the work of textile and graphic designer, but they're not the same. The process and way of thinking is different.

I'm going to present you some of these mentioned similarities and differences.

Both of them are using graphic programs just as Adobe Illustrator, Photoshop, CorelDraw, etc.

Textile designer:

- sees the pattern as definitive, self-consistent, depending on a inner structure of the textile and technology of production
- graphic feature is a component of a structure, it has decorative meaning and can be imprintable, woven or knitted
- orientation of the pattern depends on use: one- or both-sided is used mostly in furniture design, four-sided is used in fashion design and is used because of the smallest amount of trash and the patterns could be naturally connected

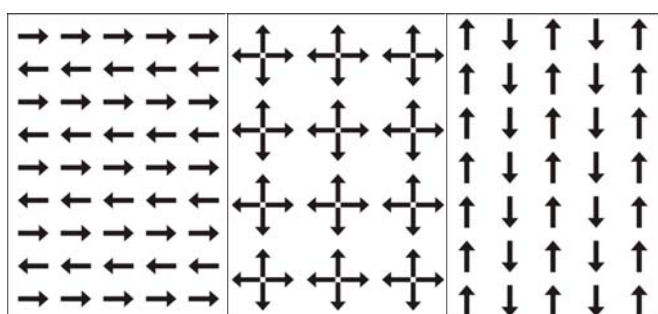


Figure1

Figure 2

Figure3

Graphic designer:

- sees the pattern as a raster of pixels or a structure that includes a topic, but prepares a space for typography or motives depending on use (for example the pattern used as a packaging design)
- pattern is most likely printed
- the orientation of the pattern is tied to used forms of reading the texts in our language, from the left side, to the right one or from up to down.

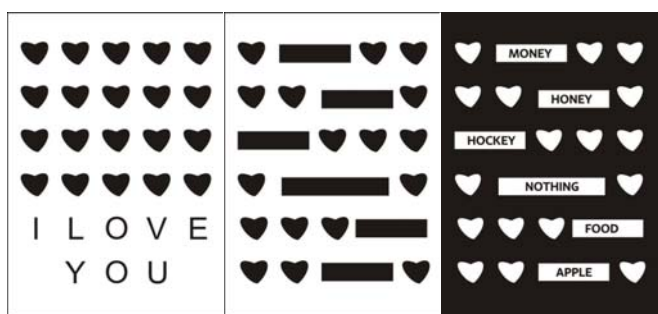


Figure4

Figure 5

Figure 6

Next difference by T-shirt designing is that the graphic designer is focusing more on the content and the textile designer on decorative part of the process.



Figure 7 T-shirt, that is probably sewn out of a striped netting by a textile designer



Figure 8 Pattern designed by a graphic designer that was printed on a T-shirt

In this moment it's not important what kind of print is it. And there also can come a moment, when a graphic designer creates a design, which is printed on the textile before it's cut and sewn into clothes or a different product.

We've been talking about the similarities and differences of creating and thinking of a graphic and a textile designer. Let's think of the possibilities of the application of fine art into textile design through computer graphics as a separate form of art. I'll use my own computer graphics that were created by frottage of the structures got by blueprint to demonstrate this idea. I recreated these structures in CorelDraw and then duplicated them horizontally and vertically. The result is a structure, that can have a various use in textile design, like housing design_curtains, bedding, fashiondesign_shirting. In the end, I'd like to mention, that the term "computer graphics" is even wider than the idea of fine art graphic pattern designed in computer, printed in printhouse in some edition size and signed.

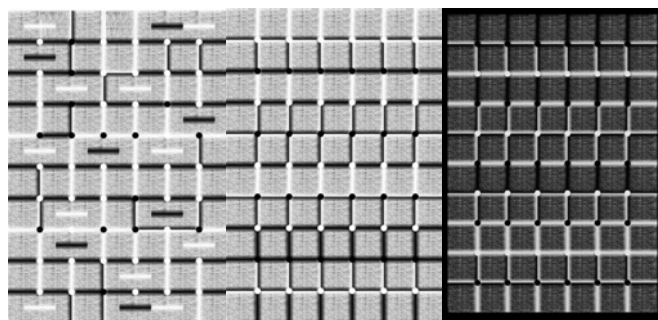


Figure 9

Figure 10

Figure 11

From the informatics point of view, we can see this term as the whole system of recognizing and presenting information in computer. From the designer point of view, the whole field of visual communication, system of glyphs, fonts, resolution of colours in use with computer programs. I think that the use of digital technology and the computer, as the tool of progress,

computer programs, graphic, designer and lots of others will motivate creative people to work with each art and designer disciplines at the same time.

I believe that the most important element in this chain will still remain the human.

1 REFERENCES

1. Gombrich E.H.: Příběh umění, Praha, Argo 1995, ISBN 8020406859
2. Kolesár Z.: Kapitoly z dejín grafického dizajnu, Bratislava, Slovenské centrum dizajnu, 2006, 213 s, ISBN 8096865854
3. Dabner D.: Grafický design v praxi, Praha, Slovart, 2004, 128 s, ISBN 8072095978.
4. Rusko P.: Počítačová grafika 2000-2010, Ružomberok, Verbum, 2010, 99 s. ISBN 9788080846602

POČÍTAČOVÁ GRAFIKA V TEXTILNOM DIZAJNE

Kreativita je v každom odbore zárukou posúvania hraníc kvality a vzniku nových objavov. Presahy medzi voľným umením a úžitkovým, ale aj umením a dizajnom prinášajú novú inšpiráciu v spolupráci umelca a dizajnéra. Na rozdieloch a podobnostiach postupu grafického a textilného dizajnéra pri tvorbe dezénu demonštrujeme aplikáciu počítačovej grafiky do textilného dizajnu.

ANALYSIS OF THE ELECTRICAL AND MECHANICAL PROPERTIES OF HYBRID YARNS DESIGNATED FOR PROTECTION AGAINST ELECTROMAGNETIC FIELD

Veronika Šafářová and Jiří Militký

*Technical University of Liberec, Faculty of Textile Engineering, Czech Republic
veronika.safarova@tul.cz*

Abstract: Hybrid yarns with enhanced electric conductivity were prepared during the research. They were designated for development of a hybrid electromagnetic shielding fabrics. These yarns were composed of polypropylene and extremely thin steel fibers in staple form. Yarns were produced in two special linear densities and they contain different conductive component content (1-60%). Electrical properties of these yarns and chosen mechanical properties depending on yarn structure and conductive component content were studied. It was found that dependence of electric resistance on clamping length is highly nonlinear for yarns containing the conductive staple metal fibers. The main aim of this paper is investigation and validation of a simple mechanistic model describing this dependence. Characteristic parameter of this model is so called specific resistivity α . This factor is used for expressing the influence of content of metal fibers on the yarns conductivity or resistivity changes. Moreover, effect of metal fiber content on Young's and dynamic modulus, tenacity and elongation of hybrid yarns was evaluated.

Keywords: hybrid yarn, metal fiber, electrical conductivity, mechanical properties.

1 INTRODUCTION

Over the last few years, there has been mounting concern about the possibility of adverse health effects resulting from exposure to radiofrequency electromagnetic (EM) fields, such as those emitted by wireless communication devices. In 2011 the World Health Organization/International Agency for Research on Cancer (IARC) has classified radiofrequency electromagnetic fields as possibly carcinogenic to humans (Group 2B), based on an increased risk for glioma, a malignant type of brain cancer, associated with wireless phone use [1]. For the reason given above, a demand for protection of human beings against undesirable influence EM signals and troublesome charges has been increasing.

The best material for shielding or absorption of EM wave must have both high electric conductivity and high magnetic permeability and that shields based on the use of metals and magnetic alloys are the best ones. In contrast, most synthetic fabrics are electrically insulating and transparent to EM radiation [2]. There are several approaches how to make electrically conductive textiles. One way how conductive fabrics can be created is by using minute electrically conductive fibers. They can be produced in filament or staple lengths and can be incorporate with traditional non-conductive fibers

to create yarns that possess varying degrees of conductivity. Another way represents conductive coatings which can transform substrates into electrically conductive materials without significantly altering the existing substrate properties. They can be applied to the surface of fibers, yarns or fabrics. The most common are metals and conductive polymer coatings.

However, electro-conductive yarns often suffer from poor mechanical properties, unexplored electrical properties and reduced elongation. Therefore, they often face problems as they are deformed, draped and subjected to stress during application. Consequently, there is a need for investigation of electrical and chosen mechanical properties of yarns with enhanced conductivity.

In our research, conventional blending and spinning textile techniques were applied to produce electro-conductive yarns, in which the conductive fibers are distributed randomly. Our aim was to produce high electro-conductive yarns preserving main properties of traditional textile structures designed for preparation of protective fabrics against electromagnetic field. In this paper an analysis of the yarn's applicability and reliability is presented. Hence, influence of metal fiber component and structure on the yarns conductivity or resistivity was studied. Dynamic modulus, tenacity and elongation changes with different metal fiber content in yarn were also

evaluated. Moreover, percolation thresholds for different yarn characteristics were examined.

2 EXPERIMENTAL

2.1 Hybrid yarns

Hybrid yarns were composed of conventional polypropylene (PP) fiber and different content of staple BEKINOX stainless steel (SS) metal fibers (1-60%). The aspect ratio (length/diameter ratio, l/d) of the SS used in this study is 6250, since the diameter of the SS is 8 μm and the fiber length of the SS is 50 mm. In this study, TREVON polypropylene fiber with a fineness 2.2 dtex and 50 mm length was used as a non conductive component. The two components were mixed at the drawing frame and a ring spinning system was used to produce blended yarns. Hybrid yarns were prepared in two different linear densities: (a) single yarn (fineness of yarns was 25 tex), (b) two ply yarns (fineness of yarns was 2x25 tex).

Figure 1 presents microscopic images of hybrid yarns with different content of conductive component. The detailed specifications of all samples are listed in Table 1.

Table 1 Specification of yarns samples

Sample ID	Material composition	Linear density [tex]
H1	99% PP / 1% SS	25
H3	97% PP / 3% SS	25
H5	95% PP / 5% SS	25
H10	90% PP / 10% SS	25
H15	85% PP / 15% SS	25
H20	80% PP / 20% SS	25
H20-50	80% PP / 20% SS	50
H40-50	60% PP / 40% SS	50
H60-50	40% PP / 60% SS	50

2.2 Characterization

The properties of yarns were tested as follows; linear density of yarns was evaluated according to ASTM D1907, tensile strength and elongation was evaluated according to ISO 2062:2009. Single-end breaking force and elongation at break of yarns were determined using Instron 4411 at constant rate of extension (500 mm/min), 500 mm gauge length, load cell 5 kg.

Velocity of the sonic pulses in yarns, resp. their acoustic dynamic modulus was tested using Dynamic modulus tester LH-551.

The yarn resistance R [Ω] at gauge lengths 0.01; 0.05; 0.1; 0.125; 0.15; 0.20; 0.25 and 0.3 was

evaluated by the two conductors method. All samples were conditioned in $20\pm 2^\circ\text{C}$ and $40\pm 5\%$ RH. Each sample at each gauge length was measured 30 times and for subsequent statistical evaluation the sample median was used to estimate location, because end-values may be measurement errors.



Figure 1 Microscopic images of two ply hybrid yarns containing (a) 15%, (b) 60% of conductive component

3 RESULTS AND DISCUSSIONS

3.1 Electrical properties

In the report [3] was found that for yarns containing the conductive metal fibers is dependence of electric resistance R on L highly nonlinear and simple mechanistic model was created:

$$\alpha = \frac{R(n+1)}{L^{n+1}} \quad (1)$$

where: α – specific resistivity factor, R – yarn resistance [Ω], n – factor connected with attenuation of electric conductivity, L – yarn length.

Main aim of this contribution is verification of proposed mechanistic model describing the dependence. The dependence of yarn resistance R on the yarn length L for chosen yarns with linear density 25 tex is shown in the Figure 2. It was confirmed that electrical resistance is nonlinear convex increasing function of clamping length. For 25 tex yarns, the model with factor $n = 1.5$ was chosen as the most suitable (based on least square method). It was found that specific resistivity factor is decreasing (conductivity of the yarn is increasing) with increasing metal fiber content (at conserving factor n) and the percolation threshold is about 5% of SS.

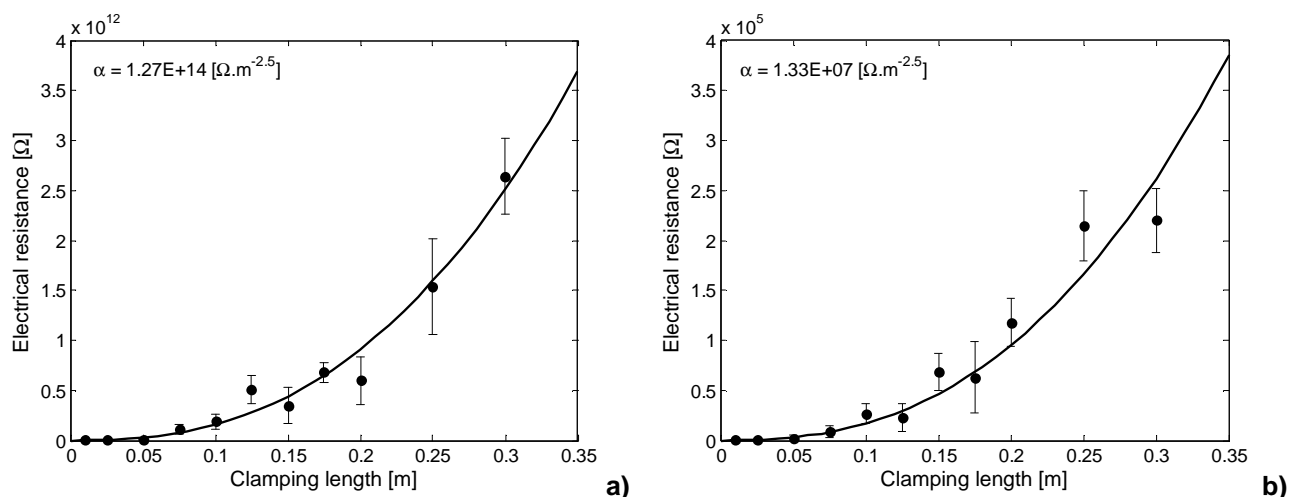


Figure 2 Dependence of electrical resistance on the yarn length (points are sample medians and solid line is model see eqn (1), $n = 1.5$ for a) yarn containing 10%, b) yarn containing 20% of metal fiber

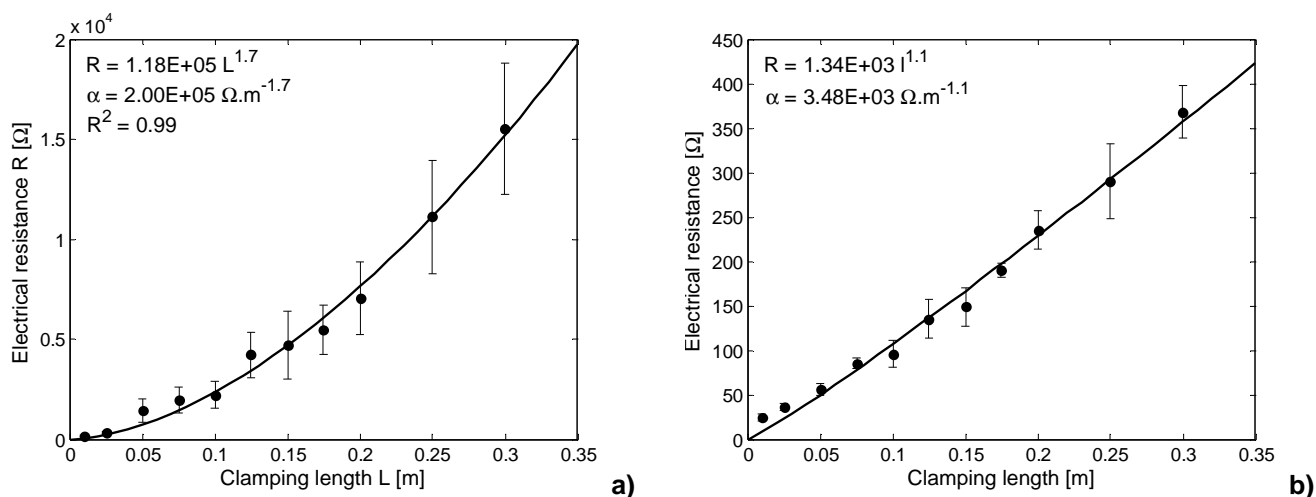


Figure 3 Dependence of electrical resistance on the yarn length (points are sample medians and solid line is model see eqn (1) for a) yarn containing 40%, b) yarn containing 60% of metal fiber

The dependence of yarn electrical resistance R on the yarn length L for chosen yarns with linear density 50 tex is shown in the Figure 3. Also in this case, it was confirmed that electrical resistance is nonlinear convex increasing function of clamping length.

It was found that factor $n = 1.7$, resp. 1.6, resp. 1.1 for yarns containing 20, 40, resp. 60% of conductive component. The higher is the metal fiber content; the lower is the factor n . For reasons given above, continuous electrically conductive path along the length of the yarn will be reached at further increment of conductive component ($P > 60\%$) and the dependence of the electrical resistance on the clamping length will get the linear tendency.

3.2 Mechanical properties

It was found, that the yarn strength and elongation is decreasing with increasing metal fiber content (from $P=1\%$ to $P=20\%$). On the other hand, static modulus, resp. dynamic modulus is slightly rising with increasing metal fiber content.

4 CONCLUSIONS

It was confirmed that dependence of electric conductivity on the length of yarn is highly nonlinear (especially for yarns with relatively low metal fiber content and low linear density) which is in contradiction with behavior of metals and some composites.

To model this dependence the simple mechanistic model with different magnitude of factor n was verified. It can be summarized that the higher the metal fiber content (at conserving factor n), the lower specific resistivity factor (higher conductivity) for 25 tex yarns. The higher metal fiber content (in the area above percolation threshold) the lower the factor n for 50 tex yarns. The dependence of electric resistance on clamping length will get linear tendency in case of yarns with higher metal fiber content ($P > 60\%$). Using the specific resistivity factor we are able to compare the yarns and study influence of content of conductive phase on yarn conductivity.

It was shown that increased content of metal fiber in yarn will decrease yarn strength and elongation, whilst static, resp. dynamic is increased.

5 REFERENCES

1. World Health Organization: Establishing a dialogue on risks from electromagnetic fields, WHO, Geneva, 2002
2. Ott HW.: Electromagnetic compatibility engineering, John Wiley & Sons, New Jersey, 2009
3. Šafářová V., Militký J.: A study of Electrical Conductivity of Hybrid Yarns Containing Metal Fibers. *Journal of Material Science and Engineering B* 2(2), 2012, pp. 197-202

ANALÝZA ELEKTRICKÝCH A MECHANICKÝCH VLASTNOSTÍ HYBRIDNÍCH PŘÍZÍ VYTVOŘENÝCH ZA ÚČELEM OCHRANY PROTI ELEKTROMAGNETICKÉMU POLI

V rámci návrhu textilií schopných odstínit elektromagnetické pole byly vytvořeny hybridní příze se zvýšenou elektrickou vodivostí. Zmíněné příze byly směšové, vyrobené z konvenčních polypropylenových a extrémně jemných nerezových ocelových vláken ve staplové formě. Příze byly připraveny ve dvou odlišných jemnostech a obsahovaly různý obsah vodivé komponenty (1 – 60 %). Během tohoto výzkumu byly studovány elektrické vlastnosti a vybrané mechanické vlastnosti závislé na struktuře příze a na obsahu kovového vlákna. Bylo zjištěno, že hybridní příze obsahující nerezová ocelová vlákna ve staplové formě vykazují vysoce nelineární závislost elektrického odporu na upínací délce. Cílem tohoto článku bylo na široké paletě vzorků prozkoumat a ověřit platnost navrženého jednoduchého mechanického modelu popisujícího tuto závislost. Charakteristickým parametrem tohoto modelu je tzv. specifická rezistivita α , pomocí které je možno vyjádřit vliv obsahu kovového vlákna na změny elektrické vodivosti nebo elektrického odporu příze. Vliv obsahu kovového vlákna na Youngův modul, dynamický modul, pevnost a prodloužení hybridních přízí byl také vyhodnocen.

EFFECT OF CONSUMER WEAR AND TEAR ON TRANSPORT PROPERTIES OF KNITTED FABRICS

Anton Schlosser, Pavol Lizák and Ľubomír Žila

Alexander Dubček University of Trenčín, Faculty of Industrial Technologies
Department of Material Engineering, Púchov, Slovak Republic
tono.schlosser@gmail.com

Abstract: Knitted fabrics are often used for production of clothes - mainly underwear and free time activities ones. It is the comfort which is very important for underwear, sports clothes and similar clothes production. It is the status of human organism in which the physiological functions are optimal. The textile materials differ from each other not only by different fibres used for production but mainly by the way of mutual arrangement of fibres which affects mainly structure and fineness of knitwear. The coefficient of knitted fabric filling is influenced by the structure of the yarn used on its production and by the yarn structure itself. All these factors influence not only coefficient of filling but also other final knitted fabric properties. By their influence the knitwear parameters are changed what subsequently affects transport properties and they have decisive influence on the thermal-physiological comfort.

In our work we focus on the influence of these parameters on the thermal-physiological comfort. In the area of thermal-physiological comfort are included thermoregulation and moisture, what can be expressed by the heat resistance and resistance to water vapor.

Keywords: fabric, filling, comfort, thermal resistance, resistance to water vapour.

1 INTRODUCTION

Clothing comfort is possible to characterize as the summary of all consumer's percepts while wearing the clothes. Clothing comfort has got two characteristics:

- Functional comfort is influenced by clothing materials properties and includes physiological, sensory and path - physiological comfort.
- Aesthetic comfort depends on cultural and social consumer's level; it is influenced by fashion, tradition, age, education, religion, colour and etc.

Physiological comfort is the status of human organism in which physiological functions are optimal and which is perceived by the individual as comfort. In this status in organism it can stay unlimited time with the feeling of comfort. The ideal status for human organism is the status of basal metabolism. The status of basal metabolism is when the organism - healthy, hungry and undressed stays in horizontal position, it does not perform any activity and lies in climatic conditions and has no feeling of cold and hot. There run only minimal metabolism functions which are necessary for keeping the functions of body's organs. Clothing helps body to keep thermal balance and gives it the sense of comfort. It creates a particular microclimate around the body, which influences subjective

feelings of a person while wearing it. Microclimate under the clothing depends on thermal status of organism, on climate conditions of environment and on clothing properties.

In Table 1 we can see physiological, psychological and physical harmony between human and environment.

Table 1 Comfort harmony between human and environment

Thickness	0.8 – 2 [mm]
Area weight	0.11 – 0.4 [kg/m ²]
Thermal permeability	14 – 22 [J/m ² .s.K]
Moisture permeability	0.44 – 0.7 [g/m ² .s.bar]
Air permeability	10 – 100 [m ³ /m ² .s]

The optional comfort conditions are if the skin temperature is 33-35°C, relative humidity near skin is 25±10%, air speed near the skin is 25±10 cm.s⁻¹ and skin is not covered in sweat.

Complex action is action of humidity which occurs swelling of hydrophilic fibres, porosity decrease, decrease of permeability of air and humidity through textiles and thereby increasing the thermal conductivity.

The knitted fabric density is one of the most important properties because it can be easily influenced by the technology and it is the result of the basic technological parameters and the way

of production. Density is also the property which influences other properties in a large scale. However, in spite of this the expression of knitted fabric density is not unambiguous and uniform. From the physical point of view the density means the amount of mass of given substance in unit volume. In the technology of knitting the density has to correspond to percept conception. There are several systems of density expression.

- linear density expression in which the system arises from loop length, however it does not correspond to the percept conception in which we have to take in consideration also the thread thickness. This type of expression is usable only with certain types of knitted fabrics. In more complicated knitted fabrics expression does not correspond to percept conception.

- square density expression defined the filling of the knitted fabric area by the structure elements. The total density is expressed by the product of columns density and courses density on water. This expression has got mainly technological importance. It corresponds to percept conception only when the knitted fabric is created by the threads of the same average.

- volume density expression defines filling of knitted fabric volume by processing thread. It is more advantageous and it is more favourable for majority of knitted fabrics. It corresponds to percept conception provided we respect the knitted fabric thickness.

- mass expression of density corresponds to a certain scale with the motion of density. Knitted fabric density we can define as the ratio of density and volume. This expression is suitable mainly for the plastic knitted fabrics where previous procedures are difficult to use.

Fibres density in the fibrous textile structure is characterized by the ratio of the total space of knitted fabric which is filled by fibres volume filling. Filling is a dimensionless quantity residing in the interval (0,1). In our work we were identifying what is the influence of the filling characterized by the share of polypropylene

polymer in the knitted fabric volume on the thermal physiological comfort. The measurements were realized on polypropylene knitted fabrics aimed at the production of sports and free-time activities clothes. The knitted fabrics were made of profiled polypropylene fibres which are made by company Chemosvit Fibrochem a.s. Svit. On the measured samples the square mass and the knitted fabric thickness were defined and with the help of these data specific mass of the knitted fabric, too. The ratio between specific mass of the knitted fabric and specific mass of polypropylene is given by the coefficient of filling. After measuring of thermal resistance and resistance to water vapour, it is possible to define the dependence of given quantity on the coefficient of filling.

2 EXPERIMENTAL

2.1 Material

Tests were performed on polypropylene knitted fabric which was scraped on helicopter abrader for 3, 6, 9 and 12 minutes. For particular samples was set their change of weight and thickness. The Figure 1 shows the knitwears with different degrees of wear.

2.2 Methods and devices

We defined square mass m_s [g.m^{-2}] on the material samples by weighing and we also measured the knitted fabric thickness h [mm]. From the given values it is possible to calculate specific knitted structure thickness ρ_{pl} [kg.m^{-3}]. The coefficient of knitted fabric filling by polypropylene fibres can be calculated by relation.

$$\mu = \rho_{pl} / \rho_v \quad (1)$$

Specific mass of fibre forming polypropylene ρ_v is 980 [kg.m^{-3}].

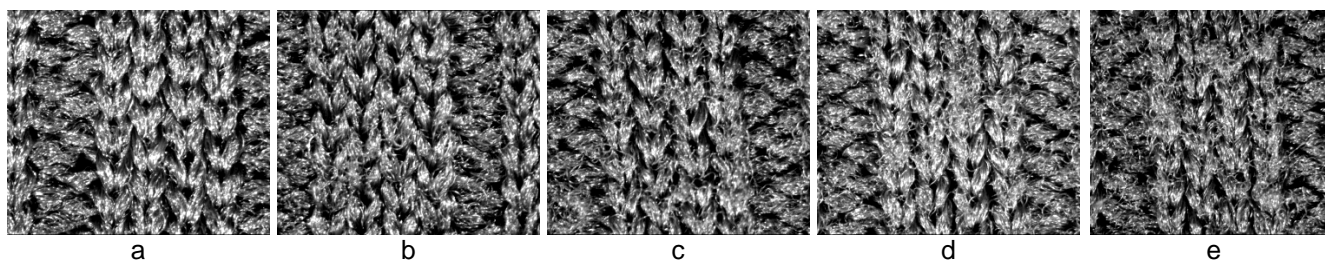


Figure 1 Samples worn out at particular time intervals (a) 0 min, (b) 3 min, (c) 6 min, (d) 9 min, (e) 12 min

Thermal resistance R_{ct} is the difference of the temperatures between two surfaces of material divided by resulting thermal flow on the surface in the gradients direction. This flow of dry heat can have conductive, conventional and radiational component or only some of them. Thermal resistance R_{ct} expressed in $[m^2.K.W^{-1}]$ is the property specific for textile materials or stratified compositions which manage dry heat flow on the given area corresponding to stable heat gradient. Heat resistance R_{ct} is defined the following way - heat resistance of marginal air layer above the surface of testing devices is deducted from heat resistance of testing sample and marginal air layer above it, both are measured in the equal conditions according to formula:

$$R_{ct} = \frac{(T_m - T_a) \cdot A}{H - \Delta H_c} - R_{cto} \quad (2)$$

T_m is the temperature of measuring unit $[^{\circ}C]$, T_a is the air temperature in the experimental space $[^{\circ}C]$, A is the area of measuring unit $[m^2]$, H is a heating input transported to measuring unit $[W]$, ΔH_c is a correcting element for heating input by the measurement of heat resistance, R_{cto} is the constant of apparatus on heat resistance measurement $[m^2.K.W^{-1}]$.

Resistance to water vapor R_{et} is the difference of water vapour pressure between surfaces of material divided by resulting evaporating thermal flow on the unit of area in the gradient direction.

Evaporating flow can consist of difusal and conventional component. Resistance to water vapour R_{et} expressed in $[m^2.Pa.W^{-1}]$ is a specific property for textile materials or composites which defines latent evaporating thermal flow running across given area and corresponding to stable water vapour gradient. To define resistance to water vapour the electric heated porotic plate is covered by membrane which leaks vapour, but not water. For a testing sample located on a membrane the thermal flow is necessary for keeping constant temperature on the plate by the measure of the vapour water speed and from this data is the sample resistance to vapours defined.

$$R_{et} = \frac{(p_m - p_a) \cdot A}{H - \Delta H_e} - R_{eto} \quad (3)$$

p_m is a balanced partial pressure of water vapors on the surface of measuring unit $[Pa]$, p_a is a partial pressure in the air in the testing area $[Pa]$, A is the area of measuring unit $[m^2]$, H is a heating input given to measuring unit $[W]$, ΔH_e is a correcting element for heating input by measurement of resistance to water vapor, R_{eto} is an apparatus constant for measurement of resistance to water vapors $[m^2.Pa.W^{-1}]$.

3 RESULTS AND DISCUSSIONS

Resulting values of individual knitted fabric samples and their coefficient of filling are introduced in the chart (Table 2).

Table 2 Parameters of individual knitted fabric samples

sample	h [mm]	$m_s [g.m^{-2}]$	$\rho_{pl} [kg.m^{-3}]$	$\rho_v [kg.m^{-3}]$	$\mu [0,1]$
A	0.700	115.205	164.578	980	0.168
B	0.796	114.379	143.692	980	0.147
C	0.848	114.296	134.783	980	0.137
D	0.940	114.296	121.591	980	0.124
E	0.990	114.214	115.367	980	0.118

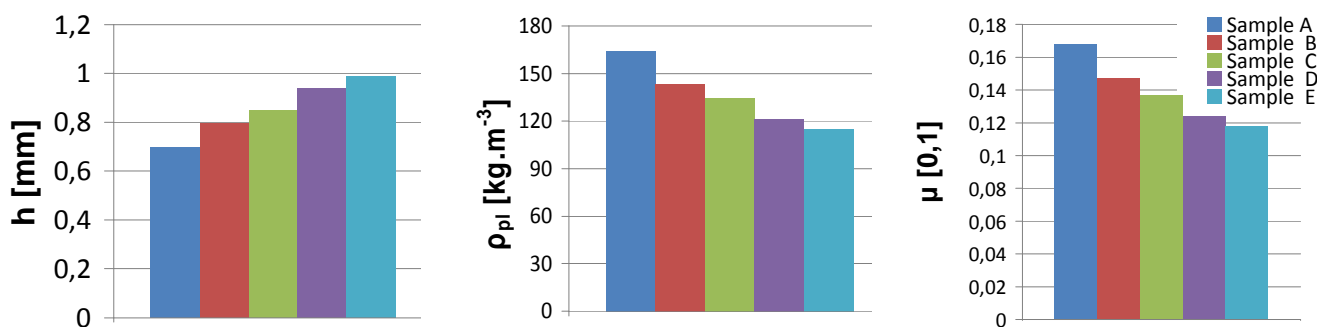


Figure 2 Filling coefficient of parameters of individual knitted fabric samples

In the chart 3 the thermal resistance values of individual samples of knitted fabrics are introduced. Graph displays the dependence of thermal resistance on filling coefficient (Figure 3).

Table 3 Thermal resistance and coefficient of filling

sample	$R_{ct} [m^2 \cdot K \cdot W^{-1}]$	$\mu [0,1]$
A	0.02670	0.168
B	0.05348	0.147
C	0.06302	0.137
D	0.07204	0.124
E	0.08175	0.118

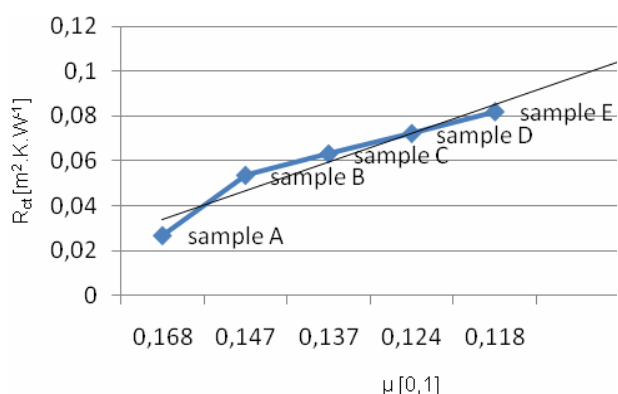


Figure 3 Coefficient of filling influence on thermal resistance

In the chart 4 there are introduced the values of resistance to water vapour of the individual kinds of knitted fabrics. The graph displays the dependence of water vapour resistance to water vapor on filling coefficient (Figure 4).

Table 4 Resistance to water vapors and filling coefficient

sample	$R_{et} [m^2 \cdot Pa \cdot W^{-1}]$	$\mu [0,1]$
A	1.220	0.168
B	0.961	0.147
C	1.480	0.137
D	1.260	0.124
E	1.610	0.118

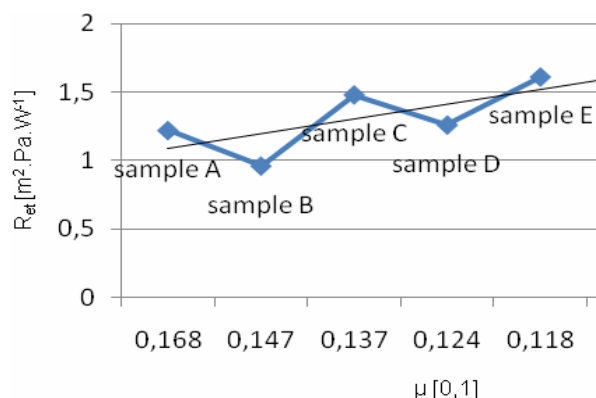


Figure 4 Coefficient filling influence on the resistance to water vapor

4 CONCLUSIONS

Following the measured values by the gradual samples abrasion came to gradual fibres releasing from the knitted fabric structure which caused its thickness increases thereby also increasing of its total volume. By growing ρ_{pl} there was a gradual decrease of filling μ . When evaluating the thermal resistance R_{ct} it came to gradual increase of heat transfer resistance proportionally with material wear. Consequently there is a reduction of heat flow in the direction from skin to the outside. In the case of water vapor resistance R_{et} evaluation it did not come to gradual increase of the material wear value, which can be justified by the fact that abrasion caused the local destruction of knitwear. These matters subsequently affect the value of the water vapor transmission resistance.

Acknowledgment: This work was supported by the project KEGA No. 003 TnUAD- 4/2014.

5 REFERENCES

- Lizák P., Militký J.: Technické textilie, 1st ed., M Print, Lipt. Sielnica, 2002
- Kočí V.: Vazby pletenin, SNTL - Nakladatelství technické literatury, Praha 1980
- Lizák P.: Evaluation methods of materials structure, 1st ed., Krakow, Towarzystwo Słowaków w Polsce, 2011

VPLYV ZMENY PARAMETROV SPOTREBITEĽSKÝCH VLASTNOSTÍ NA TRANSPORTNÉ VLASTNOSTI PLETENÍN

Textilné materiály sa od seba odlišujú nielen odlišným druhom vlákien použitých na ich výrobu ale najmä spôsobom vzájomného usporiadania vlákien, čo ovplyvňuje hlavne väzba a jemnosť pleteniny. Koeficient zaplnenia pleteniny je ovplyvňovaný štruktúrou priadze použitej na jej výrobu a štruktúrou samotnej pleteniny. Všetky tieto faktory ovplyvňujú nie len koeficient zaplnenia ale aj ďalšie výsledné vlastnosti pleteniny.

A PROCEDURE OF 3D SURFACE RECONSTRUCTION OF UNICOLOR AND PATTERNED FABRICS AND PILLS DETECTION

Lenka Techniková¹, Maroš Tunák¹ and Jiří Janáček²

¹Technical University of Liberec, Faculty of Textile Engineering, Liberec, Czech Republic

²Academy of Sciences of the Czech Republic, Institute of Physiology, Prague, Czech Republic
lenka.technikova@tul.cz

Abstract: This paper deals with an objective procedure of effective and fast 3D surface reconstruction of unicolor and patterned fabrics with pills and subsequent pills detection. The main purpose of the procedure is based on a gradient field method which makes a 3D fabric surface just from a set of 4 sample images. The principal of the gradient field method relates with methods called Shape from shading. The methods Shape from shading are capable to create 3D images due to shadows of an object realized by a lateral illumination of the object. When the 3D fabric surfaces are prepared, the pills detection is possible to do with using of simple tools of image analysis. The method is suitable not only for unicolor fabrics but even for patterned fabrics where the segmentation of pills is very difficult.

Keywords: fabric pilling, 3D fabric surface reconstruction, gradient field method, pills detection.

1 INTRODUCTION

Pilling is a serious problem associated with fibers protruding from a fabric surface. Pill is a small ball of entangled fibers connects with a top of the fabric surface. Traditionally, pilling is evaluated by human experts - a subjective method of a pilling evaluation is still the most used evaluation of pilling in textile industry. A human expert compares a sample with series of standards photographs according to standards ASTM [1], etc. However, the subjective visual method has several significant disadvantages as inconsistency and inaccuracy of the rating results. Therefore, a development of more reliable and objective methods is desirable.

Many researchers have tried to develop an objective method of the fabric pilling evaluation with using different principles. Semnani and Ghayoor [2] tried to apply corner detectors for finding the crossing points of yarns and for detecting of the disturbance of regularity caused by pills. A method edge flow was used by Xiaojun et al. [3] for pills extraction from RGB images. In next studies, Xin et al. [4] and Chen et al. [5] segmented pills with using of template matching techniques.

The methods mentioned above solved a problem of the pills detection in unicolor fabrics. However, the pills detection in patterned fabrics is necessary as well. This study describes a method for the pills detection in unicolor and even in patterned fabrics. Firstly, a gradient field method

is used for a 3D fabric surface reconstruction. Due to estimation of gradient images, an influence of a fabric pattern on the pills segmentation is eliminated. Thereafter, a pills extraction is possible to do with using of simple tools of image processing techniques.

2 EXPERIMENT

2.1 Experimental Samples and Sample Image Capturing

For experiment of the pills detection, several fabrics with various material, weave, color, density, pilling grade, pattern, and so on were used. The experimental samples were tested on a Martindale abrasion tester for a resistance to pilling. In this study, a representative set of 2 samples was selected for illustration of efficiency of the method: first sample is unicolor felted fabric in a twill weave and second sample is woven fabric in a plain weave with checked pattern (Figure 1).

The gradient field method, used for 3D reconstruction of fabrics with pills, requires a creation of the shadows of pills for a quality surface reconstruction. So, between basic elements for using of the gradient field method belong the pill shadows and necessary to make a set of 4 images for each of the samples. A principle of creation of the set of 4 sample images follows. A sample is laterally illuminated from 4 sides step by step: from above I_a , below I_b , then from the right I_r and finally from the left side I_l .

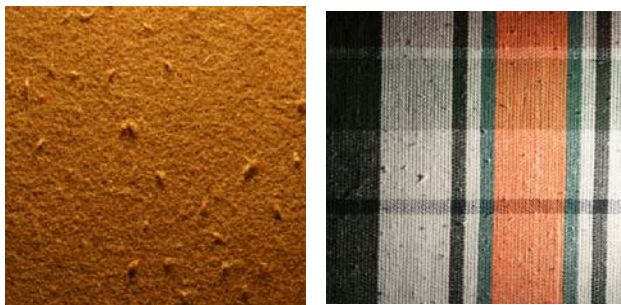


Figure 1 A representative set of the samples: unicolor and patterned fabrics

During individual illumination of the sample, image of the sample is captured by a camera placed over the sample. Therefore, the set of 4 images is captured for each of the samples. Images of the samples are captured in RGB scale and subsequently converted on gray level images.

2.2 3D Fabric Surface Reconstruction

When the set of 4 images of the sample is prepared, a 3D fabric surface reconstruction is possible to realize with using of special algorithm [6] in software MatLab. The principal of the method is focused on estimation of 2 gradient images and their processing in 3D image. Therefore, the gradient images have to be firstly estimated. In this study, the gradient images are

estimated by subtracting of the images in relevant directions. The gradient image in horizontal direction g_x is obtained by subtracting of the sample image illuminated from left I_l from the sample image illuminated from right I_r . The next one, the gradient image in vertical direction g_y is acquired by subtracting of the sample image illuminated from above I_a from the sample image illuminated from below I_b .

The gradient field method is capable to make a 3D surface from such images. The principal of the gradient field method is based on trying to make a gradient field of the image integrable. If the gradient field is integrable, it is possible to reconstruct the surface using Frankot-Chellappa algorithm, for details see [6]. Efficiency of the method is illustrated on the representative set of samples in Figure 2 (a-f). The gradient images g_x , g_y of the samples (a, b, d, e) and their 3D surfaces (c, f) reconstructed by the gradient field method are all presented in Figure 2. In the gradient images, pills are obviously emphasized in the fabric surface and their subsequent detection is quite simple. Specially, it can be seen in the gradient images g_x , g_y of patterned sample that the fabric pattern is relatively eliminated and an influence of the pattern on the pills segmentation is reduced.

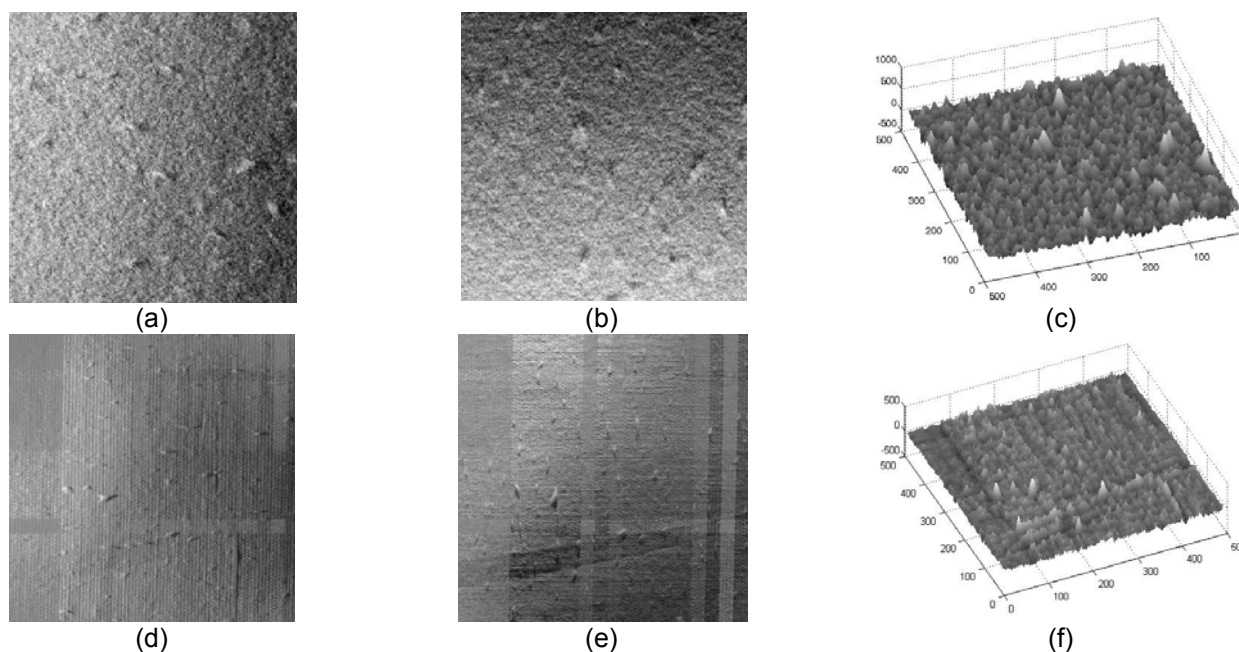


Figure 2 The gradient images g_x and g_y of (a), (b) unicolor and (d), (e) patterned sample. 3D fabric surfaces of (c) unicolor and (f) patterned sample

2.3 The Pills Detection

Next step embodies the pills detection in 3D images of the fabrics using simple image processing techniques in software MatLab. Generally, pills segmentation plays important role in the objective methods for the pilling evaluation. In this work, a local thresholding algorithm according to method Niblack [7] was applied for a separation of pills from the background of a fabric. The principal of the algorithm is based on computation of the local threshold for each pixel according to local mean $m(i,j)$ and standard deviation $\sigma(i,j)$ of all pixels in pixel surroundings (i,j) of a window which is sliding over an image. An expression for calculation of a local threshold $T(x,y)$ for each pixel with coordinates x,y in the pixel surroundings (i,j) of the window is:

$$T(x,y) = m(i,j) + k \cdot \sigma(i,j) \quad (1)$$

Demonstration of the efficiency of the pills segmentation is presented on the representative set of samples in Figure 3 where (a, c) the original and (b, d) final binary images with detected pills as white objects are shown.

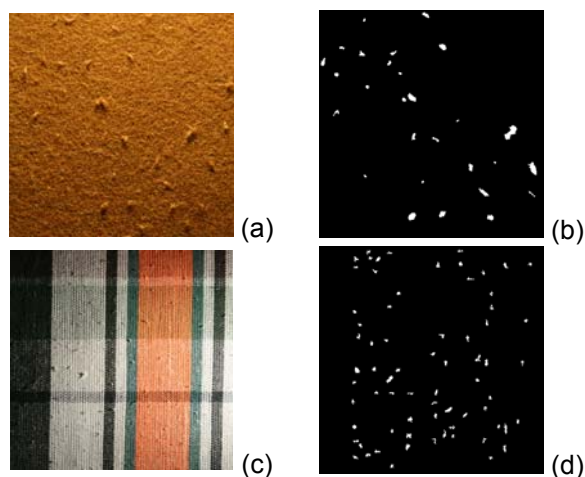


Figure 3 The original set of (a) unicolor and (c) patterned fabric and (b), (d) their binary images with detected pills

3 CONCLUSION

The paper presented a new procedure of the pills detection in unicolor and patterned fabrics. Among the main advantages of the objective method belong relatively cheap devices for the image capturing, fast 3D fabric surface

reconstruction, using the pill shadows in benefit of quality 3D reconstruction, the reduction of an influence of the fabric pattern on the pills detection and using simple image processing techniques for the pills segmentation. Generally, the pill shadows created by illumination during image capturing signify significant barrier for the pills segmentation. However, the gradient field method requires the pill shadows for quality surface reconstruction. Due to estimation of the gradient images and their processing in 3D image, a pattern of fabric is quite eliminated in the sample image and the method is possible to apply not only for unicolor fabrics but even for patterned fabrics.

Acknowledgement: The report was supported by the Student Grant Competition 2014 of Technical University of Liberec, project number: 21036.

4 REFERENCES

1. ASTM D4970/D4970M. Standard Test Method for Pilling Resistance and Other Related Surface Changes of Textile Fabrics: Martindale Tester. International American Society for Testing and Materials, USA, 2012
2. Semnani D., Ghayoor H.: Detecting and Measuring Fabric Pills Using Digital Image Analysis, World Academy of Science, Engineering and Technology. Vol. 49, 2009, pp. 897-900
3. Xiaojun L., Huabing H., Yushu L., Hong Z.: The Evaluation System of Fabric Pilling Based on Image Processing Technique, IEEE Image Analysis and Signal Processing. Vol. 1, 2009, pp. 44-47
4. Xin B., Hu J.: Objective Evaluation of Fabric Pilling using Image Analysis Techniques, Textile Research Journal. Vol. 72 (no 12), 2002, pp. 1057-1063
5. Chen X., Xu Z., Chen T., Wang J., Liqing L.: Detecting Pills in Fabric Images based on Multi-scale Matched Filtering, Textile Research Journal. Vol. 79 (no 15), 2009, pp. 1389-1395
6. Agrawal A., Raskar R., Chellappa R.: What is the Range of Surface Reconstructions from a Gradient Field? 9th European Conference on Computer Vision. Vol. 2, 2006, pp. 578-591
7. Khurshid K., Siddiqi I., Faure C., Vincent N.: Comparison of Niblack inspired binarization methods for ancient documents, Proc. SPIE 7247. Document Recognition and Retrieval XVI, 2009

MONITORING OF NANOFIBER LAYER STRUCTURE WITH THE AID OF IMAGE ANALYSIS

Maroš Tunák and Michaela Řičicová

*Technical University of Liberec, Faculty of Textile Engineering, Czech Republic
maros.tunak@tul.cz*

Abstract: Measurement of the geometrical and other properties as well as directional orientation of fibrous structures is an important part of quantitative measurements in textile metrology. Most of the measurements are currently performed either manually or with the use of specialized software, where evaluation of fibrous systems characteristics is not performed automatically but is affected by subjective human decisions. For this purpose characteristics of interest must be routinely estimated, requiring fast, robust and reliable procedures. Such quantitative characteristics are fundamental basis for following modelling and prediction of utility properties of final products. This paper is dealing with objective procedures for estimation of quantitative characteristics of nanofiber layers with the tools of image analysis. The basic characteristics extracted from images of nanofiber layers were parameters of pores between nanofibers, detection and characterization of defects occurring in such layers, description of preferred nanofibers orientation, and evaluation of distribution of nanofibers diameter. The effectiveness of algorithms was tested on a set of grayscale images of polycaprolactons nanofiber structures formed by electrospinning with different concentrations of polymer. Digital images of nanofiber layers were captured by scanning electron microscopy and sequence of image procedures was performed in Matlab environment.

Keywords: Nanofibers, Image Analysis, Pores, Defects, Orientation, Diameter.

1 INTRODUCTION

Quantitative characteristics of fibrous system are important part of quantitative measurements in textile metrology. Geometrical and other characteristics as well as directional orientation of fibrous structures are fundamental basis for following modeling and prediction of utility properties of products. Processing of image data allows us to understand image content and to perform quantitative and qualitative descriptions of objects of interest. In textiles structures, typical objects can be fibers, threads, cross sections of fibers, etc., and the systems containing objects can be webs, fiber layers, woven fabrics, knitted fabrics, nonwoven textiles, nanofibrous layers, cross-sections of layers, etc. This paper is dealing with objective procedures for estimation of quantitative characteristics of nanofiber layers with the tools of image analysis. The basic characteristics extracted from images of nanofiber layers were parameters of pores between nanofibers, detection and characterization of defects occurring in such layers, description of preferred nanofibers orientation, and evaluation of distribution of nanofibers diameter. The effectiveness of algorithms was tested on a set of grayscale images of polycaprolactons nanofiber structures formed by electrospinning with different

concentrations of polymer (14, 16, 18 and 20% of PCL). Five images of nanofiber layers for all concentration were taken by scanning electron microscopy. To detect basic parameters of nanofiber structures were created algorithms in MatLabenvironment.

2 IMAGE ANALYSIS OF FIBROUS SYSTEMS GEOMETRY

2.1 Measurement of fiber diameter and distribution of fiber diameter in fibrous system

The fiber diameter is one of the most important structural characteristic in textile fibrous systems and distribution of fiber diameters extracted from images characterize fibrous system in view of variability. Various techniques and algorithms for fiber diameter measurement for nonwovens and nanofibrous layers have been proposed, e.g. [1]. The idea is based on computation of Euclidean distances for all background pixels (nanofibers in this case) to nearest nonzero pixel (pores) from binary negative image in Figure 1c. The results can be seen in Figure 1d and is known as distance transform map, where Euclidean distance is displayed as gray level. The brightness pixels in distance transform matrix represent axis of nanofibers and shortest distance

to background. Automatically can be found by using morphological operation - skeletonization. It removes pixels on the boundaries of objects but does not allow objects to break apart. The pixels remaining make up the image skeleton. The values of Euclidean distances corresponding for pixels of image skeleton represent desired nanofiber semi diameters. The results of nanofiber diameter measurement, detailed description of method and more examples see [2].

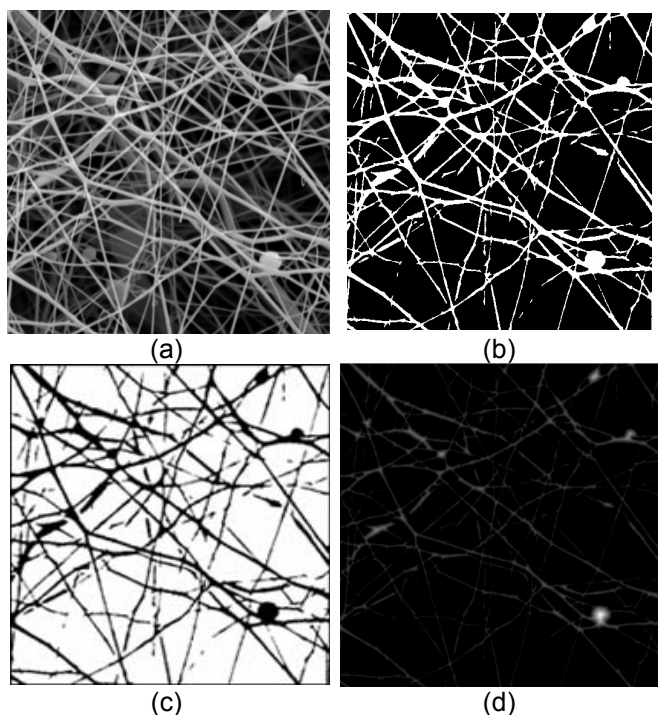


Figure 1 (a) Monochromatic image of nanofibrous layer (14% PCL), (b) binary image, (c) negative image, (d) distance transform map

2.2 Measurement of porosity and geometrical characteristics of pores in fibrous systems

Pore geometry is one of the most important parameters of textile fibrous systems which influence thermo-physiological properties, air permeability, transport properties, absorbance of liquids, filtration properties etc. The aim of image processing is objective determination of area of pores between the yarns in woven and knitted fabrics, pores in nonwoven fabrics as well as in nanofibrous structures. Distribution of characteristics of pores is important for prediction of above mentioned properties.

The aim of image processing is determination of distribution of area of pores between the

nanofibers from gray level image (Figure 2a). For this reason the binary image (Figure 2b) was converted from grayscale by using a global thresholding (thresh level is founded experimentally). Negative of binary image is then obtained where pores as objects are displayed by white and background represented by nanofibers is displayed by black (Figure 2c). Small objects may also be visible in binary images, which can be caused by random noise and it is necessary to remove these from binary image. Operation morphological opening is used to remove such small connected objects. Objects connected to image border represented incomplete objects were also removed. Small holes, breaks and gulfs can be seen inside many objects, operation morphological closing with disk structuring element of size 3 pixels was used for filling these types of defects (Figure 2d). From such pre-processed images characteristics as number of pores, total area of pores, average area of pores, average perimeter and other shape characteristics of pores can be extracted. Results for all samples obtained from prior analysis, detailed description of used method and examples of all samples see [2].

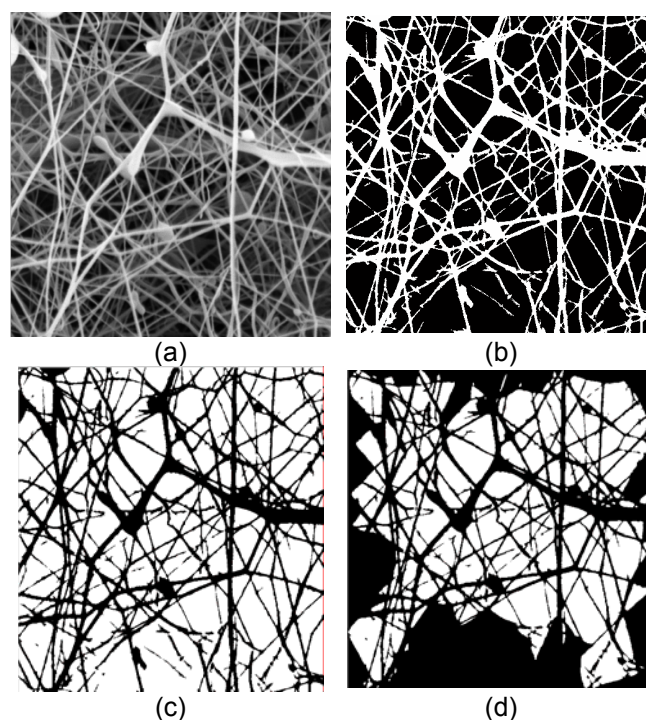


Figure 2 (a) Monochromatic image of nanofibrous layer (14% PCL), (b) binary image, (c) negative image, (d) image without incomplete objects

2.3 Detection and quantification of defects in fibrous systems

Defects, irregularities and inhomogeneity in regular fibrous structures (woven, knitted, nonwoven fabrics) as well as in random structures (nonwoven fabrics, fibrous and nanofibrous layers (Figure 3)) are undesirable and cause reduction of quality. The aim of this section is to propose image processing methods suitable for detection of ball-shaped defects occurred in nanofibrous layers (caused by low concentration of PCL).

As can be seen in Figure 3a, for segmentation of ball-shaped defect global thresholding cannot be effectively used. Matching by correlation turns out to be more efficient. Correlation is quite simple in principle. The correlation problem is to find all places in the image that match a given sub-image or template (in this case simulated ball-shaped object (see Figure 3a in right bottom corner)).

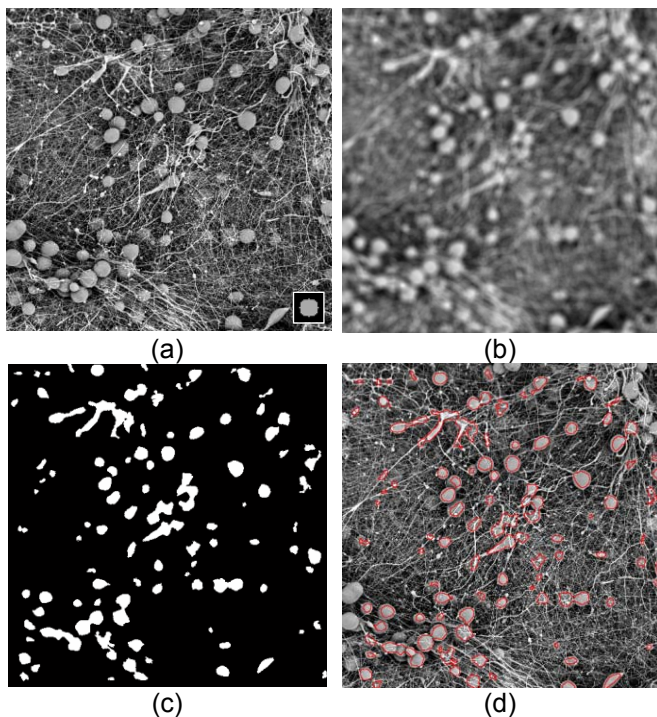


Figure 3 (a) Monochromatic image of nanofibrous layer (14% PCL) with template, (b) correlation map, (c) negative image, (d) objects borders (red color)

One approach for finding matches is to treat template as a spatial filter and compute the sum of product for each location of image. Then the best matches are locations of the maximum values (as grey levels) in the resulting correlation image (Figure 3b). For finding the location of best matches we can threshold the correlation image near its maximum and obtained binary image

(Figure 3c). Borders of localized ball-shaped objects are displayed in Figure 3d. The results of defect detection and parameters of such objects can be found in [2]. 20% PCL nanofiber layers do not contain any defects.

2.4 Estimation of the fiber system orientation and its distribution

Estimation of object orientation in grey level image is based on utilization of 2D discrete Fourier transform, which transforms image from the spatial domain to the frequency domain. The key point is that dominating direction (gradients of image function) in spatial domain corresponds to large magnitudes of frequency components distributed along the straight lines in the Fourier spectrum. The idea is based on transforming power spectrum to binary image via thresholding, where only significant frequencies remain. Global thresholding was used for binarization of the image, with the threshold value being set to 0.5 of the maximum of the logarithm of the power spectra. Directional orientation of significant frequencies in the frequency domain rotated by 90° corresponds to the directional orientation of objects in the spatial domain. In the corresponding binary image we consider a cluster of white pixels as a region of interest and analyze it further. Orientation and length of major and minor axes of the “covering” ellipse, that has the same normalized second central moment as the region, are computed. It is obvious that its orientation reflects the predominant directions of objects in the spatial domain (for detailed description see [3]). Described method is used for estimating the orientation of fibers or objects in the whole image. However, it turns out that for textile fibrous layers or nanofibrous layers more detailed analysis would be more suitable. By the local point of view image area is divided into K many small, non-overlapping pieces (sub-windows) covering it, and estimating the characteristic of interest (orientation) for each piece independently from the others. As a result we obtain many estimates of the characteristic of interest T_1, \dots, T_K , one for each sub-window of the original image, and instead of averaging them in order to get just one value we can estimate the distribution of T_i values by either histogram or kernel estimator.

The image of 18% PCL nanofibrous layer is divided into sub-windows of size 25×25 pixels and orientation estimation is done individually for every sub-window. Results of estimating the orientation in the form of a grey-level map can be

seen in Figure 4b, where preferred orientation of objects for every sub-window is represented by the directional vector displayed in red.

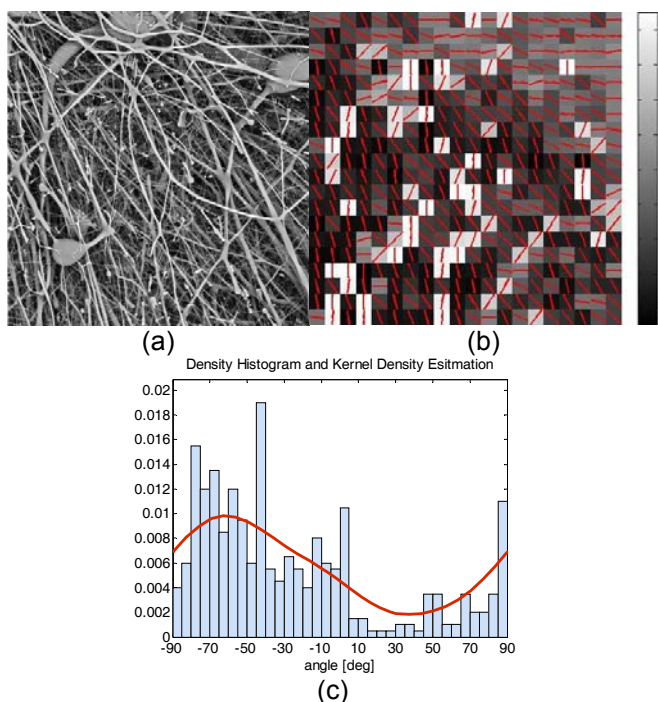


Figure 4 (a) Monochromatic image of nanofibrous layer (18% PCL), (b) grey level map of orientation (sub-window size 25×25 pixels), (c) density histogram and kernel density estimation of orientation

Distribution of estimates of the orientations in the respective sub-windows in the form of density histogram and kernel density estimates are shown in Figure 4c.

We can see that the distribution of orientation of fibers prevails in -60° direction. For more examples of analysis performed on all samples see [2].

3 CONCLUSION

In this work our interest is orientated in the field of developing new procedures and algorithms for objective measurement of quantitative characteristics of fibrous textile materials especially for nanofibers layers with the tools of image analysis. The basic characteristics extracted from digital images of nanofiber layers were characteristics of nanofiber pores, parameters of defects occurred in such layers, orientation of nanofiber, and estimation of nanofiber diameters. Results show that proposed algorithms can be effectively used for fast and robust estimation of such quantitative characteristics.

4 REFERENCES

1. Ziabari M., Mottaghtalab V., McGovern S.T. and Haghi A.K.: A New Image Analysis Based Method for Measuring Electrospun Nanofiber Diameter, *Nanoscale Research Letters* 2, 2007, pp. 597-600
2. Řičicová M.: Monitoring of Nanofiber Layer Structure with the Aid of Image Analysis, Diploma Thesis, Technical University of Liberec, 2013
3. Tunák M., Antoch J., Kula J. and Chvojka J.: Estimation of Fiber System Orientation for Nonwoven and Nanofibrous Layers: Local Approach based on Image Analysis, *Textile Research Journal* 84 (9), 2014, pp. 989-1006

MONITOROVÁNÍ STRUKTURY NANOVLÁKENNÝCH VRSTEV POMOCÍ OBRAZOVÉ ANALÝZY

Měření geometrických vlastností, směrové orientace a dalších vlastností vláknenných struktur je důležitou součástí kvantitativního měření v textilní metrologii. V současné době je většina měření prováděna buď manuálně, nebo s využitím specializovaného software, kde odhad charakteristik vláknenných systémů není prováděn automaticky, ale je zatížen subjektivním pohledem. Proto pro odhad takovýchto charakteristik se požadují rychlé, robustní a spolehlivé procedury. Odhadnuté charakteristiky pak mohou sloužit pro následující modelování a predikci užitečných vlastností výsledných produktů. Tento příspěvek se zabývá objektivními postupy pro odhad kvantitativních charakteristik nanovláknenných vrstev s použitím nástrojů obrazové analýzy. Základními zjišťovanými vlastnostmi vytvořených nanovláknenných vrstev jsou parametry nanovláknenných pórů, charakteristiky vyskytujících se defektů, směrová orientace a průměry nanovláken. Účinnost algoritmů byla testována na sadě monochromatických snímků polykaprolaktonových nanovláknenných struktur vytvořených elektrostatickým zvlákněním lišících se koncentrací zvlákněvaného polymeru. Digitální obrazy nanovláknenných vrstev byly pořízeny rastrovací elektronovou mikroskopií a algoritmy byly navrženy v programovém prostředí MatLab.

THERMAL PROPERTIES OF HIGH PERFORMANCE NONWOVEN PADDING FABRICS AT SUB ZERO TEMPERATURES

Mohanapriya Venkataraman, Rajesh Mishra, Jiri Militky, Dana Kremenakova,
Arumugam VeerakumaR and Srabani Misra

*Department of Material Engineering, Faculty of Textile Engineering
Technical University of Liberec, Czech Republic*

Abstract: *This research focuses on evaluation of nonwoven fabrics used as padding for thermal insulation clothing. The thermal insulation of textile fabrics depends on properties like thermal conductivity, thermal resistance, thermal diffusivity, thermal absorptivity, thermal effusivity, density and thickness. Experiments were conducted with an objective of studying heat transfer by conduction through the different thickness of fabrics used as thermal insulators especially at temperatures below 0°C. The nonwoven padding fabrics with different composition of polypropylene/polytetrafluoroethylene and 100% polypropylene were used in this work. Alambeta and C-Therm Thermal conductivity analyzer (TCi) have been used to measure the thermal properties. The relationship between the thermal conductivity, thermal resistance, thermal absorptivity, thermal diffusivity and thermal effusivity with fabric density of the selected fabrics were studied. It was observed that fabric density and thickness had a significant effect on the thermal properties.*

Keywords: *Nonwoven padding fabric, Thermal conductivity analyzer, Sub zero temperature, Thermal insulation, Thermal diffusivity.*

1 INTRODUCTION

Textile structures made directly from fiber rather than yarn are defined as nonwoven fabrics [1]. They provide warmth in coats, jackets, and outerwear. Nonwoven interlinings are incorporated into articles of clothing, as a layer of fabric inserted between the face and the lining of a garment, drapery, or quilt, during production to perform a range of functions [2]. Nonwovens are either sewn to the wrong side of the lining or the inner side of the outer shell fabric as insulation, padding, or stiffening fabric. Sewn and bonded interlinings are based on the types of processing methods used. During the sewing process, sewn interlinings are incorporated between the shell and the lining material. By using bonding process like heat sealing, bonded interlinings are fused to the shell, lining or another inlay material. The ratio between sewn to bonded interlinings is about 20:80. In quilting, a layer of down or fiberfill is placed between two layers of fabric, and then held in place by stitching or sealing in a regular, consistent, all-over pattern on the goods [3]. Past studies have shown that the number of layers is directly proportional to thermal insulation property desired. It is also revealed that the increase in velocity of air reduces the thermal insulation [4]. PTFE coated fabrics

have shown the highest water vapor permeability on studying the thermal and moisture vapor transmission properties of different types of laminated fabrics along with other fabric layers [5].

2 EXPERIMENTAL

2.1 Materials

Eleven nonwoven thermal insulation padding fabrics were used for this study. Of the chosen fabrics, nine were 100% polypropylene and the other two were composed of polypropylene and polytetrafluoroethylene (PTFE).

2.2 Methods

C-Therm Thermal conductivity analyzer (TCi) was used to measure the thermal properties like conductivity, resistance and effusivity of the nonwoven wraps. The fabrics were cut to 10 cm x 10 cm dimension and the weight of the samples was measured. Images were taken from confocal microscope and scanning electron microscope in order to compare the physical structure of the three nonwoven fabric samples and to determine if any difference was noticeable. All the samples were conditioned in standard atmospheric temperature of about 25±2°C and 65±2% relative humidity before testing.

Alambeta Conductivity Tester

Alambeta measuring device is a fast measuring equipment for transient and steady state thermo-physical properties (thermal insulation and thermal contact properties) [6].

Thermal conductivity analyzer

The C-Therm (TCi) thermal conductivity analyzer allows determining accurate values for thermal conductivity and thermal effusivity of aerogel treated nonwoven material at sub zero temperatures without extensive sample preparation or damage to the sample.

3 RESULTS AND DISCUSSION

Evaluation of various techniques for measurement of thermal properties of nonwoven padding fabrics were carried out. Before conducting the measurements, all samples of nonwoven padding fabrics were conditioned at standard atmospheric conditions ($27\pm 2^\circ\text{C}$, $65\pm 2\%$ RH) for 24 hours. The tested data were statistically analyzed using data analysis software ORIGIN LAB (origin pro 8).

Scanning Electron Microscopy (SEM)

Using Scanning electron microscope (SEM), images were taken on microscopic scale for the cross section area of the fabrics with different magnification. The physical structure confirmed to be different for all fabrics due to varied fabric densities, open structure and construction. Three similar composition and structure of SEM images of the fabric are randomly chosen and presented in Figure 1.

Thermal conductivity is the property of a material to conduct heat and is temperature dependent. It is fundamental to determine the heat transfer through fabrics. For textile materials, still air in the fabric structure is the most important factor for conductivity value, as still air has the lowest thermal conductivity value when compared to all fibers ($\lambda_{\text{air}} = 0.025$). The thermal conductivity at sub zero temperatures was measured using TCi thermal conductivity analyzer. Results are shown in Figure 2.

Thermal resistance is a measure of a material's ability to prevent heat from flowing through it. It is a function of the thickness and thermal conductivity of a fabric and is influenced by fabric structure. Under certain

climatic conditions, if the thermal resistance of clothing is low, heat energy will tend to gradually decrease, giving rise to a cool feeling. From the Figure 3, the results of thermal resistance derived from Alambeta measured at room temperature and TCi thermal conductivity analyzer at -10°C and -20°C can be seen. It is clearly shown that the thermal resistance increases as the thickness of the fabric increases. The same trend of values is shown both in Alambeta and TCi.

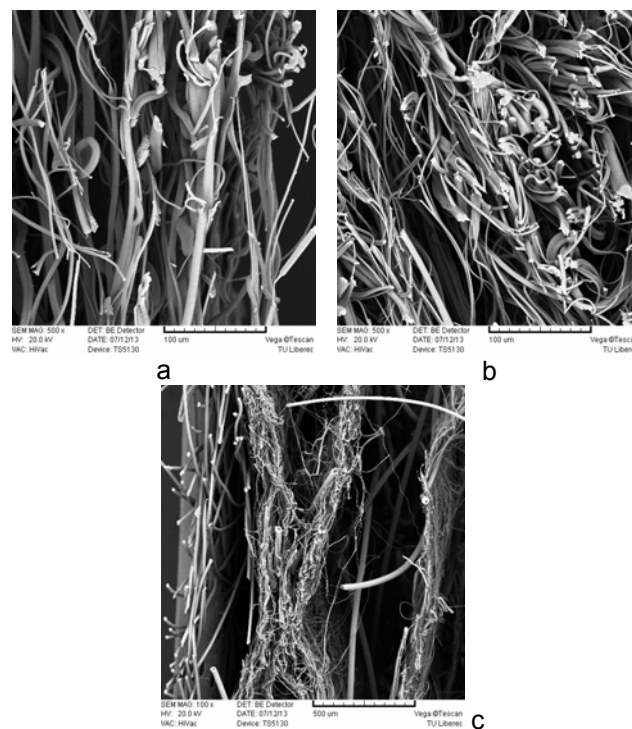


Figure 1 SEM images of selected nonwoven padding fabric samples (a) D2 (b) M1 (c) M9.

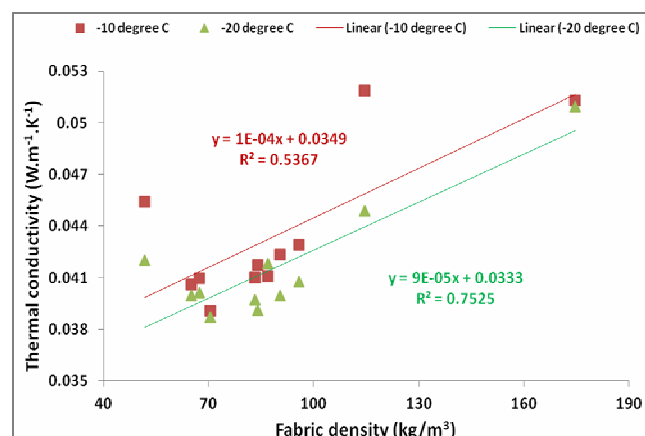


Figure 2 Thermal conductivity of nonwoven padding fabrics (TCi Thermal conductivity analyzer)

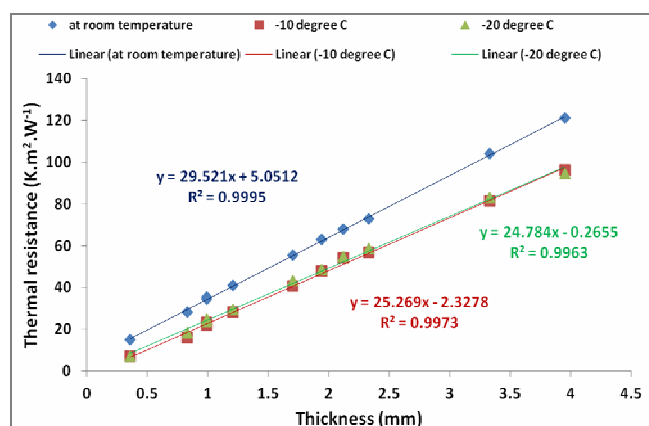


Figure 3 Thermal resistance of nonwoven padding fabrics

4 CONCLUSION

On statistically analyzing the results of this study, it was observed that fabric density and thickness of the nonwoven padding fabrics have a significant effect on the thermal properties. The fabric thickness and density play a major role in defining the thermal properties of the fabric like thermal conductivity, thermal resistance, thermal diffusivity, thermal absorptivity and thermal effusivity. Since the thermal conductivity of the nonwoven padding fabric depends on the fabric weight, thickness and fibre geometry, the values show low correlation between fabrics. Therefore, air transports very low quantity of thermal energy by conduction and thermal conductivity decreases as porosity increases. The same trend of values is shown both in Alambeta and TCi. From ANOVA results, the thermal resistance values of the fabrics measured from Alambeta and TCi showed significant difference and thermal resistance values of the fabrics

have an insignificant difference between temperatures. The difference in temperatures did not show much difference in the thermal resistance values.

In conclusion, fabric thickness and density play a major role in the thermal properties of the fabric. Evaluation of various techniques for measurement of thermal properties also gave insights into the suitability of instruments and techniques for measurement of thermal properties. The results showed that the selected nonwoven fabrics are suitable for usage as thermal insulators at subzero temperatures.

5 REFERENCES

1. Frydrych I., Dziworska G. and Bilaska J.: Comparative analysis of the thermal insulation properties of fabrics made of natural and man-made cellulose fibres, *Fibre Text East Eur.* Vol. 39, 2002, pp. 40-44
2. Varkiyani S.M.H., Rahimzadeh H., Bafekrpoor H. and Jeddi A.A.A.: Influence of punch density and fibre blends on thermal conductivity on nonwoven, *The Open Text J.* Vol. 4, 2011, pp. 1-6
3. Mazzuchetti G., Lopardo G. and Demichelis R.: Influence of nonwoven fabrics' physical parameters on thermal and water vapor resistance, *J Ind Text.* Vol. 36, 2007, pp. 253-264
4. Matusiak M.: Investigation of the thermal insulation properties of multiplayer textiles, *Fibre Text East Eur* Vol. 56, 2006, pp. 98-102
5. Kuvandykova D.: A new transient method to measure thermal conductivity of asphalt, *C-Therm Technol* Vol. 7, 2010, pp. 1-10

COLOR DIFFERENCE EVALUATION AT HIGH CHROMATIC COLORS

Michal Vik, Martina Viková and Markéta Kašparová

*Technical University of Liberec, Faculty of Textile, Liberec, Czech Republic
marketa.kasparova@centrum.cz*

Abstract: In 1976, the International Commission on Illumination, CIE, defined a new color space called CIELAB. It was created to be a visually uniform color space. At the same time the color difference equation ΔE^*_{ab} was developed to communicate color tolerances. However, CIELAB is not truly visually uniform, making colors having the same ΔE^*_{ab} magnitude in different regions of the color space appears of different magnitude. Instead of developing a new color space, the color science community has developed several other color difference equations that use higher order mathematics to give more or less weight to CIELAB values in different areas of the color space, resulting in color difference equations that better correlate with visually perceived differences. We propose a method to improve existing color-difference formulas with additional visual data from color discrimination experiment. Published data used for development and testing of new color difference formulas are limited in chroma. In presented work was used high chroma dataset for testing of prediction performance of well known color difference formulas. Five color difference equations (ΔE^*_{ab} , ΔE_{94} , $\Delta E_{CIEDE00}$, ΔE_{CMC} , and DIN99) were evaluated to determine which best correlates with the perceived color difference. The experimental data could provide references for the improvement of uniform color space and color-difference formula.

Keywords: colorimetry, color difference, color difference formula, visual assessment, textiles, gamut.

1 INTRODUCTION

The color quality control for many color industries has been an important event to fulfil the living requirement of human, such as the reproduction of a treasure-artistic work, high quality color communication of high-art valuable color images between media, and also one of the most important applications in many industries. We know that one observer “sees” a color somewhat differently from another observer. He will also see a color differently at different times. His judgments are influenced by both physiological and psychological factors. The single observer is, therefore, not very reliable. For a reproducible judgment a panel of observer is imperative. This is not practical, however, in everyday circumstances.

In 1976, the International Commission on Illumination, CIE, defined a color space called CIELAB [1]. It was created to be a visually uniform color space. At the same time the color difference equation ΔE_{ab} was developed to communicate color tolerances. Unfortunately, for some applications the perceptual uniformity of CIELAB is not sufficient, especially when color tolerances need to be defined. Data derived from color discrimination experiments (e.g., RIT-DuPont [2]) show the disagreement between

perceived differences and Euclidean distances in CIELAB. Suprathreshold ellipsoids, which approximately define all colors with similar perceived distance to a color center, are of particular interest. As the CIELAB color space is not visually uniform for small color differences ($\Delta E^*_{ab} < 5$) it is preferable to use the DIN99 color space [3]. DIN99 is uniform for small color differences and hence it is possible to compare the errors of different colors in DIN99 coordinates [4]. In CIELAB one may only compare color differences from non-Euclidian calculations like color differences based on CIE2000, CIE94 or CMC [5–7]. Only in the three dimensional DIN99 color coordinates (ΔL_{99} , Δa_{99} , Δb_{99}) it is possible to visualize the dispersion of measured color coordinates. When using any of the color difference formulae the problem is transferred into a one dimensional color difference scale (ΔE) and the possibility of visualization in a three-dimensional color space is lost. Therefore we used the DIN99 color space in this work.

2 MATERIALS AND METHODS

The normal color vision and color discriminating ability of observers were examined using the Ishihara Test and the Farnsworth Munsell 100 Hue Test, and each observer took a short-term

(about two hours) training to be familiar with the process of estimating color difference. Visual assessments were carried out using a set of 94 acryl fabric samples dyed with cationic (basic) dyes with high chromacity. Each sample was cut to precise 2×2 cm dimensions and mounted onto custom manufactured grey paper holders. Each sample mounting could slide in a bar on a custom designed display easel, as shown in Figure 1.

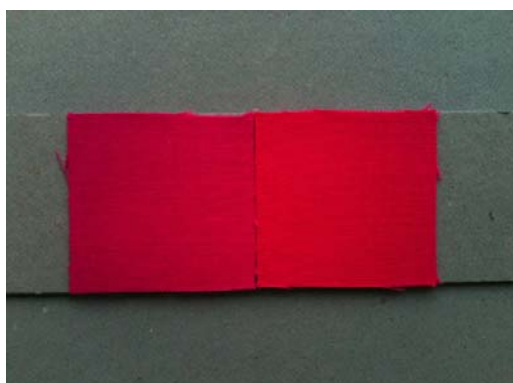


Figure 1 Picture of colored samples adjustment

The easel was viewed at a 45° angle and was located in an ATColor standard lightbox, illuminated with a fluorescent F7 daylight simulator with a correlated color temperature of 6500±100 K and constant illuminance of approximately 1300 lx in the middle of the display board. All extraneous light was eliminated. The light source was carefully controlled during the experiment in order to diminish variability at constant room temperature.

With this setup sharp dividing lines were produced with no shadows. Test samples were measured spectrophotometrically using a Datacolor International SF600 spectrophotometer with the following setup: specular included, UV included, illuminant D65 and 10 degree standard observer and 30 mm aperture size. Each measurement was based on an average of 4 readings. Average color coordinates are shown in graph on Figure 2.

Our basic approach was to measure the set of color different pair of samples and compare the color coordinates. In a first step the distance matrix of each pair of samples was calculated. In a data set with 94 elements 4464 color distances ΔE are present.

The evaluation of differences was carried out based on an ISO 105-A02 gray scale evaluation procedure. For each sample pair the question

asked was: "Which grey scale difference is in closest agreement with the difference between the displayed sample pair. The result can be between two steps, such as 3-4 or 4-5, etc. A total of 8928 visual assessments were thus conducted. A correlation coefficient (COQ) and other well-known criteria [8-11] were used to evaluate the performance of color difference formulae.

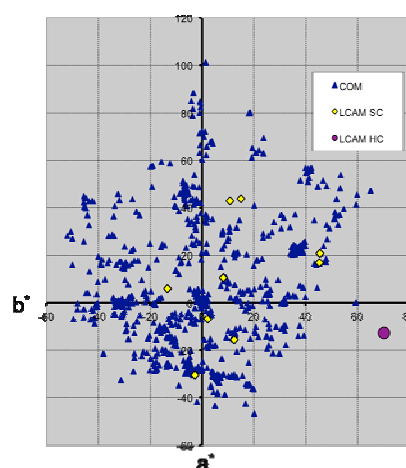


Figure 2 Color coordinates of LCAM HC (high chroma) test center in CIELAB color space

3 RESULTS AND DISCUSSION

As discussed earlier, the different color difference equations give weightings in different parts of the color space to better match the differences seen by the human eye. This means that different areas of the color space will show difference more than others and different factors of the color difference are more perceivable than others. Table 1 shows two examples of how visual ranking and calculated rankings agree for standard form of tested color difference formulas. A result presented in Table 1 shows insignificant difference between color difference formulas in multidimensional scaling techniques.

These results indicate that various color difference equations may not provide optimal results at set decisive ΔE values, and weighting functions should be optimized for each formula in order to appropriately compare their performance. Such optimization was made for each tested formula and results are shown in Table 2.

Table 1 Summary of performance criteria for various color difference formulae

Criterion	ΔE^*	ΔE_{CMC2}	ΔE_{CIE942}	ΔE_{DIN99d}	ΔE_{CIE00}
COQ	0.80	0.80	0.79	0.82	0.81
ϕ	0.23	0.52	0.51	0.41	0.46
WDC	28.02	19.35	19.89	23.05	21.50
D%	11.20	45.72	45.95	30.49	38.21
PF/3	66.41	66.66	68.44	67.94	68.38
STRESS	40.28	40.42	41.04	39.11	39.45

Table 2 Summary of performance criteria for optimized various color difference formulae

mag opt	2	1.3	1.4	1.8	1.9
Criterion	ΔE^*_{opt}	ΔE_{CMC2}_{opt}	ΔE_{CIE942}_{opt}	ΔE_{DIN99d}_{opt}	ΔE_{CIE00}_{opt}
COQ	0.80	0.80	0.79	0.82	0.81
ϕ	0.42	0.60	0.61	0.56	0.58
WDC	22.62	16.71	17.51	19.17	19.73
D%	32.28	59.87	63.67	56.07	60.83
PF/3	66.41	66.66	68.44	67.94	68.38
STRESS	40.28	40.42	41.04	39.11	39.45

A result presented in Table 2 shows specifically at optimized decisive ΔE values, characterized as magnitude (mag opt), when applicable, WDC coefficients are ranked in the order shown: CMC<CIE94<DIN99< CIEDE2000<CIELAB. Nevertheless we can see, that difference in this criterion is only 6% in comparison to obviously 15 and more % measured for mid and low chroma samples.

However, the statistical significance of any differences in the performance of the models must be determined for solid conclusions to be drawn. In this study, pairs were selected with a range of high chroma around one color center. Data presented show, that border between accepted and rejected pairs is rather fuzzy than sharp. Such problem is well known, however in comparison to other studies in our test observers were more tolerant in hue term in comparison to chroma.

4 CONCLUSION

Analysis of color measurements is a typical problem of multivariate statistics: Usually color coordinates of a colorimetric controlled process are located in an ellipsoid in the color space, sphere in uniform color space respectively. The new dataset can be used in the development of additional color difference models and comparison of their performances. Several metrics were used to compare the performance of

color difference models against experimental visual data. However, different conclusions may be drawn depending on the performance metric(s) used. Our results shows, that during evaluation of high chroma samples performance improvement of color difference formulas decrease in comparison to CIELAB color space.

5 REFERENCES

1. Hunt R.W.G.: The Reproduction of Colour. Chichester, England: John Wiley & Sons Ltd., 2004
2. Berns R.S., Alman D.H., Reniff L., Snyder G.D., and Balonon-Rosen M.R.: Visual determination of suprathreshold color-difference tolerances using probit analysis, *Color Research and Application* 16(5), 1991, pp. 297-316
3. DIN6176: Farbmetrische Bestimmung von Farbabständen bei Körperfarben nach der DIN-99-Formel, Technical report, DIN, Deutsches Institut für Normung e.V., 2001
4. Cui G., Luo M.R., Rigg B., Roesler G., and Witt K.: Uniform colour spaces based on the DIN99 colour-difference formula, *Color Research and Application* 27(4), 2002, pp. 282-290
5. CIE Publication No. 142: Improvement to Industrial Colour-Difference Evaluation, Technical report, Central Bureau of the CIE, Vienna, Austria, 2001
6. CIE Publication No. 116: Industrial Colour-Difference Evaluation, Technical report, Central Bureau of the CIE, Vienna, Austria, 1995
7. Clarke F.J.J., McDonald R. and Rigg B.: Modification to the JPC79 Color-difference

- Formula, *J. Soc. Dyers Color* 100, 1984, pp. 128-132
8. Guan S.S., Luo M.R.: A colour-difference formula for assessing large color differences, *Color Research and Application* 24, 1999, pp. 344-355
 9. Alder C., Chaing K.P., Chong T.F., Coates E., Khalili A.A., Rigg B.: Uniform chromaticity scales - New experimental data, *J. Soc. Dyers Color* 98, 1982, pp. 14-20
 10. Schultz W.: The usefulness of colour-differences formulae for fixing colour tolerances. In: Color Metrics, edited by Vos JJ, Friele LFC, and Walraven PL. Soesterber: AIC/Holland, 1972, pp. 245-265,
 11. Garcia P., Huertas R., Melgosa M., Cui G.: Measurement of the relationship between perceived and computed color differences, *J. Opt. Soc. Am. A* 24, 2007, pp. 1823-1829
 12. Kruksal J.B.: Multidimensional scaling by optimizing goodness of fit to a nonmetric hypothesis, *Psychometrika* 29, 1964, pp. 1-27

HODNOCENÍ BAREVNÝCH ROZDÍLŮ U MATERIÁLŮ S VYSOKOU ČISTOTOU ODSŤÍNU

Percentuálně jednotný barevný prostor je nutný především pro kontrolu kvality a různých barevných technologických aplikací. Barevný prostor CIELAB byl navržen pro tento účel v roce 1976. Používá se u mnoha standardů, jako je tisk, grafické umění, nátěry a v automobilovém průmyslu. Nicméně, CIELAB není vizuálně rovnoměrně odstupňovaný, takže barvy, které mají stejnou velikost ΔE^* v různých oblastech barevného prostoru se zobrazí v různé velikosti. K překonání nerovnoměrnosti CIELAB, byly vytvořeny různé vzorce (např., CMC, DIN99, a CIEDE2000).

Barevné rozdílové vzorce jsou navrženy pro zpřesnění parametrů, které jsou předdefinovaných funkcí do obrazových dat. Existují dva hlavní problémy s tímto přístupem:

1. Vizuální data z jediného experimentu jsou obvykle řídky rozložena v CIELAB a jsou spojovány souborem údajů získaných různými psychofyzickými metodami (např. způsoby stálých podnětů nebo metodou šedé stupnice), je vysoce kontroverzní.
2. Vizuální údaje mohou být vybrány tak, aby výsledný barevný rozdíl rovnice tvořil shluk, a tím ztrácí schopnost zobecňování.

Cílem této práce není vytvářet rovnice pro výpočet barevných rozdílů, ale vést ke zlepšení stávajících rovnic pomocí vizuálních dat. Možné použití je pro zvýšení přesnosti predikce kolem jednotlivých barevných center s vysokou čistotou. Vizuální experimenty na těchto barevných centrech by mohlo zlepšit standardizované rovnice, za předpokladu, že byly provedeny za podobných podmínek.

INSTRUCTIONS FOR AUTHORS

The journal „**Vlákna a textil**” (Fibres and Textiles) is the scientific and professional journal with a view to technology of fibres and textiles, with emphasis to chemical and natural fibres, processes of fibre spinning, finishing and dyeing, to fibrous and textile engineering and oriented polymer films. The original contributions and works of background researches, new physical-analytical methods and papers concerning the development of fibres, textiles and the marketing of these materials as well as review papers are published in the journal.

Manuscript

The text should be in ***single-column format***.

The original research papers are required to be written in English language with summary. Main results and conclusion of contribution from Slovak and Czech Republic should be in Slovak or Czech language as well.

The other parts of the journal will be published in Slovak language; the advertisements will be published in a language according to the mutual agreement.

The first page of the manuscript has to contain:

The title of the article (16 pt bold, capital letters, centred)

The initials of the **first name** (s) and also **surnames** of all authors (12 pt, normal, centred)

The complete address of the working place of the authors, e-mail of first author (12 pt, italic, centred)

Abstract (10 pt, italic)

Key words (10 pt, italic)

The manuscript has to be written in A4 standard form, in **Arial**.

Do not number the pages and do not use footnotes. Do not use business letterhead.

Figures, tables, schemes and photos should be numbered by Arabic numerals and titled over the table and under the figure or

picture. The total number of figures and tables should not be more than 10.

Photos and schemes have to be sufficiently contrastive and insert in text as pictures.

Mathematical formulae should be centred on line and numbered consecutively on the right margin.

Physical and technical properties have to be quantified in SI units, names and abbreviations of the chemical materials have to be stated according to the IUPAC standards.

References in the text have to be in square brackets and literature cited at the end of the text. References have to contain names of all authors.

1. Surname N., Surname N.: Name of paper or Chapter, In *Name of Book (in Italics)*, Publisher, Place of Publication, YYYY, pp. xxx-yyy
2. Surname N., Surname N.: Name of paper, *Name of Journal (in Italics)* Vol. (No.), YYYY, pp. xxx-yyy
3. Surname N., Surname, N.: Title of conference paper, *Proceedings of xxx xxx*, conference location, Month and Year, Publisher, City, Surname N. (Ed.), YYYY, pp. xxx-yyy
4. Surname N., Surname N.: Name of Paper, Available from <http://www.exact-address-of-site>, Accessed: YYYY-MM-DD

Authors are kindly requested to deliver the paper to be published by e-mail (in Word form).

Address of the Editor Office:

Marcela Hricová

FCHPT, STU in Bratislava

Radlinskeho 9

812 37 Bratislava,

Slovakia

e-mail: marcela.hricova@stuba.sk